I. A NUCLEAR MAGNETIC RESONANCE STUDY OF METAL CARBONYLS IN THE SOLID STATE, AND

II. STUDIES OF THE SURFACE CHEMISTRY OF RHODIUM SUPPORTED ON ALUMINA

Thesis by

James W. Gleeson

In Partial Fulfillment of the Requirements

for the Degree of

Doctor of Philosophy

California Institute of Technology
Pasadena, California

1982

(Submitted November 17, 1981)

ACKNOWLEDGEMENTS

I thank Professor W. Henry Weinberg for valuable advice during my final two years at Caltech. The efforts of Professor Sunney I. Chan in maintaining the financial support for the research are much appreciated. I am indebted to the late Professor Robert W. Vaughan for his inspiring example as a scientist and as a person.

I thank the present and former members of the Vaughan and Weinberg groups, especially Mike Duncan, Mike Templeton, Jeff Reimer, and Albert Highe, for helpful advice and discussions and for being pleasant to work with.

The assistance of the staff of the Chemistry and Chemical Engineering Division, especially John Yehle, George Griffith, Ray Reed, Seichi Nakawatase, and Eric Siegel, in constructing and maintaining the equipment used in these studies is greatly appreciated. Professor George R. Rossman was very generous in allowing the use of his infrared spectrometer. Kathy Lewis was most patient and accommodating in typing this thesis.

The financial support of Caltech and the Office of Naval Research is gratefully appreciated.

Finally, and most importantly, I would like to thank two people for assistance of many sorts during the past five years, as well as the previous twenty one, my parents, Mr. James A. and Mrs. Dora R. Gleeson.

ABSTRACTS

Part I

The principal components of the ^{13}C nuclear magnetic resonance chemical shift tensors of metal carbonyls containing between one and six metal atoms were determined from the powder patterns of the solid compounds. The tensors of terminally-bound CO groups are highly anisotropic (380 ± 60 ppm) and nearly axially symmetric. The tensors of bridging CO groups are much less anisotropic, due to significant asymmetry in the electron orbitals about the CO internuclear axis. The tensors vary only slightly for different transition metals. There is no intramolecular rearrangement of the metal carbonyls in the solid state at frequencies $\gtrsim$ 10 kHz, except in $Fe_3(CO)_{12}$.

Part II

The surface chemistry of rhodium supported on alumina was studied using infrared spectroscopy and quantitative measurements of the gases adsorbed and evolved during various procedures. First, the behavior of alumina-supported Rh upon heating in the presence of CO, CO_2, O_2 and H_2 was studied. The loss in the capacity to adsorb CO after heating to 525 K increases in the order O_2, H_2, vacuum < CO_2 < CO. Upon heating in CO, some CO is oxidized to CO_2 with oxygen from the surface, while the dicarbonyl-forming Rh^I is reduced to Rh°. The Rh° agglomerates, accounting for the substantial loss in capacity to adsorb CO. Upon heating in CO_2, the dicarbonyl-forming Rh^I is also deactivated. There is little loss in the capacity

to adsorb CO upon heating in H_2, O_2 or vacuum.

Second, the adsorption of H_2S and its interaction with CO on Rh supported on alumina was studied. The dissociation of H_2S on the Rh at 300 K produces H_2 and is inhibited by preadsorbed CO. Rh also facilitates the reaction of H_2S with surface oxygen below or at 373 K, in which water is produced. After exposure of the Rh to H_2S, CO adsorbs in the linear, but not in the dicarbonyl or bridging modes. Exposure of a CO-precovered surface to H_2S displaces much of the bridging CO, but only slowly removes the dicarbonyl and linear CO. Exposure to H_2S strongly inhibits the removal of adsorbed CO by O_2, but exchange of adsorbed and gas phase CO occurs readily.

TABLE OF CONTENTS

Part I:

A ^{13}C Nuclear Magnetic Resonance Study of Metal Carbonyls in the Solid State

Chapter 1:

Introduction

Many chemical reactions require breaking bonds involving carbon, hydrogen and/or oxygen atoms that typically have bond energies of $\gtrsim$ 80 kcal/mol. This can often be facilitated by the process of catalysis, in which weaker, temporary bonds are made between one or more of the reactants and an additional material, the catalyst, that is recovered unchanged after the reaction. Bonds to transition metals are well suited for this and transition metal catalysts are consequently used extensively in industry.

An example of a reaction catalyzed by a transition metal is the oxidation of CO, shown in Fig. 1. Although the thermodynamics of the reaction are not affected by the presence of the catalyst since there is no net change in the catalyst, the kinetics are affected strongly. The activation energy for dissociating the oxygen molecule is nearly eliminated in the presence of the metal. In contrast, it is more difficult for the dissociated oxygen to react with the CO in the presence of the metal, and additional energy is needed to break the bonds to the metal in desorbing the product. The overall effect of the catalyst is, however, highly beneficial toward reaction, such that the reaction proceeds readily at room temperature in the presence of a catalyst **(1)**, whereas a temperature of ~ 900°C is needed merely to sustain this reaction after ignition in the absence of a catalyst **(4)**. To understand the reason for the high catalytic activity of transition metals, we consider the energies, number and symmetries of the valence orbitals that bind to the reactants **(5-7)**. The example above illustrated the point that one or more of the reactants must be activated through binding to the metal, but the binding must not be so strong as to prevent further reaction and desorption of the product. In fact, typical binding energies of various species to transition metals in metal complexes and on metal surfaces lie in the range 25-70 kcal/mol **(8-10)**, somewhat below the energies of the bonds to be broken in the reactants and reformed in the products. In each

transition metal atom, there are empty s, p and d valence orbitals of various symmetries so that, in principle, different reactants may be bound in proximity to one another, increasing the chances of reaction. While the remaining sites of metal atoms of a metal surface are involved in bonds to other metal atoms, the remaining sites in metal complexes are occupied by ligands that can be chosen to optimize the catalytic properties of the complex.

Transition metals bind species such as hydrogen atoms and alkyl groups with covalent bonds qualitatively similar to those in organic compounds. Bonds to the most electronegative elements probably possess significant ionic character. In addition to these types of bonding found in the main group elements, transition metals also participate in coordinate or donor-acceptor bonding, illustrated in Fig. 2 for the bonding of CO to a transition metal. The CO "donates" a pair of electrons from one of its filled orbitals to an empty orbital of the metal and accepts electrons from the metal into an unoccupied orbital. The bonding of phosphines, molecular nitrogen, nitriles, isonitriles and other molecules to transition metals is of this type.

The ability of transition metals to bind reactants in more than one manner increases the number of ways it can promote the reaction. It is common for a reactant bound in a coordinate manner to change to bonding in a covalent manner after reaction with another species. A striking example of this is found in a molybdenum complex in which both hydrogen and ethylene ligands are bound. The hydrogen ligand exchanges with the hydrogens of the coordinatively bound ethylene at a rate of ~ 500 Hz at 7°C, almost certainly via a covalently bound ethyl group **(11)**. This process models an important step in metal-catalyzed olefin hydrogenation.

Despite the much greater importance of transition metals dispersed on rela-

tively inert supports as catalysts in industry, most of the fundamental understanding of the bonding of molecules to transition metals has been obtained from studies of molecular transition metal complexes. In addition to the information concerning the syntheses and reactions of the metal complexes, a variety of physical methods are available for their characterization, among them: X-ray crystallography, infrared, optical, nuclear and electron magnetic resonance and photoelectron spectroscopies, methods for measuring magnetic susceptibilities, and mass spectrometry **(12)**. The use of many of these techniques to study the binding of reactants to dispersed transition metals is hindered by particular features of the dispersed metals. For example, their amorphous nature prevents the use of X-ray crystallography, while their light scattering properties inhibit the use of optical spectroscopy. The reduced concentration of metal-reactant bonds relative to that in solid or even dissolved metal complexes causes substantial problems in the application of nuclear magnetic resonance and sometimes infrared spectroscopy. Recently, however, there has been a burgeoning of sensitive electron spectroscopies appropriate for studying transition metal crystals and molecules bound to them for gas phase pressures less than about 10^{-4} Torr.

The use of nuclear magnetic resonance spectroscopy to study metal complexes has focused primarily on determining the geometrical structures of the metal complexes and the intramolecular rearrangements that they may undergo **(13-16)**. These studies are carried out with the metal complex in a solution, in which the resonances of the various nuclei of a given element depend on the precise chemical environment of the nucleus. They differ from each other by amounts of the order of ppm and are often easily resolved in the spectrum. The temperature dependence of the resonance frequencies can provide information about intramolecular rearrangements of the complex **(15,16)**.

For compounds in the solid state in general, it is much more difficult to resolve the resonances of the nuclei of a given element. This is because there are several effects on the resonance frequency of a nucleus that are dependent on the orientation of the molecule with respect to the externally applied magnetic field, such as the dipole-dipole interactions between nuclei, the chemical shift interaction, and the interaction of a quadrupolar nucleus with electric field gradients at the nucleus. These are averaged by the rapid tumbling of the molecule in a liquid but are not averaged in the solid state. An advantage of obtaining the spectrum of a solid is that the unaveraged interactions can provide more information about the molecule than the averaged interactions. Recently, there have been advances which allow one to selectively reduce the effects of the various interactions on the observed spectrum by applying the exciting radiation to the sample in a particular manner **(17-19)**.

In Part I of this thesis, the bonding of CO in transition metal carbonyls will be examined with ^{13}C nuclear magnetic resonance. It is desirable to understand the bonding of CO to metals because of the importance of metal-catalyzed reactions involving CO: reduction by hydrogen to methane and higher hydrocarbons **(20,21)**, oxidation to CO_2 **(1,2)** and reaction with alcohols to make carboxylic acids, and with olefins and hydrogen to make aldehydes **(7)**. Supported transition metals are generally used in the first two reactions, while soluble metal complexes are used in the latter two. There is much effort toward comparing the bonding of CO in metal complexes to that on metal surfaces **(9)**, and it seems clear that the general features of the bonding are similar in the two cases.

The metal carbonyls will be studied by measuring the nuclear magnetic resonance spectra of the solids. The major interaction that will determine the shape of the spectrum will be the unaveraged chemical shift interaction. The spectra

will be simple enough to be interpreted in terms of certain aspects of the electronic structure of these compounds. Comparisons among the metal carbonyls and between metal and organic carbonyls will be made.

References

1. T. Engel and G. Ertl, Advan. Catal. **28**, 1 (1979).

2. G. Ertl, Proc. 7th Intern. Congr. Catal., Preprints, P2, Tokyo, 1980.

3. *JANAF Thermochemical Tables*, 2nd ed., Office of Standard Ref. Data, Washington, 1971.

4. R. V. Green, in *Encyclopedia of Chemical Technology*, 2nd ed., Vol. 4, p. 430, Wiley-Interscience, New York, 1964.

5. F. A. Cotton and G. Wilkinson, *Advanced Inorganic Chemistry*, 3rd ed., p. 528, Wiley-Interscience, New York, 1972.

6. *The Nature of the Surface Chemical Bond*, T. Rhodin and G. Ertl, eds., North-Holland, Amsterdam, 1979.

7. G. W. Parshall, *Homogeneous Catalysis*, p. 5, Wiley-Interscience, New York, 1980.

8. J. A. Connor, Top. Curr. Chem. **71**, 71 (1977).

9. E. L. Muetterties, T. N. Rhodin, E. Band, C. F. Brucker and W. R. Pretzer, Chem. Rev. **79**, 91 (1979).

10. I. Toyoshima and G. A. Somorjai, Catal. Rev.-Sci. Eng. **19**, 105 (1979).

11. J. W. Byrne, H. U. Blaser and J. A. Osborn, J. Amer. Chem. Soc. **97**, 3871 (1975).

12. R. S. Drago, *Physical Methods in Inorganic Chemistry*, Reinhold, New York, 1965.

13. B. E. Mann, Advan. Organometal. Chem. **12**, 135 (1974).

14. O. A. Gansow and W. D. Vernon, in *Topics in Carbon-13 NMR Spectroscopy*, Vol. 2, G. C. Levy, ed., Wiley-Interscience, New York, 1976.

15. E. Band and E. L. Muetterties, Chem. Rev. **78**, 639 (1978).

16. J. Evans, Advan. Organometal. Chem. **16**, 319 (1977).

17. M. Mehring, *High Resolution NMR Spectroscopy in Solids*, Springer-Verlag, New York, 1976.

18. U. Haeberlin, *High Resolution in Solids — Selective Averaging*, Academic Press, New York, 1976.

19. R. W. Vaughan, Ann. Rev. Phys. Chem. **29**, 397 (1978).

20. V. Ponec, Catal. Rev.-Sci. Eng. **18**, 151, (1978).

21. M. A. Vannice, Catal. Rev.-Sci. Eng. **14**, 153 (1976).

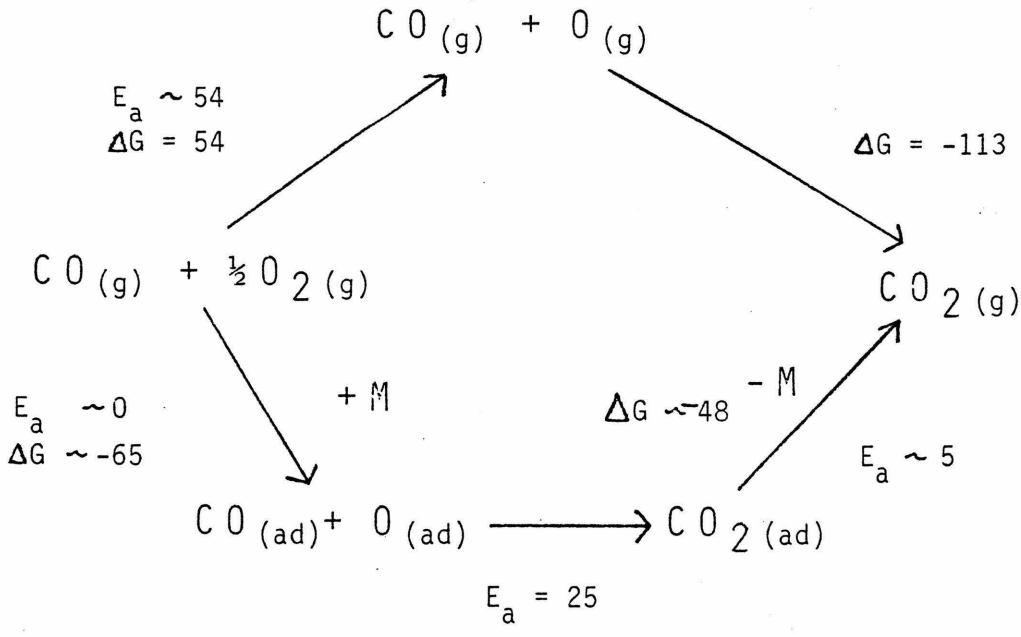

Figure 1. Catalysis of CO Oxidation by a Group VIII Transition Metal (M). The activation energy, E_a, and ΔG are in kcal/mol for the reaction at 400 K **(1–3)**. Values are for low coverages of $CO_{(ad)}$ and $O_{(ad)}$.

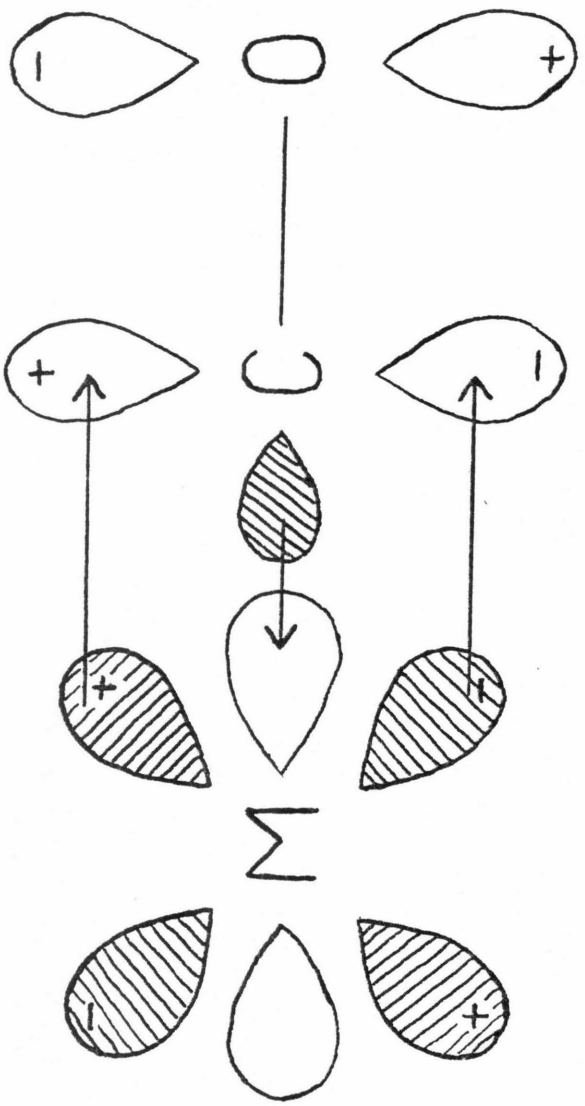

Figure 2. Donor-Acceptor Bonding of CO to a Transition Metal

Chapter 2:

^{13}C NMR Chemical Shift Tensors of Metal Carbonyls

Abstract

The principal components of the ^{13}C NMR chemical shift tensors of metal carbonyls containing between one and six metal atoms were determined from their powder patterns. The tensors of terminally-bound CO groups are highly anisotropic (380 ± 60 ppm) and nearly axially symmetric. The tensors of bridging CO groups are much less anisotropic, due to significant asymmetry in the electron orbitals about the C-O internuclear axis. The tensors vary only slightly for different transition metals. There is no intramolecular rearrangement of the metal carbonyls in the solid state at frequencies greater than 10 kHz, except in $Fe_3(CO)_{12}$.

1. Introduction

Despite the plethora of studies of the interaction of CO with transition metals, many fundamental details of the bonding are not completely understood. From semiempirical and even sophisticated *ab initio* theoretical calculations of metal carbonyls, there has yet to emerge a consistent description of such aspects as the relative importance of σ and π bonding, and variations in electronic structure with the type of transition metal and bonding geometry **(1)**. Relative and absolute electronic energy levels have been determined experimentally using electronic absorption and photoelectron spectroscopies, respectively **(1,2)**. Vibrational and NMR spectroscopies are sensitive to specific aspects of the electronic structure, such as the degree of π-backbonding from the metal to the CO and to specific electronic excitation energies **(2-4)**. The isotropic chemical shifts measured in ^{13}C NMR studies of liquids have been correlated to other parameters such as the CO stretching frequency **(3-4)** and atomic charge populations from theoretical studies **(5)**. Unfortunately, a number of changes in the bonding can cause changes in the isotropic chemical shift that are comparable to the differences observed. NMR studies of metal carbonyls have been more successful in characterizing intramolecular rearrangements in solution that indicate the lability of the carbonyl bonds and serve as models for motion of CO adsorbed on metal surfaces **(6-8)**.

There is inherently a greater amount of information in the NMR of solids than liquids since in liquids the angular dependence of the chemical shift interaction, as well as that of other interactions, is averaged by the rapid tumbling of molecules. The chemical shift tensor can be defined by three principal components: σ_{11}, σ_{22} and σ_{33}, and three principal directions in the molecule or crystal along which the magnetic field at the nucleus is shifted from the externally applied field by the amounts equal to the three principal components **(9-11)**.

For a chemical shift tensor with axial symmetry, which will at least be approximately the case throughout this study, two of the components and directions coincide:

$$\sigma_{22} = \sigma_{33} = \sigma_{\perp} \tag{1}$$

The chemical shift along the unique direction is defined as σ_{11}. We further note that the average, or isotropic, chemical shift and the chemical shift anisotropy are defined, respectively, as:

$$\bar{\sigma} = (\sigma_{11} + 2\sigma_{\perp})/3 \tag{2}$$

and

$$\Delta\sigma = |\sigma_{\perp} - \sigma_{11}| \quad . \tag{3}$$

NMR spectra of solids can also be affected by intramolecular rearrangements **(12)**. Since the chemical shift tensor depends on the angle of the applied magnetic field with respect to the molecule, not simply the average chemical environment of the observed nucleus, a greater number of rearrangements may change the spectra of solids than of liquids, and in ways more characteristic of the rearrangement.

In general, the principal components, but not the principal directions of the chemical shift tensor, are determined from polycrystalline samples, or powders. However, we will see that the tensors of the CO groups of metal carbonyls are axially symmetric, or nearly so, the unique direction being along the C-O internuclear axis. Thus we obtain, at least approximately, the complete tensors from the powder patterns of metal carbonyls.

Initial studies of the ^{13}C NMR chemical shift tensors of metal carbonyls have been carried out. Mahnke et al. **(13)** by relaxation time measurements in solution, evaluated the chemical shift tensors of $Ni(CO)_4$ and $Fe(CO)_5$, which were

later confirmed by NMR measurements of the solids **(14)**. By analyzing the diamagnetic and paramagnetic contributions of each chemical shift component, they argued that the differences among the spectra of CO, $Ni(CO)_4$ and $Fe(CO)_5$ could be explained in terms of π-backbonding. This will be discussed later with respect to the present results. Spiess et al. **(14)** showed that the temperature-dependent changes in the spectrum of solid $Fe(CO)_5$ were the result of exchange between axial and equatorial CO groups. Such exchange also occurs in the liquid state **(15,16)**.

In the present study, we examine the sensitivity of the chemical shift interaction in metal carbonyls to the type of transition metal, the presence of metal-metal bonding and the mode of CO bonding, i.e. terminal or bridged. We will see that the mode of bonding has a particularly large effect. The motional properties of metal carbonyls in the solid state will also be discussed.

2. Experimental Procedures

The $Cr(CO)_6$ and $W(CO)_6$ were obtained from Alfa-Ventron and the other metal carbonyls were obtained from Strem Chemicals. The ^{13}CO (90% enriched) was obtained from Merck, Sharp and Dome. The metal carbonyls were enriched in ^{13}C by direct exchange of ^{13}CO with the metal carbonyls. Enrichment of $Cr(CO)_6$, $Mo(CO)_6$ and $W(CO)_6$ was carried out in the gas phase at 360 K, while exchange with the other carbonyls was performed in solution at 300 K. The typical extent of enrichment was 5%, except for $(\eta^5-C_5H_5)_2Fe_2(CO)_4$, which was 80% of the carbonyl groups. Samples were ~ 0.5 g each.

NMR spectra of the polycrystalline samples were taken on a largely home-built spectrometer, similar to that described previously **(17)**. An external lock system held the 2.35 Tesla magnet to drifts of less than 2 ppm over eight hours. A single coil (5 mm I.D.) double resonance probe **(18)**, tuned for ^1H resonance at

99.8 MHz and ^{13}C resonance at 25.1 MHz, was used to obtain the spectrum of $(\eta^5-C_5H_5)_2Fe_2(CO)_4$. A decoupling field of 12 Gauss was applied continuously at the ^1H resonance frequency while the ^{13}C resonance was observed. The spectra of the other carbonyls were obtained using a single resonance probe with a 8 mm I.D. coil and tuned to 25.1 MHz All chemical shift values are reported on the σ scale ($-\delta$ scale) relative to tetramethylsilane (TMS).

Spin-lattice relaxation times of the ^{13}C nuclei were ~ 20 min. and depended on the orientation of the molecules with respect to the external magnetic field. With a pulse repetition time of 50 min, spectra were obtained that were free of distortions from relaxation effects. To remove experimental artifacts, pulses with 0° and 180° phase shifts were alternately applied to the sample and the decays alternately added and subtracted. Approximately 128 free induction decays were accumulated for each sample, and then Fourier transformed.

The spectrum of a sample at a low temperature was obtained by first allowing the sample to magnetically equilibrate in the magnet at 300 K. The sample was then brought to 77 K by immersing in liquid N_2 between the magnet pole faces but outside the NMR coil. Finally, the sample was quickly placed in the coil, pulsed and a decay recorded. The temperature of the sample at this point is estimated to be 100 ± 20 K. With this procedure, possible problems resulting from long spin-lattice relaxation times at low temperatures were avoided. Also, the purpose of these experiments was to determine if there were gross changes in the spectra due to the presence of temperature-dependent motions on the NMR timescale. Therefore, it was not necessary to know the temperature precisely.

3. Results

Principal components of the chemical shift tensor for the ^{13}C nuclei of the CO groups of nine metal carbonyls were determined from their ^{13}C NMR powder patterns. The principal components of these carbonyls, along with those of related carbonyls measured by other authors are listed in Table 1. Illustrative spectra are presented in Figs. 1-4 and are described below.

A. $Mo(CO)_6$, $Cr(CO)_6$ and $W(CO)_6$

Shown in Fig. 1 is the ^{13}C NMR spectrum of $Mo(CO)_6$ at 300 K. The solid line is a nonlinear least-squares fit to the experimental points of a theoretical chemical shift powder pattern convoluted with a Lorentzian broadening function. The chemical shift tensor of the carbon nucleus is axially symmetric due to the four-fold rotational symmetry about the Mo-C-O internucleus axis in the molecule **(19)** (slight deviations from the idealized symmetry in the crystal are ignored here).

The principal components of the chemical shift tensor, σ_{11} and $\sigma_{\perp}$, obtained from the fit to the $Mo(CO)_6$ spectrum may be used to calculate the isotropic chemical shift, $\bar{\sigma}$, using Eq. (2). The value found, -203 ppm, should be equal both to the center of mass of the spectrum, -208 ppm, as well as to the isotropic chemical shift obtained from the spectrum of dissolved $Mo(CO)_6$, -202 ppm **(20)** in the absence of intermolecular effects. The agreement is well within the experimental error of 15 ppm. Similar agreement was found for other metal carbonyls **(13,14,21-24)**, and is typical of ^{13}C chemical shifts in general **(9)**.

Only the $\sigma_{\perp}$ components, which were observed easily, were determined directly from the powder patterns of $Cr(CO)_6$ and $W(CO)_6$ because of the low signal-to-noise. The values of σ_{11} were calculated from Eq. (2) using the values of $\bar{\sigma}$ for

these carbonyls in solution **(20)**. Theoretical powder patterns calculated with these values matched the experimental spectra well within experimental error.

We note that it was not necessary to include effects of motional averaging of the chemical shift interaction in fitting the experimental spectra. That the chemical shift interaction is not being averaged for the metal carbonyls here is also supported by the similarity of the principal components determined to the unaveraged components of CO **(25,26)**, $Ni(CO)_4$, $Fe(CO)_5$ **(13,14)** and $Rh_2(CO)_4Cl_2$ **(24)**, as seen in Table 1. Thus, for the hexacarbonyls, the frequency of intramolecular rearrangements that would average the chemical shift interaction must be less than 10 kHz, the linewidth due to chemical shift anisotropy.

B. $Ru_3(CO)_{12}$, $Os_3(CO)_{12}$ and $Ir_4(CO)_{12}$

To investigate possible changes in the ^{13}C chemical shift interaction from bonding CO to a metal cluster rather than to a single metal atom in a complex, several cluster carbonyls were examined. In $Ru_3(CO)_{12}$ and $Os_3(CO)_{12}$, four CO groups are bound terminally to each metal atom. There are two equatorial CO groups in the plane of the metal triangle and one axial CO on each side of this plane and perpendicular to it, resulting in D_{3h} symmetry for these molecules **(27,28)**. In $Ir_4(CO)_{12}$, three CO groups are bound terminally to each atom of the Ir tetrahedron resulting in T_d symmetry for the molecule **(29)**.

The spectrum of $Ru_3(CO)_{12}$ at 300 K is shown in Fig. 2, along with a fit of a single theoretical chemical shift powder pattern. We would expect the spectrum to be a superposition of two equally intense chemical shift powder patterns from the axial and equatorial CO groups. Also, the two tensors are not required to be axially symmetric by the molecular symmetry. However, we see that a single powder pattern of a nearly axially symmetric tensor fits the data quite well. As with the carbonyls containing a single metal atom, the isotropic chemical shift,

-201 ppm, and the center of mass of the spectrum, -196 ppm are within experimental error of the isotropic chemical shift in solution, -199.7 ppm **(30)**. Here, also, there is no evidence for averaging of the chemical shift interaction by intramolecular rearrangements.

The signal-to-noise of the spectra of $Os_3(CO)_{12}$ and $Ir_4(CO)_{12}$ was low. The chemical shift tensors of both carbonyls were assumed to be axially symmetric. Also, $\bar{\sigma}$ in solid $Os_3(CO)_{12}$ was set equal to that of dissolved $Os_3(CO)_{12}$ **(30)** and used to calculate σ_{11} as before.

C. $Rh_6(CO)_{16}$ and $(\eta^5-C_5H_5)_2Fe_2(CO)_4$

All spectra described so far have been of CO bound terminally to a single metal atom of a complex or cluster. To investigate the bonding of CO to more than one metal atom in a multicentered or bridging configuration, the powder patterns of $Rh_6(CO)_{16}$ and $(\eta^5-C_5H_5)_2Fe_2(CO)_4$ were measured. $Rh_6(CO)_{16}$ contains triply-bridging CO groups and $(\eta^5-C_5H_5)_2Fe_2(CO)_4$ doubly-bridging CO groups. The spectra are shown in Fig. 3.

In $Rh_6(CO)_{16}$, two CO groups are bound terminally to each Rh atom, while the remaining four triply bridge alternate faces of the Rh octahedron **(31)**. The spectrum will be a superposition of the powder patterns of the terminal and bridging CO groups, with a relative intensity of 3:1. The chemical shift tensor of the bridging CO groups is axially symmetric due to the three-fold rotational symmetry about the C-O axis. With the above two restrictions, in addition to setting the isotropic chemical shifts in the solid equal to those in solution **(32)**, the experimental spectrum is fit uniquely and well.

The chemical shift tensor of the terminally-bound CO groups in $Rh_6(CO)_{16}$ is typical of terminally-bound CO groups in general, both in anisotropy and near

axial symmetry. The anisotropy of the tensor of the bridging CO, however, is only 194 ppm, or about half that of terminally-bound CO. The change results almost exclusively from a shift of σ_{11}. Evidence that the difference is not due to motional averaging is *(a)* the typical powder pattern of the terminal CO groups, *(b)* the lack of exchange on the NMR timescale of CO groups among the Rh atoms of $Rh_6(CO)_{16}$ in solution at 343 K **(28)**, and *(c)* the similarity of the spectra of the solid at 300 and 100 K. The only change in the spectrum that occurs at 100 K is that the intensity from 0 to +80 ppm increases to match the theoretical fit to the 300 K spectrum more closely. This could be due to freezing out some low frequency vibrational motions that average the chemical shift interaction to a small extent.

To determine the chemical shift tensor of a doubly-bridging CO group, the ^{1}H-decoupled powder pattern of $(\eta^5-C_5H_5)_2Fe_2(CO)_4$ was measured. There is one CO is bound terminally to each of the Fe atoms, while the other two symmetrically bridge the Fe-Fe bond **(33-35)**. There are cis and trans forms, depending on the relative positions of the cyclopentadienyl and terminal CO groups. The infrared spectrum of the sample used here indicates a mixture of the two forms. However, the isotropic chemical shifts in solution differ by only 0.2 ppm **(36,37)**, an insignificant amount in this study.

The experimental spectrum shown in Fig. 3b is due to the carbon nuclei of the CO groups since they were selectively enriched to 80% by exchange with ^{13}CO. The small contribution of the carbons of the cyclopentadienyl groups was removed by measuring the spectrum of an unenriched sample and subtracting an appropriate intensity from the spectrum of the enriched sample. The number of fitting parameters was reduced as for $Rh_6(CO)_{16}$ to obtain a unique fit.

The chemical shift tensor of the terminal CO groups was nearly axially symmetric and had an anisotropy of 444 ppm, which are typical of terminal CO groups in other metal carbonyls. The anisotropy of the tensor of the bridging CO group is even less than that of the triply-bridging CO group in $Rh_6(CO)_{16}$, 138 ppm vs. 194 ppm, again because the σ_{11} component has shifted. The deviation from axial symmetry of the tensor of the doubly-bridging CO is somewhat greater than that of terminally-bound CO, with $\sigma_{33} - \sigma_{22} = 20$ ppm.

Although the cis and trans forms of $(\eta^5\text{-}C_5H_5)_2Fe_2(CO)_4$ rearrange on the NMR timescale in solution at 238 K **(36-38)**, motional averaging is unlikely in the solid based on the typical powder pattern of the terminal CO groups and the similarity of the powder patterns of the sample at 300 and 100 K. Thus, the tensors of both doubly- and triply-bridging CO groups are much less anisotropic than those of terminally-bound CO groups.

D. $Fe_3(CO)_{12}$

In solid $Fe_3(CO)_{12}$, two CO groups doubly bridge a single edge of the Fe_3 triangle, while the ten terminally-bound CO groups are of four types based on slightly different chemical environments **(39)**. We would expect a superposition of powder patterns from terminal and bridging CO groups, as in $(\eta^5\text{-}C_5H_5)_2Fe_2(CO)_4$, but with a relative intensity of 5 terminal:1 bridging.

In the spectrum of $Fe_3(CO)_{12}$ at 300 K in Fig. 4, however, we see that this is not the case. There is no indication of a feature that could be attributed to the σ_{11} component of the powder pattern of the bridging CO groups, in contrast to the spectrum of $(\eta^5\text{-}C_5H_5)_2Fe_2(CO)_4$. More definitively, there is intensity over much, but not all of the range expected for terminal CO groups. The spectrum is well fit with a powder pattern of a single theoretical chemical shift tensor with an anisotropy of 327 ppm, compared to 425 ppm for $Fe(CO)_5$ **(14)**. However, the

broadening function that must be convoluted with the chemical shift powder pattern to fit the experimental spectrum is more than five times as large as that used for the other carbonyls, and is physically unreasonable.

The spectrum of the sample at 100 K is shown in Fig. 4b. Although the spike has been reduced in intensity somewhat the spectrum has not changed greatly from that of the sample at 300 K. Thus, any intramolecular rearrangement that averages the chemical shift interaction must have a small activation energy.

4. Discussion

A. Chemical Shift Tensors of Terminal CO Groups

The ^{13}C chemical shift tensors of all CO groups bound terminally in metal carbonyls are quite similar. Anisotropies lie in the range 320-440 ppm, and are large in comparison with the anisotropies of tensors for carbon nuclei in other compounds **(9)**, which are usually less than 200 ppm. Even when not required to be so by the local symmetry about the carbon nucleus, the tensors of terminally-bound CO groups are nearly axially symmetric, with asymmetry values, $(\sigma_{33} - \sigma_{22})/(\sigma_{11} - \bar{\sigma}) \lesssim 0.1$.

In order to interpret these results in terms of the bonding and electronic structure about the carbon nucleus, we first review the analysis of Mahnke, Sheline and Spiess (MSS) **(13)** for CO, $Ni(CO)_4$ and $Fe(CO)_5$. They use the conventional theoretical development **(40)** in which the chemical shift components are divided into diamagnetic and paramagnetic contributions:

$$\sigma = \sigma^{(d)} + \sigma^{(p)} \tag{4}$$

which, for axial symmetry, are given by:

$$\sigma_{11}^{(d)} = \frac{e^2}{2mc} < 0 \left| \sum_i \left(\frac{1}{r_i} - \frac{z_i^2}{r_i^3} \right) \right| 0 > \tag{5}$$

$$\sigma_{\perp}^{(d)} = \frac{e^2}{4mc} < 0 \left| \sum_i \left(\frac{1}{r_i} + \frac{z_i^2}{r_i^3} \right) \right| 0> \tag{6}$$

$$\sigma_{\parallel}^{(p)} = \frac{e^2}{mc^2} \sum_K (E_o - E_K)^{-1} < 0 \left| \sum_i L_{zi} \right| K> < K \left| \sum_i L_{zi} r_i^{-3} \right| 0> \tag{7}$$

$$\sigma_{\perp}^{(p)} = \frac{e^2}{mc^2} \sum_K (E_o - E_K)^{-1} < 0 \left| \sum_i L_{\perp i} \right| K> < K \left| \sum_i L_{\perp i} r_i^{-3} \right| 0> \tag{8}$$

where e, m and c are the electron charge, electron mass and speed of light, respectively; r_i is the length of the vector (x_i, y_i, z_i) between the electron and gauge origin, L_z and $L_\perp$ are the electron orbital angular momenta about and orthogonal to the unique axis, z, and $|0>$ and $|K>$ are the ground and an excited state of the molecule with energies E_o and E_K, respectively. The indices K and i extend over all the excited states and all the electrons of the system, respectively. The relative values of $\sigma^{(d)}$ and $\sigma^{(p)}$ depend on the choice of gauge, but their sum, σ, a physical observable, does not. However, by choosing the carbon nucleus as the gauge origin, $\sigma^{(d)}$ is dominated by the C_{1s} electrons, while the valence electrons, which dominate the bonding, largely determine $\sigma^{(p)}$. Calculations by MSS using self consistent field and semiempirical wavefunctions and Flygare's approximation of Eqs.(5) and (6) above **(41)** show that this is the case for CO, $Ni(CO)_4$ and $Fe(CO)_5$. We expect this to hold for the other metal carbonyls.

MSS point out that for CO, as for all linear molecules, $< 0|L_z|K>$ is zero (the wavefunctions are eigenfunctions of L_z and are orthogonal to each other). Therefore $\sigma_{\parallel}^{(p)}$ is zero, according to Eq. (7). Since the values of σ_{11} and $\sigma_{\parallel}^{(d)}$ for CO, $Ni(CO)_4$, and $Fe(CO)_5$ are approximately equal, $\sigma_{\parallel}^{(p)}$ must also be approximately zero for $Ni(CO)_4$ and $Fe(CO)_5$. The electron orbitals in CO are symmetric

about the C-O internuclear axis. This symmetry is not significantly reduced upon bonding CO to Ni and Fe in $Ni(CO)_4$ and $Fe(CO)_5$. In physical terms, there is free circulation of the electrons about the C-O internuclear axis. The data presented here indicate that this is a general result for CO bound terminally in metal carbonyls containing between one and six transition metal atoms.

B. Chemical Shift Tensors of Bridging CO Groups and Comparison with Organic Carbonyls

For the doubly-bridging CO groups in $(\eta^5-C_5H_5)_2Fe_2(CO)_4$ and the triply-bridging CO groups in $Rh_6(CO)_{16}$, the σ_{11} values are more negative, i.e. are shifted in the paramagnetic direction, by 182 and 266 ppm, respectively, compared to the σ_{11} values of free and terminally-bound CO. Since we expect any variation in $\sigma_{11}^{(d)}$ to be much less than this **(13)**, there is a substantial paramagnetic contribution to σ_{11} for bridging CO. Thus, the electron orbitals of bridging CO are not symmetric about the C-O internuclear axis, in contrast to those of terminally-bound CO. In physical terms, the circulation of electrons about the C-O internuclear axis is not free for bridging CO.

We note that a similar phenomenon occurs in the bonding of cyano and acetylene groups. The difference beween the σ_{11} values of HCN and CN bound terminally in a Pt compound is only 13 ppm **(42)**. Upon replacing the hydrogens of HCN or C_2H_2 with methyl groups, however, the σ_{11} values shift 40-50 ppm in the paramagnetic direction **(43-46)**.

We may also compare the chemical shift tensors of metal-bridging CO to those of organic carbonyls. Although experimental chemical shift values are not available for H_2CO, reliable theoretical calculations have been made **(47)**, and are consistent with the experimental values for CH_3CHO and $(CH_3)_2CO$ **(46)**. In addition to the principal components of the chemical shift tensor, the

calculations also provide their associated principal directions which are needed to fully define the chemical shift tensor. The association of principal values and directions for terminal and triply-bridging CO groups is unambiguous due to the axial symmetry about the C-O internuclear axis.

The chemical shift values of CO, H_2CO and the triply-bridging CO groups of $Rh_6(CO)_{16}$ are presented in Fig. 5 as a correlation diagram. Principal components along a given direction with respect to the C-O internuclear axis are connected by dashed lines. Because of the reduced symmetry in doubly-bridging CO, its principal components cannot be connected unambiguously in this diagram. It seems likely, though, that the least negative component corresponds to the chemical shift parallel to the C-O internuclear axis as in terminal and triply-bridging CO. In any case, the chemical shift components of, and therefore the bonding in, H_2CO are much different from those in free and metal-bound CO. Thus, despite the geometric similarity of doubly-bridging CO and H_2CO, and the similar CO bond distances and stretching frequencies of triply-bridging CO **(48,49)** and H_2CO **(50,51)**, the bonding in H_2CO is not a good model for the bonding of CO to metals.

C. Variations in Chemical Shift with Transition Metal

Variations in the ^{13}C chemical shift tensors among the carbonyls of different transition metals are most clearly demonstrated through the $\sigma_\perp$ values, as shown in Fig. 6. Although the error in any particular measurement is relatively large, two trends are evident: decreasingly paramagnetic values of $\sigma_\perp$ both in going across and down in the transition series. We also note that there are values both above and below the value of $\sigma_\perp$ for free CO. To explain these trends, we again review the analysis due to MSS.

As with the σ_{11} component, variations in $\sigma_\perp$ are due primarily to variations in the paramagnetic term. In free CO, there is only one low-lying excited state of the proper symmetry to contribute to $\sigma_\perp^{(p)}$. In a molecular orbital formalism, this excited state is formed from the ground state by promoting an electron from the 5σ to the 2π orbital. MSS argue that to the extent that the 2π orbital is stabilized by backbonding from the d orbitals of the metal, the $5\sigma \rightarrow 2\pi$ excitation energy will be lowered and the paramagnetic contribution to $\sigma_\perp$ will be increased. Based on the increasingly paramagnetic shifting of $\sigma_\perp$ observed in the series CO ~ $Ni(CO)_4$ < $Fe(CO)_5$, they conclude that π-backbonding is significant in $Fe(CO)_5$ but much less so in $Ni(CO)_4$.

In contradiction to the above analysis, however, the 2π orbital would be destabilized, not stabilized, through interaction with filled d orbitals. It would be better to think of the metal d orbitals, which are intermediate in energy between the 5σ and 2π orbitals of CO, as stabilizing the excited state formed from the $5\sigma \rightarrow 2\pi$ transition. The excitation energy would thus be lowered and the paramagnetic contribution to $\sigma_\perp^{(p)}$ would be increased by the presence of the d orbitals, as is observed for $Fe(CO)_5$.

This stabilization of the excited state would decrease as the d energy level decreases. Photoelectron spectra of carbonyls containing one **(1,2,52)** and more than one **(53,54)** metal atom indicate that the d energy levels generally decrease with increasing atomic number of the metal within a row or column. Therefore, the above arguments may be used to explain the decreasely paramagnetic value of $\sigma_\perp$ that is observed for increasing atomic number of the metal for the carbonyls in general. Since lower d levels would also lead to increased σ bonding and decreased π bonding, the $\sigma_\perp$ values, and thus the σ values for terminal CO, may be related to these fundamental properties, as concluded by MSS. The chemical shift may also be correlated with other properties that are determined

by the extent of σ and π bonding such as metal-CO bond energies and CO and metal-C stretching force constants.

Although the variation in $\sigma_\perp$ among the transition metals was explained by differences in the stabilization of the excited state formed from a $5\sigma \rightarrow 2\pi$ transition, this is highly simplified. In metal carbonyls, the metal and CO orbitals are mixed and form a new set of orbitals based on the particular molecular symmetry. There are then many excited states that contribute to $\sigma_\perp$. In addition, it is not obvious to what extent the matrix elements $<0|L_\parallel|K>$ and $<K|L_\perp/r^3|0>$ change upon bonding CO to a metal or among the various metal carbonyls.

The simplified approach of effectively considering the bonding to the metal as a perturbation of the bonding in CO is supported by the small magnitude of the trend to be explained. In addition, the trend holds in the cases where there is no change in molecular symmetry: for $M(CO)_6$, where M = Cr, Mo and W, and for $Ru_3(CO)_{12}$ and $Os_3(CO)_{12}$. Also, calculations show that the largely metal-derived orbitals contribute $\lesssim$ 5 ppm to the chemical shift values of $Cr(CO)_6$ and $W(CO)_6$ **(55)**. However, by considering only the stabilization of the excited state from a $5\sigma \rightarrow 2\pi$ transition by the metal d orbitals, $\sigma_\perp$ of metal-bound CO is always predicted to be more paramagnetic than $\sigma_\perp$ of free CO. However, the $\sigma_\perp$ values of $Os_3(CO)_{12}$, $Rh_6(CO)_{16}$ and $Ir_4(CO)_{12}$ are less paramagnetic than that of free CO. Thus, a more sophisticated analysis is necessary to relate the $\sigma_\perp$ values of metal carbonyls to that of free CO to determine the extent of π backbonding in the metal carbonyls.

D. Intramolecular Rearrangements of Metal Carbonyls in the Solid State

A final aspect that we would like to consider is that of intramolecular rearrangements in the metal carbonyls. Of the carbonyls studied here, only in $Fe_3(CO)_{12}$ is the chemical shift interaction motionally averaged. In previous

studies, $Fe(CO)_5$, but neither $Ni(CO)_4$ **(14)** nor $Rh_2(CO)_4Cl_2$ **(24)**, was shown to be undergoing intramolecular rearrangement. Most rearrangements would change the angle of the external field with respect to the C-O internuclear axis, averaging the chemical shift interaction and narrowing the spectrum. Thus, there is little intramolecular rearrangement of the metal carbonyls in the solid state, in contrast to those of dissolved carbonyls containing one **(8)** and more than one **(6,7)** metal atoms. This is probably the result of intermolecular packing forces in the crystal lattice.

An example of a rearrangement that cannot be taking place in the carbonyls in the present study, ignoring $Fe_3(CO)_{12}$ for the moment, at rates $\gtrsim$ 10 kHz, is twisting of three or four CO groups with respect to the rest of the molecule, e.g.:

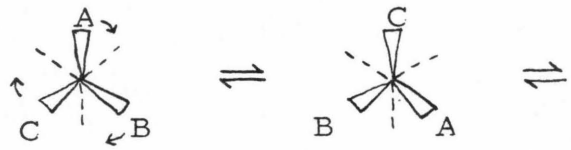

Other examples would include most exchanges of CO groups among metal atoms in which the CO groups change from terminal to bridging positions or vice versa in the intermediate or transition state, e.g.:

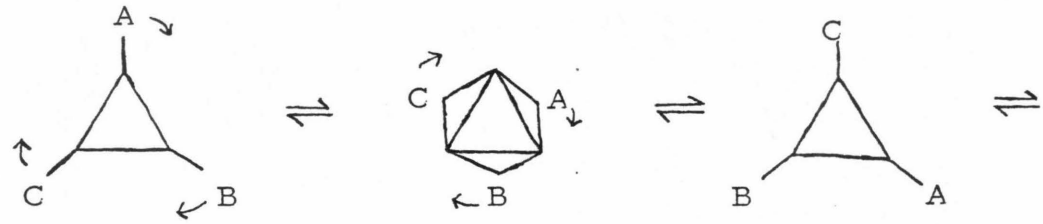

A mechanism that would not affect the NMR spectrum would be cycling of the axial CO groups on one side of the Ru_3 triangle in $Ru_3(CO)_{12}$:

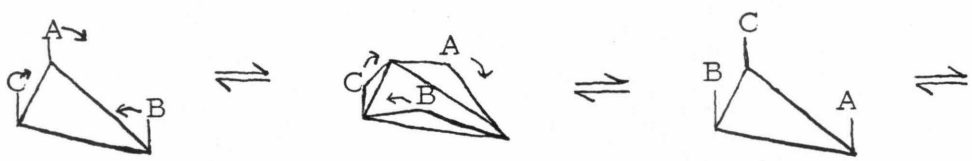

However, in only one metal carbonyl, $[(\eta^5-C_5H_5)RhCO]_3$, has a similar mechanism been clearly demonstrated **(56)**.

The final class of rearrangements that will be discussed involves motion of the metal cluster within the "shell" formed by the CO groups **(57)**. In the liquid state, it is difficult to distinguish this mechanism from the above types in which some CO groups move with respect to the rest of the molecule since both redistribute CO groups among the various sites of the molecule. Motion of the metal cluster within the CO shell, though, would leave the spectrum of the solid relatively broad, whereas the other mechanisms would lead to substantial narrowing. Even the partial narrowing expected in the former case would be enough to discount it from occurring in most of the metal carbonyls, with the exception of $Fe_3(CO)_{12}$.

In $Fe_3(CO)_{12}$, rotation of the Fe_3 cluster would exchange CO groups among terminal and bridging positions. The weak temperature dependence of the powder pattern indicates that the rate of rearrangement is at least comparable to the linewidth. In the fast exchange limit, this mechanism would not change $\sigma_\perp$ substantially, but the value of σ_{11} observed would become $\sim [5(+70) - 179]/6 = +28$ ppm, based on the chemical shift values of $Fe(CO)_5$ and the bridging CO groups of $(\eta^5-C_5H_5)_2Fe_2(CO)_4$. Small librational motions and deviations from idealized symmetry (C_{2v} for the molecule, icosahedral for the carbonyl shell) would result in further narrowing of the spectrum and smoothing of the shoulders, consistent with the observed spectrum. This mechanism is further supported by the fact that the Fe-Fe distances may either expand or remain the same during the reorientation of the Fe_3 cluster with little or no change in the positions of the CO groups **(57)**. Intermolecular interactions which would be expected to hinder CO motion in the solid state would have little effect on this mechanism. A crucial test of this mechanism would be motional narrowing of the ^{57}Fe NMR

spectrum.

5. Conclusions

From measurements of the principal components of the ^{13}C NMR chemical shift tensors of a series of metal carbonyls, we find that:

1. The chemical shift tensors of CO groups bound terminally in metal carbonyls are highly anisotropic (380 ± 60 ppm) and axially symmetric. They vary only slightly with the transition metal. The electron orbitals are symmetric about the C-O internuclear axis.

2. The tensors of CO groups that bridge two or more metal atoms are much less anisotropic due to significant asymmetry in the electron orbitals about the C-O internuclear axis. This suggests that there is a greater perturbation of the electronic structure of CO in bridged than in terminal bonding to a metal. However, the bonding in metal-bridging CO is distinct from that in organic carbonyls, which is not apparent from a consideration of isotropic chemical shifts or vibrational frequencies.

3. There is little or no intramolecular rearrangement of the metal carbonyls in the solid state at frequencies greater than 10 kHz, except in $Fe_3(CO)_{12}$.

We have seen that it is possible to draw conclusions about the bonding and electronic structure of metal carbonyls from chemical shift measurements. To put these on a quantitative basis requires wavefunctions and energies of the ground and excited states that are more accurate than those presently available for metal carbonyls. The present results also serve as important references for interpreting ^{13}C NMR spectra of CO that is adsorbed or that has reacted on metal surfaces **(24)**. In particular, terminal and bridging CO should be easily distinguishable from each other and from CO that has reacted with hydrogen or

some organic group, based on their chemical shift powder patterns and/or isotropic chemical shifts.

Acknowledgments

This study was supported by the Office of Naval Research under contracts N000014-77-F-0008 and N000014-79-F-0014. Helpful comments were offered by Drs. W. H. Weinberg, T. M. Duncan, W. A. Goddard and S. I. Chan.

References

1. E.g., see A. H. Crowley, Prog. Inorg. Chem. **26**, 45 (1979).

2. P. S. Braterman, *Metal Carbonyl Spectra* (Academic, New York, 1975).

3. O. A. Gansow and W. D. Vernon, in *Topics in Carbon-13 NMR Spectroscopy*, edited by G. C. Levy, (Wiley-Interscience, New York, 1976), Vol. 2, Ch. 5.

4. B. E. Mann, Advan. Organometal. Chem. **12**, 135 (1974).

5. A. F. Schreiner and T. L. Brown, J. Am. Chem. Soc. **90**, 3366 (1968).

6. E. Band and E. L. Muetterties, Chem. Rev. **78**, 639 (1978).

7. J. Evans, Advan. Organometal. Chem. **16**, 319 (1977).

8. R. D. Adams and F. A. Cotton, in *Dynamic NMR Spectroscopy*, edited by L. M. Jackman and F. A. Cotton, (Academic Press, New York, 1975), Ch. 12.

9. M. Mehring, *High Resolution NMR Spectroscopy in Solids*, Vol. 11 of *NMR: Basic Principles and Progress* (Springer, New York, 1976).

10. U. Haeberlen, *High Resolution NMR in Solids: Selective Averaging*, Advan. Magn. Reson. Suppl. 1 (Academic, New York, 1976).

11. R. W. Vaughan, Ann. Rev. Phys. Chem. **29**, 397 (1978).

12. H. W. Spiess, Chem. Phys. **6**, 217 (1974).

13. H. Mahnke, R. K. Sheline and H. W. Spiess, J. Chem. Phys. **61**, 55 (1974).

14. F. A. Cotton, A. Danti, J. S. Waugh and R. W. Fessenden, J. Chem. Phys. **29**, 1427 (1958).

15. R. Bramley, B. N. Figgis and R. S. Nyholm, Trans. Faraday Soc. **58**, 1893 (1962).

16. R. W. Vaughan, D. D. Elleman, L. M. Stacy, W. K. Rhim and J. W. Lee, Rev. Sci.

Instrum. **43**, 1356 (1972).

17. M. E. Stoll, A. J. Vega and R. W. Vaughan, Rev. Sci. Instrum. **48**, 800 (1977).

18. L. O. Brockway, R. V. G. Ewens, and M. W. Lister, Trans. Farad. Soc. **34**, 1350 (1938).

19. O. A. Gansow, B. Y. Kimura, G. R. Dobson and R. A. Brown, J. Am. Chem. Soc. **93**, 5922 (1971).

20. B. E. Mann, J. Chem. Soc., Chem. Commun. 1173 (1971).

21. P. C. Lauterbur and R. B. King, J. Amer. Chem. Soc. **87**, 3266 (1965).

22. P. Chini, S. Martinengo, D. J. A. McCaffrey and B. T. Heaton, J. Chem. Soc., Chem. Commun. 310 (1974).

23. T. M. Duncan, J. T. Yates, Jr. and R. W. Vaughan, J. Chem. Phys. **73**, 975 (1980).

24. A. A. V. Gibson, T. A. Scott and E. Fukushima, J. Magn. Reson. **27**, 29 (1977).

25. K. Jackowski and W. T. Raynes, Mol. Phys. **34**, 465 (1977).

26. R. Mason and A. I. M. Rae, J. Chem. Soc (A), 778 (1968).

27. E. R. Corey and L. F. Dahl, Inorg. Chem. **1**, 521 (1962).

28. S. H. H. Chaston and F. G. A. Stone, J. Chem. Soc. (A), 500 (1969).

29. A. Forster, B. F. G. Johnson, J. Lewis, T. W. Matheson, B. H. Robinson and W. G. Jackson, J. Chem. Soc., Chem. Commun., 1042 (1974).

30. E. R. Corey, L. F. Dahl and W. Beck, J. Am. Chem. Soc. **85**, 1202 (1963).

31. B. T. Heaton, A. D. C. Towl, P. Chini, A. Fumagilli, D. J. A. McCaffrey and S. Martinengo, J. Chem. Soc., Chem. Commun., 523 (1975).

32. O. S. Mills, Acta Crystallogr. **11**, 620 (1958).

33. R. F. Bryan, P. T. Greene, D. S. Field and M. J. Newlands, J. Chem. Soc., Chem. Commun., 1477 (1969).

34. R. F. Bryan and P. T. Greene, J. Chem. Soc. (A), 3064 (1970).

35. O. A. Gansow, A. R. Burke and W. D. Vernon, J. Am. Chem. Soc. **94**, 2550 (1972).

36. D. C. Harris, E. Rosenberg and J. D. Roberts, J. Chem. Soc., Dalton Trans., 2399 (1974).

37. R. D. Adams and F. A. Cotton, J. Am. Chem. Soc. **95**, 6589 (1973).

38. F. A. Cotton and J. M. Troup, J. Am. Chem. Soc. **96**, 4159 (1974).

39. N. F. Ramsey, Phys. Rev. **86**, 243 (1952); **78**, 699 (1950).

40. W. H. Flygare and J. Goodisman, J. Chem. Phys. **49**, 2314 (1968).

41. M. E. Stoll, R. W. Vaughan, R. B. Saillant and T. Cole, J. Chem. Phys. **61**, 2896 (1974).

42. F. Millett and B. P. Dailey, J. Chem. Phys. **54**, 5434 (1971).

43. S. Mohanty, Chem. Phys. Lett. **18**, 581 (1973).

44. S. Kaplan, A. Pines, R. G. Griffin and J. S. Waugh, Chem. Phys. Lett. **25**, 78 (1974).

45. A. Pines, M. G. Gibby and J. S. Waugh, Chem. Phys. Lett. **15**, 373 (1972).

46. R. Ditchfield, quoted in B. R. Appleman and B. P. Dailey, Advan. Magn. Reson. **7**, 231 (1974).

47. P. Chini, G. Longoni and V. G. Albano, Advan. Organometal. Chem. **14**, 285 (1976), and references therein.

48. F. A. Cotton and G. Wilkinson, *Advanced Inorganic Chemistry*, (Wiley-Interscience, New York, 1972), 3rd ed., p. 693.

49. R. B. Lawrence and M. W. P. Strandberg, Phys. Rev. **83**, 363 (1951).

50. E. S. Ebers and H. H. Nielsen, J. Chem. Phys. **6**, 311 (1938).

51. C. Furlani and C. Cauletti, in *Structure and Bonding 35: New Theoretical Aspects*, edited by J. D. Dunitz et al. (Springer-Verlag, New York, 1978), p. 119.

52. E. W. Plummer, W. R. Salaneck and J. S. Miller, Phys. Rev. B **18**, 1673 (1978).

53. J. C. Green, E. A. Seddon and D. M. P. Mingos, J. Chem. Soc., Chem. Commun. **94** (1979).

54. D. Cozak and S. Butler, Can. J. Chem. **55**, 4056 (1977).

55. R. J. Lawson and J. R. Shapley, J. Am. Chem. Soc. **98**, 7433 (1976).

56. B. F. G. Johnson, J. Chem. Soc., Chem. Commun., 703 (1976).

Table 1

Principal Components, Isotropic Values and Anisotropies of the ^{13}C NMR Chemical Shift Tensors of Metal Carbonyls[a,b]

	σ_{11}	σ_{22}	σ_{33}	$\bar{\sigma}_{solid}$[c]	$\bar{\sigma}_{soln}$	$\Delta\sigma$	Ref. ($\bar{\sigma}_{soln}$)
$Cr(CO)_6$	+70	-353	-353		-212	423	20
$Mo(CO)_6$	+75	-343	-343	-203	-202	417	20
$W(CO)_6$	+71	-324	-324		-192	395	20
$Ru_3(CO)_{12}$	+63	-319	-348	-201	-200	397	30
$Os_3(CO)_{12}$	+55	-292	-292		-176	347	30
$Ir_4(CO)_{12}$	+53	-277	-277	-167		322	
$Rh_6(CO)_{16}$							
terminal	+80	-305	-315		-181	390	32
bridging	-102	-296	-296		-231	194	
$(\eta^5\text{-}C_5H_5)_2Fe_2(CO)_4$							
terminal	+85	-354	-354		-211	444	
bridging	-179	-309	-328		-272	138	36,37
$Fe_3(CO)_{12}$	+6	-316	-325		-212	327	30,36
CO	+90[d]	-316[d]	-316[d]		-181	406	26
$Ni(CO)_4$[e]	+69	-326	-326	-194	-191	395	21
$Fe(CO)_5$[e]	+70	-355	-355	-213	-212	425	22
$Rh_2(CO)_4Cl_2$[f]	+99	-299	-306	-186	-180	402	23

(a) Values are in ppm, relative to TMS.
(b) Uncertainties are ±15 ppm for the components and ±30 ppm for the anisotropies.
(c) Where values of $\bar{\sigma}$ are not listed, they are assumed to be equal to $\bar{\sigma}_{soln}$ (see text).
(d) Calculated using the estimate for $\Delta\sigma$ in the absence of motional averaging **(25)**.
(e) Ref. **(14)**.
(f) Ref. **(24)**.

Figure Captions

Figure 1: ^{13}C NMR spectrum of polycrystalline $Mo(CO)_6$ at 300 K. The solid line is a fit of a theoretical chemical shift powder pattern to the experimental points. The principal components of the chemical shift tensor are indicated, along with the isotropic chemical shift. The separation between points is 4 ppm.

Figure 2: ^{13}C NMR spectrum of polycrystalline $Ru_3(CO)_{12}$ at 300 K. The theoretical fit (solid line) is for a single chemical shift powder pattern.

Figure 3: ^{13}C NMR spectra of polycrystalline: *(a)* $Rh_6(CO)_{16}$ and *(b)* $(\eta^5-C_5H_5)_2Fe_2(CO)_4$ at 300 K. The spectra were deconvoluted as described in the text into the contributions from the terminal (---) and bridging (···) CO groups in each compound.

Figure 4: ^{13}C NMR spectra of $Fe_3(CO)_{12}$ at: *(a)* 300 K and *(b)* 100 K. The principal components for $Fe(CO)_5$ are indicated. While there is considerable spectral intensity near $\sigma_\perp$, there is little intensity near σ_{11} at both temperatures.

Figure 5: Principal components of the chemical shift tensor for various types of CO bonding. Components associated with the same direction of the external magnetic field, H_o, with respect to the C-O internuclear axis are connected by dashed lines. The components for the triply-bridging CO groups in $Rh_6(CO)_{16}$ are connected in the diagram. The components of the doubly-bridging CO groups in $(\eta^5-C_5H_5)_2Fe_2(CO)_4$ (···) cannot be associated with directions unambiguously from the powder patterns alone and are not connected.

Figure 6: Values of the $\sigma_\perp$ components of terminally-bound CO in metal carbonyls taken from Table 1. In cases of nonaxial symmetry, the value

of $(\sigma_{22} + \sigma_{33})/2$ was used. The value for Fe is that of $Fe(CO)_5$. The trend to lower magnitude of $\sigma_\perp$ with increasing atomic number across and down the transition metals is evident.

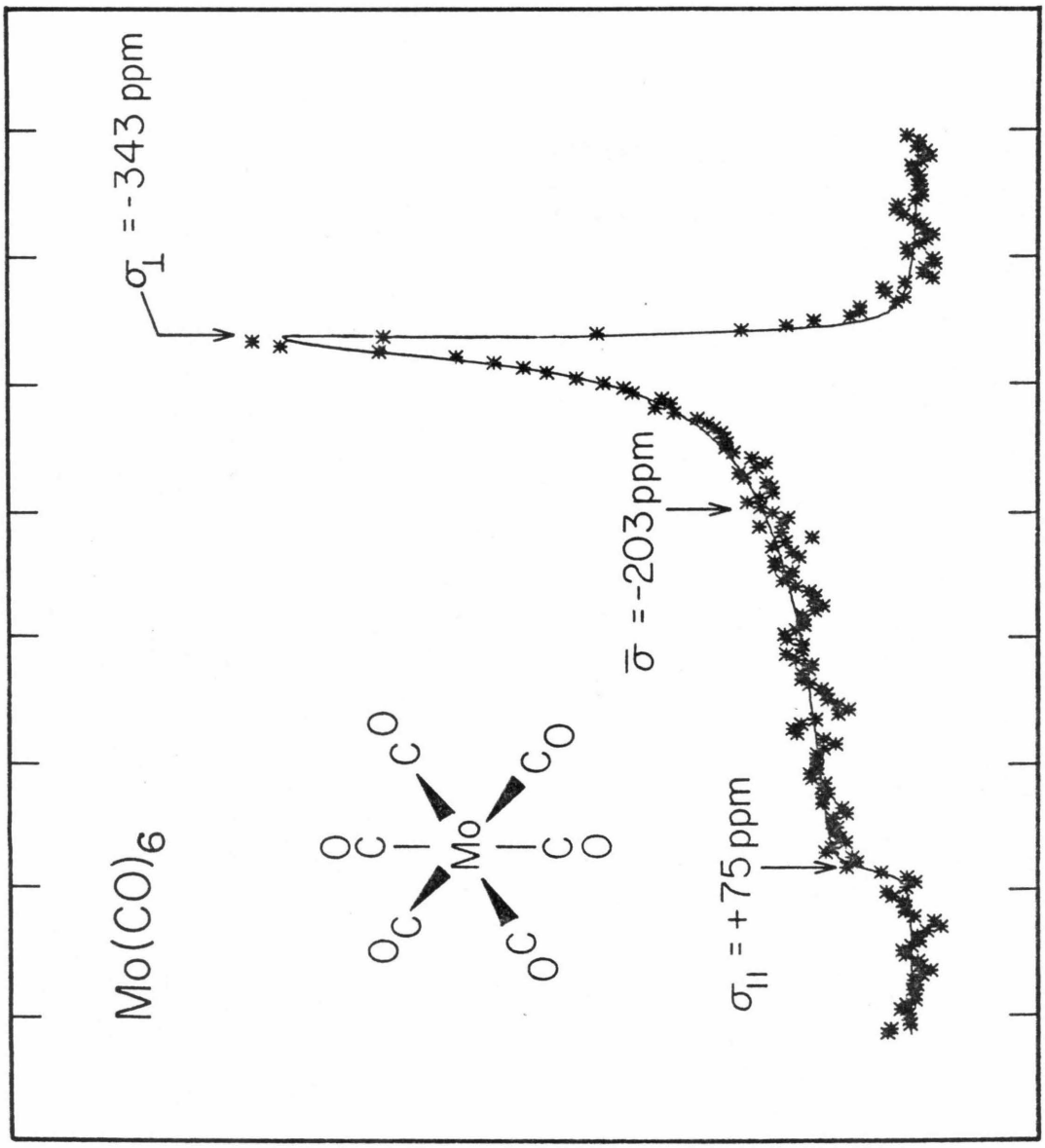
Mo(CO)6
σ⊥ = -343 ppm
σ̄ = -203 ppm
σ∥ = +75 ppm
+200
0
-200
-400
σ, (ppm), RELATIVE TO TMS
Mo
C
O

Figure 1

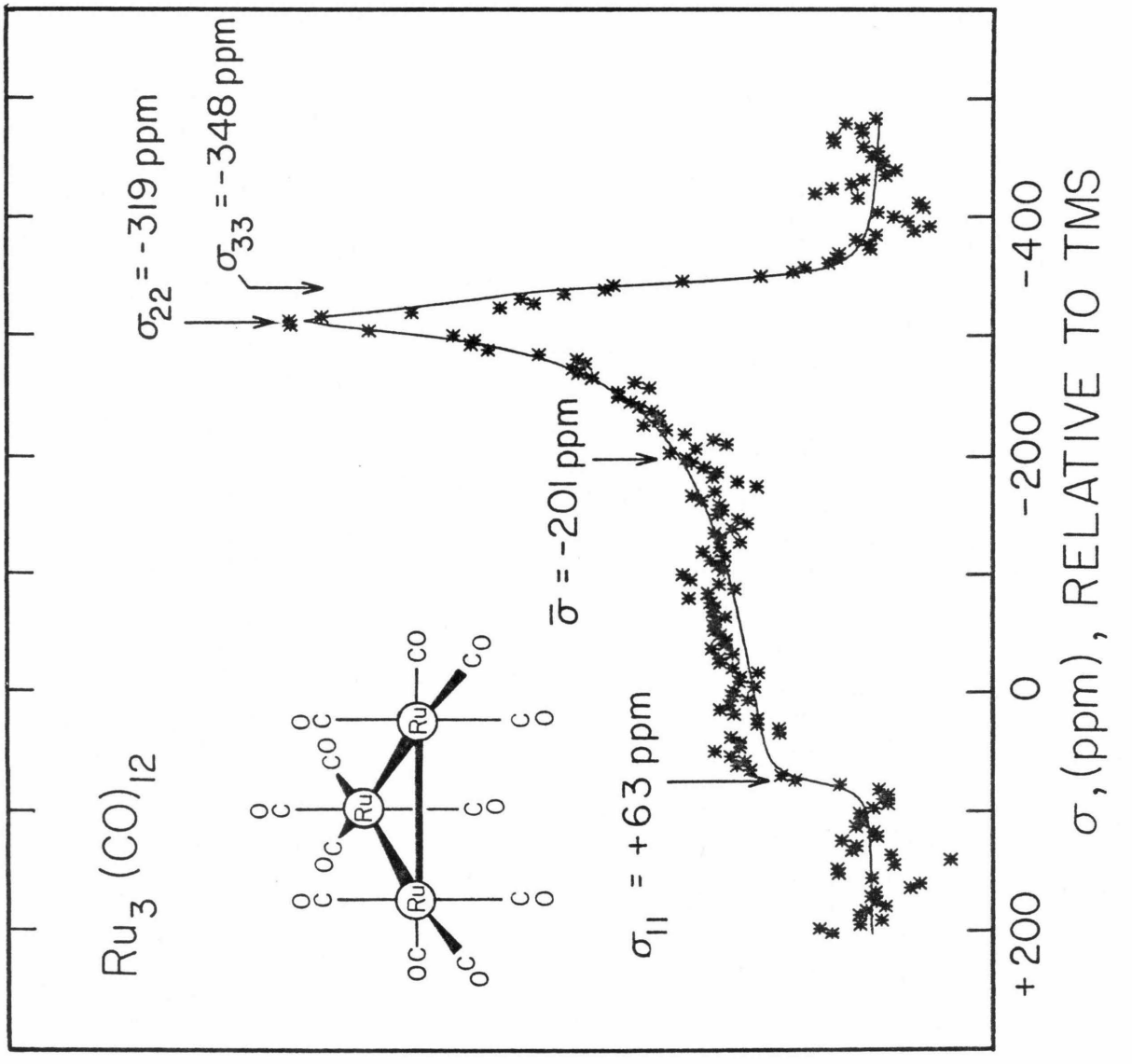
$Ru_3(CO)_{12}$
σ_{22} = -319 ppm
σ_{33} = -348 ppm
$\bar{\sigma}$ = -201 ppm
σ_{11} = +63 ppm
+200
0
-200
-400
σ,(ppm), RELATIVE TO TMS

Figure 2

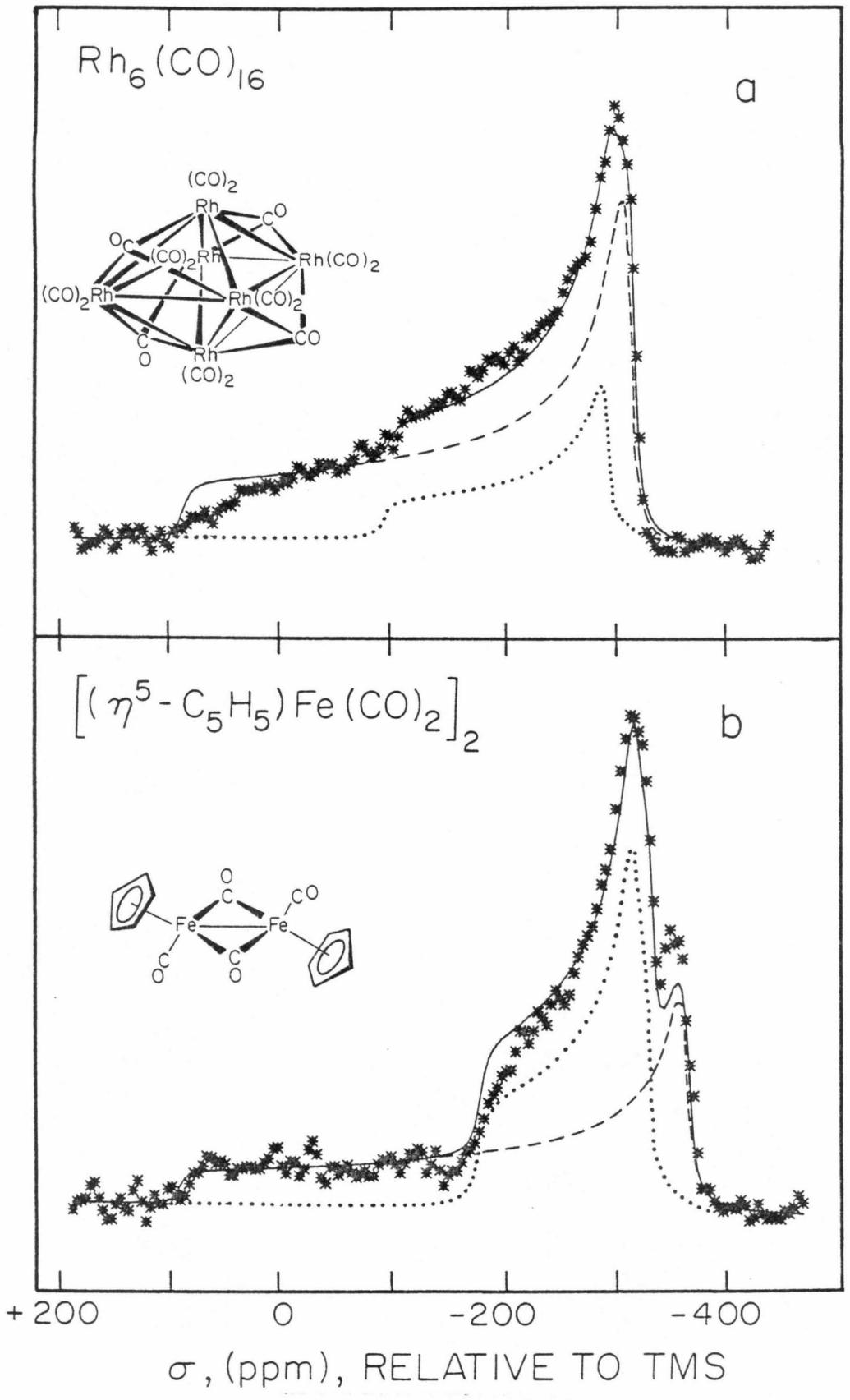
$Rh_6(CO)_{16}$
a
$[(\eta^5-C_5H_5)Fe(CO)_2]_2$
b
+200
0
-200
-400
σ, (ppm), RELATIVE TO TMS

Figure 3

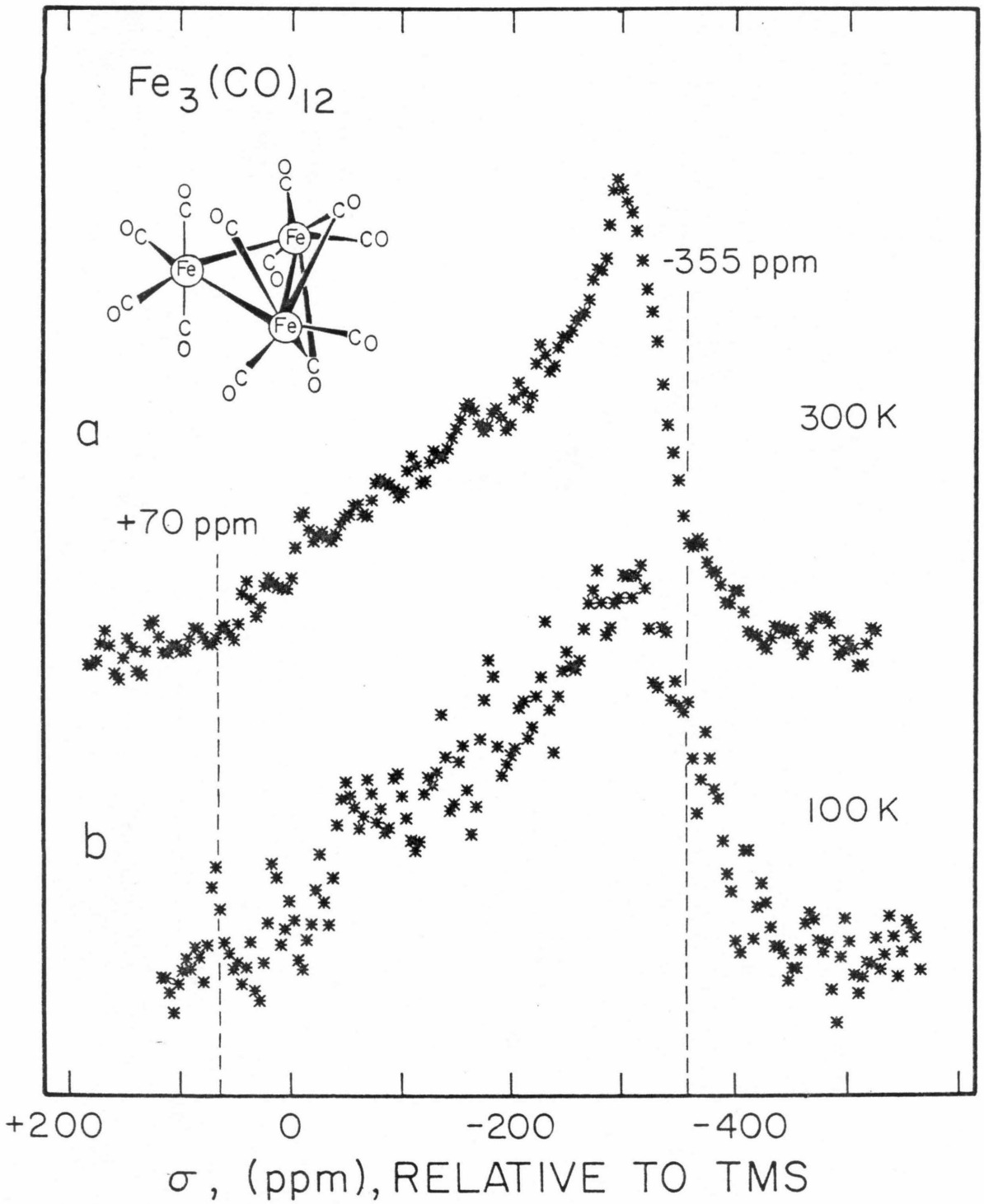
$Fe_3(CO)_{12}$
-355 ppm
300 K
a
+70 ppm
100 K
b
+200
0
-200
-400
σ, (ppm), RELATIVE TO TMS

Figure 4

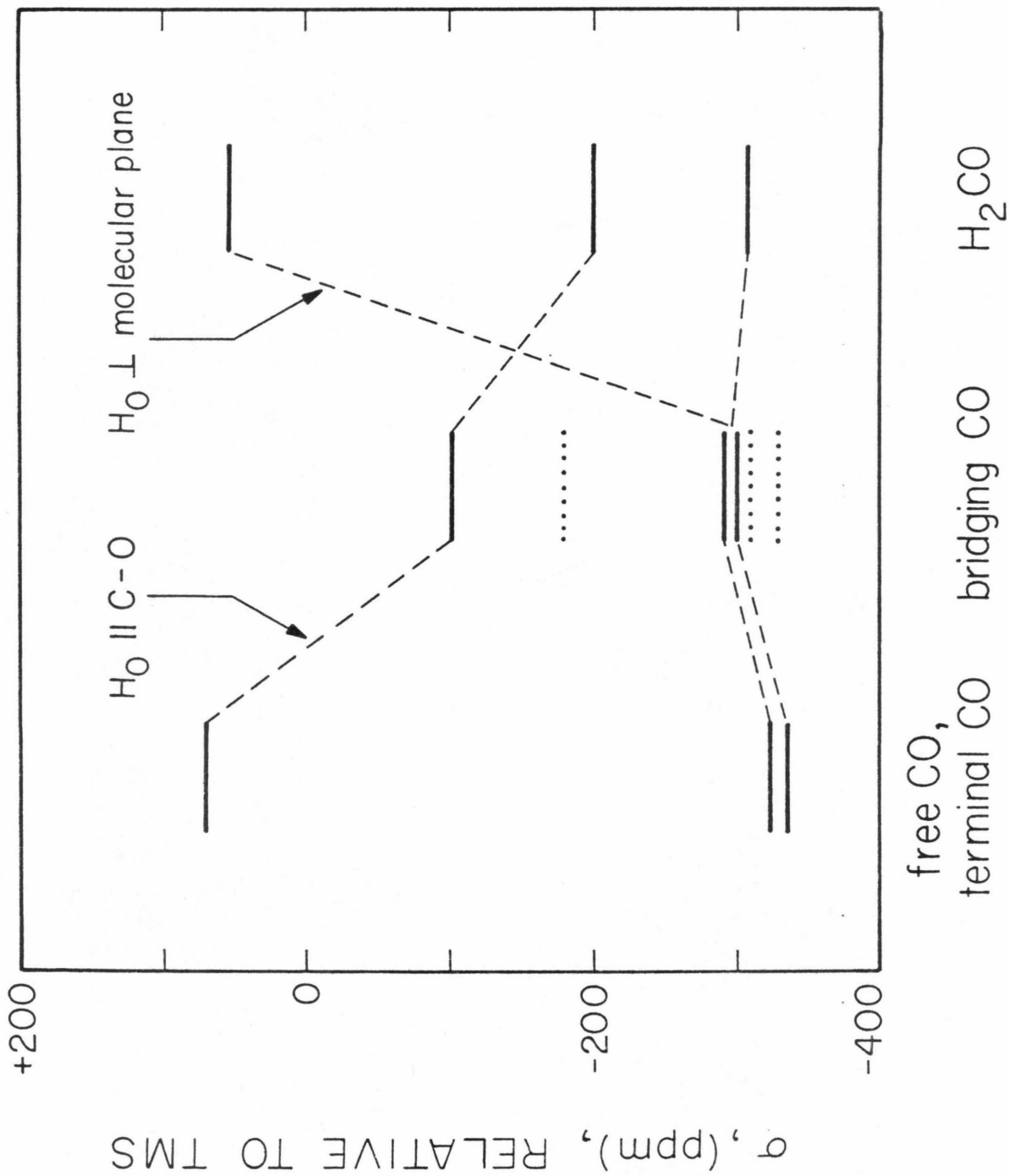
+200
0
-200
-400
σ, (ppm), RELATIVE TO TMS
H0 ∥ C-O
H0 ⊥ molecular plane
free CO,
terminal CO
bridging CO
H2CO

Figure 5

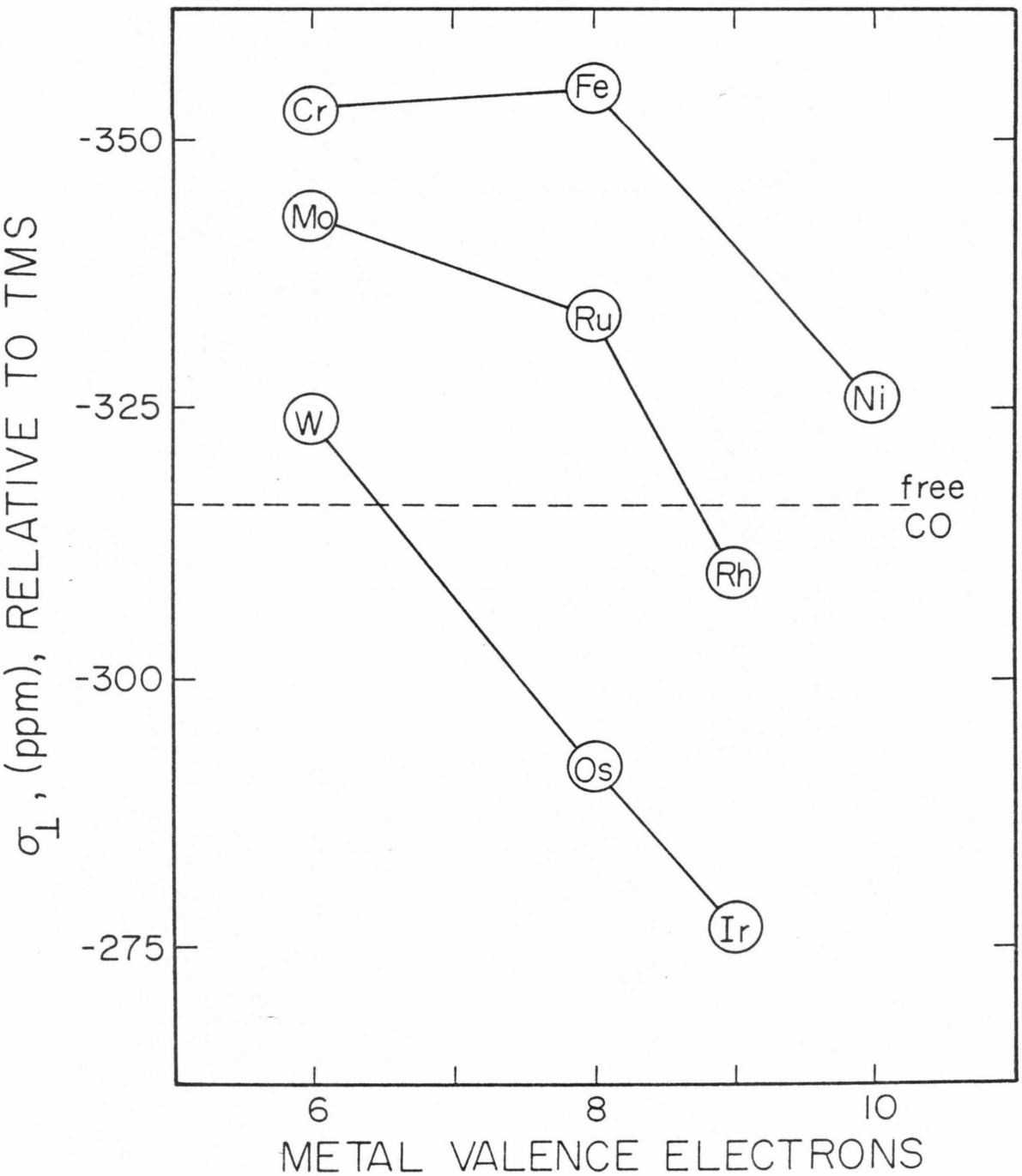
Cr
Fe
Mo
Ru
Ni
W
free
CO
Rh
Os
Ir
-350
-325
-300
-275
$\sigma_\perp$, (ppm), RELATIVE TO TMS
6
8
10
METAL VALENCE ELECTRONS

Figure 6

Part II:

Surface Chemistry of Rhodium Supported on Alumina

Chapter 3:

Introduction

In Part I of this thesis, an example of the use of NMR spectroscopy in elucidating some details of the bonding in a metal complex was presented. An important application of such knowledge is in understanding the functioning of metal catalysts, since the catalytic properties of the metal are determined largely by how they bind the reactants at their surfaces. Of course, it would be more relevant to study the surface-adsorbed species itself.

This is a difficult task. The proposed form of the adsorbed species, which is a reaction intermediate, must be consistent with the kinetics of the overall reaction, though the kinetics rarely, if ever, imply a specific intermediate. More definitive are experiments in which the reactants are isotopically labelled and the distribution of the label in the product determined (1). For example, in a recent study of methanol synthesis from CO and H_2 over rhodium supported on titania, $^{13}C^{16}O$ and $^{12}C^{18}O$ were used as reactants and the major products were $^{13}CH_3{}^{16}OH$ and $^{12}CH_3{}^{18}OH$ (2). The absence of scrambling of the labels implies that the carbon and oxygen atoms bound in the methanol must have been bound to each other in all the intermediate steps of the reaction. However, the exact nature of the reaction intermediates is still not known.

It is desirable to observe the reaction intermediate directly, such as by spectroscopic means. Unfortunately, as remarked in Chapter 1, the application in studies of surface species of most of the physical methods used in characterizing molecular metal complexes is hindered by insufficient sensitivity or by particular characteristics of the catalyst material. By far the most widely used spectroscopic method in studies of species adsorbed on supported metals has been infrared

spectroscopy (3-5). A given functional group often has characteristic vibrational frequencies that are resolvable from those of other functional groups and thus can be used to identify the species. Often, more specific information can be obtained. For example, if a surface hydroxyl group is involved in hydrogen bonding can be determined by the frequency of its OH stretching mode (3,4). A drawback of infrared spectroscopy is that the intensities of the peaks in a spectrum often cannot be related to the concentration of the species responsible for that peak (3). Thus, it is highly beneficial to have an independent means of quantifying the effects seen in the infrared spectrum, such as through mass balances or by another spectroscopic technique, such as NMR (6).

In Part II of this thesis, the surface chemistry of rhodium supported on alumina is studied using infrared spectroscopy and quantitative measurements of the gases taken up by and evolved from the samples during the various procedures. Supported Rh is an especially active catalyst for olefin hydrogenation (7,8) and is also active for hydrogenation of CO to methane (9) and oxygenated hydrocarbons (10), reduction of NO, and oxidation of CO (11). Supported Rh is unusual in binding two CO (or NO (12,13)) groups to a single Rh atom (9), in addition to binding CO in linear and bridging modes on clustered Rh, similarly to other Group VIII transition metals (14). These sites are distinguishable using infrared spectroscopy (9).

In the first study, the changes in these three CO adsorption sites upon heating in CO, CO_2, and H_2 will be examined. In another study, the interaction of H_2S, a common catalyst poison, with Rh/alumina is examined. Supported Rh was shown to be especially resistant to poisoning

by SO_2 (11), and it is of interest to determine if this is related to its unusual surface chemistry. The effect of H_2S on the reactivity of adsorbed CO toward $CO_{(g)}$ and O_2 is also examined.

References

1. A. Ozaki, Isotopic Studies of Heterogeneous Catalysts, Academic Press, New York, 1977.
2. A. Takeuchi and J. R. Katzer, J. Phys. Chem. 85, 937 (1981).
3. L. H. Little, Infrared Spectra of Adsorbed Species, Academic Press, New York, 1966.
4. M. L. Hair, Infrared Spectroscopy in Surface Chemistry, Dekker, New York, 1967.
5. G. L. Haller, in Spectroscopy in Heterogeneous Catalysis, p. 19, Academic Press, New York, 1979.
6. T. M. Duncan, J. T. Yates, Jr. and R. W. Vaughan, J. Chem. Phys. 73, 975 (1980).
7. G. C. A. Schmit and L. L. Van Reijen, Advan. Catal. 10, 61 (1945).
8. O. Beeck, Rev. Mod. Phys. 17, 61 (1945).
9. A. C. Yang and C. W. Garland, J. Phys. Chem. 61, 1504 (1957).
10. P. C. Ellgen, W. J. Bartley, M. M. Bhasin and T. P. Wilson, in Hydrocarbon Synthesis from CO and Hydrogen, E.L.Kugler, ed., p. 147, Academic Press, New York, 1979.
11. J. C. Summers and K. J. Baron, J. Catal. 57, 380 (1979).
12. H. Arai and H. Tominaga, J. Catal. 43, 131 (1976).
13. H. C. Yao, S. Japar and M. Shelef, J. Catal. 50, 407 (1977).
14. N. Sheppard and T. T. Nguyen, Advan. Infrared Raman Spectr. 5, 67 (1978).

Chapter 4:

"Deactivation of CO Adsorption Sites upon Heating Rh/Alumina in CO, CO_2, H_2 and O_2"

Abstract

The behavior of alumina-supported Rh upon heating in the presence of CO, CO_2, O_2 and H_2 was studied using infrared spectroscopy and quantitative measurements of the gases taken up and evolved during various procedures. The loss in the capacity to adsorb CO after heating to 525 K increases in the order O_2, H_2 vacuum < CO_2 < CO. Upon heating in CO, some CO is oxidized to CO_2 with oxygen from the surface, while the dicarbonyl-forming Rh^I is reduced to Rh^0. The Rh^0 agglomerates, accounting for the substantial loss in capacity to adsorb CO. Upon heating in CO_2, the dicarbonyl-forming Rh^I is also deactivated. There is little loss in capacity to adsorb CO after heating in H_2, O_2 or vacuum.

1. Introduction

There has been much interest in the fundamental interactions of small molecules on supported Rh. In a classic infrared study of CO on alumina-supported Rh, Yang and Garland **(1)** identified three modes of adsorption:

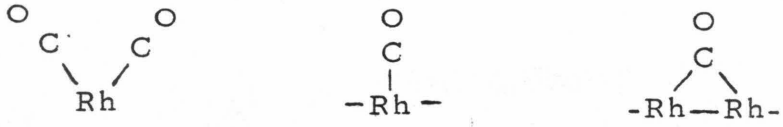

which we will refer to, respectively, as dicarbonyl, linear and bridged. The linear and bridged modes occur on two- or three-dimensional Rh clusters, and are common to most other supported and unsupported Group VIII transition metals **(2)**. Only on supported Rh, Ru **(3)** and Os **(4-6)** has CO been shown to adsorb in the dicarbonyl mode. The Rh dicarbonyl appears to be isolated from the clustered Rh **(7-10)**, though this is still controversial **(11)**.

The oxidation state of the dicarbonyl Rh also appears to differ from that of the clustered Rh. Whereas the clustered Rh is almost surely Rh^0, several studies suggest that the dicarbonyl Rh is Rh^I (Rh^{1+}).

The intensities of the infrared bands of the dicarbonyl are not changed by treatment of alumina-supported Rh with O_2 at 300 K either before or after exposure to CO or even by treatment with O_2 at 473 K before exposure to CO. This suggests that the dicarbonyl Rh may be oxidized to some extent. However, the bands are lower in frequency than those of CO in Rh^{III} complexes **(1,10,13)**. Alumina-supported $Rh_6(CO)_{16}$ that had been treated under vacuum or with H_2 above 425 K, a procedure that produces a surface that is similar to that obtained by reducing an alumina-supported Rh salt **(14)**, has been studied using X-ray photoelectron spectroscopy **(15)**. The results are consistent with the existence of Rh^0 and/or Rh^I species, but not Rh^{II} or Rh^{III} species. The absence of strong ESR signals **(9,16,18)** and the linewidth of ^{13}C NMR spectra **(9)** from

Rh/alumina with adsorbed CO indicate that there are few unpaired electrons. Thus, there can be few magnetically isolated dicarbonyls containing Rh^{II} or Rh^{0}. We note that the Os species that forms supported di- and tri-carbonyls is also oxidized (Os^{II}) **(4,18)**. The dicarbonyl of Ru, the only other metal shown to form a supported multicarbonyl species, is probably oxidized also, since its infrared bands are very similar in frequency to those of the Os^{II} dicarbonyl **(3)**. However, the results of temperature programmed reduction of highly dispersd Rh/alumina by H_2 have been interpreted as indicating reduction to Rh^{0} **(19)**.

The Rh dicarbonyl species also differs in reactivity from CO adsorbed on the clustered Rh. The CO of the dicarbonyl exchanges with gas phase CO more readily **(20)** and is more easily desorbed upon evacuation **(1,7-11,21)**, but is less easily removed by O_2 **(1,10,13)** and NO **(22)** than is the CO on the clustered Rh. The dependence of various Rh-catalyzed reactions on the dispersion and oxidation state of the Rh **(23-27)** may often be based on such reactivity differences.

It has been noticed that the dicarbonyl species is gradually removed both during adsorption-desorption-readsorption cycles **(1,7,11)** and in *in situ* infrared studies of CO hydrogenation over supported Rh catalysts **(21)**. Fujimoto *et al.* **(21)** have demonstrated that the first step in the decomposition of dicarbonyl species upon heating is loss of a CO. Whether the remaining site is especially reactive or inactive, and whether this change is reversible or not, is not clear.

In the present study, changes in the sites for CO adsorption on Rh/alumina upon heating are investigated. We used infrared spectroscopy and quantitative measurements of the CO taken up and the gases evolved while heating between 300 and 525 K. Heating to 525 K was found to cause a substantial loss in capacity to adsorb CO. Employing estimates of CO and Rh among the various adsorp-

tion modes based on the NMR results of Duncan *et al.* **(9)**, a model to account for this deactivation is proposed. By heating Rh/alumina in the presence of CO_2, O_2 or H_2 instead of CO, a strong dependence of deactivation on the gas phase is observed.

2. Experimental Procedures

The 2.0% by weight Rh dispersed on alumina was prepared as described previously **(7)**. Briefly, $RhCl_3 \cdot 3H_2O$ is dissolved in a water:acetone (1:10) suspension of alumina and sprayed onto a CaF_2 disc preheated to 365 K. The disc, with a coverage of ~ 11 mg of sample per cm^2 is mounted in a stainless steel infrared cell with CaF_2 windows. The cell is then attached to a stainless steel vacuum system and heated under vacuum to 450 K. The sample is reduced with three charges of H_2 (Matheson, 99.9995%) at 425 K and 200 Torr, evacuated at 450 K for 12 hr and cooled to 300 K. The procedure for heating the samples in various gases was to fill the cell with ~ 50 Torr of the gas, close off the cell, heat at the desired temperature for 12 hr and then cool to 300 K. The alumina samples were prepared exactly as were the Rh/alumina samples, with the exception that $RhCl_3 \cdot 3H_2O$ was not added to the water:acetone suspension of the alumina.

Quantitative measurements of the gases taken up (removed from the gas phase) by and evolved from the samples were made using either the infrared samples, or, for greater precision, 0.2 g samples packed loosely in the bottom of glass tubes and pretreated *in situ* as above. The measurements were made in the constant volume system at pressures of a few Torr to ± 0.01 Torr with a capacitance manometer.

The amounts of CO, CO_2 and H_2 in the gas phase were conveniently monitored manometrically by condensing the CO_2 in a glass tube at 77 K and condensing CO and CO_2 on dehydrated alumina at 77 K. The methane formed on heating to 525

K was determined by mass spectrometry or infrared spectroscopy. The concentration of all other gases was less than 5×10^{-6} mol per gram of sample, as shown using mass spectrometry.

Transmission infrared spectra were obtained with a Perkin-Elmer 180 grating spectrometer with a linear absorbance scale. The double beam mode was used without any compensating sample in the reference beam. The spectral resolution at 2000 cm^{-1} was set at 2.6 cm^{-1}. All spectra were recorded with the sample at ~ 310 K.

The ^{13}CO (Merck Isotopes, 90% enriched) and the unenriched CO (Matheson, Research) were obtained in glass breakseal bulbs and used without further purification. The O_2 (Matheson, Research) was passed through a trap at 77 K before use. The CO_2 (Matheson, Bone Dry) was purified by three freeze-pump-thaw cycles and sublimed at 195 K immediately before use. The alumina was "Alon-C" (Cabot), a fumed alumina with a particle size of ~ 15 nm. Two lots with BET surface areas of 90 and 115 m^2/g were used and are designated as alumina-90 and alumina-115.

3. Results

A. Infrared Spectra Rh/Alumina Heated in CO

Qualitative changes in the types and amounts of CO adsorption sites present after heating Rh/alumina in CO above room temperature were followed using infrared spectroscopy. Shown in Fig. 1 is the spectrum of Rh/alumina-90 exposed to 50 Torr of CO at 300 K. The peaks, according to the original assignment **(1)**, for which there is now general agreement **(7-14,21,22)**, are due to the symmetric and asymmetric CO stretches of the dicarbonyl species at 2103 cm^{-1} and 2034 cm^{-1}, respectively, and the stretches of CO bound to one and more than one Rh atom of a Rh cluster at 2070 and 1875 cm^{-1}, respectively. The

rotational structure about the missing Q branch at 2143 cm^{-1} of gas phase CO is also seen. The ratio of CO molecules adsorbed per Rh atom in this sample is 1.0. The peak assignments for the infrared spectra in Figs. 1-4 are summarized in Table 1.

After isolating the sample, heating at 425 K for 12 hr, and cooling to 300 K, the intensity of the dicarbonyl doublet has decreased to ~35% of that before heating. There is little change in the peaks due to linear and bridging CO. When ^{13}CO adsorbed on Rh/alumina is heated to 425 K, a broad peak at ~2280 cm^{-1} from adsorbed $^{13}CO_2$ appears. The corresponding peak of adsorbed $^{12}CO_2$ is not easily seen after heating in ^{12}CO because of spectral interference by atmospheric CO_2.

After heating this sample at 525 K for 12 hr and cooling to 300 K, the dicarbonyl doublet is absent, while again the bands from linear and bridging CO have not changed greatly. There is a further increase in the $^{13}CO_2$ band at 2280 cm^{-1} when ^{13}CO is used. This band is removed upon evacuation at 300 K, indicating that the CO_2 must be weakly adsorbed. After evacuation, treatment with H_2 and reevacuation, all at 450 K, which was the procedure used to reduce the $RhCl_3$ dispersed on the alumina, there are no bands from adsorbed CO. After reexposing the sample to 50 Torr of CO at 300 K, the bands are similar in intensity, but shifted somewhat higher in frequency compared to those after heating at 525 K. The higher frequency peak of the dicarbonyl appears at 2110 cm^{-1}, but is much weaker than before heating. Similar results are obtained when the sample is heated in 100 Torr at O_2 at 450 K before the H_2 treatment in the regeneration procedure.

At frequencies outside the CO stretching region (2200-1700 cm^{-1}) there is no change upon adsorption of CO at 300 K. Only small increases were observed

near 1475 and 1280 cm^{-1} after heating at 425 K. Upon heating at 525 K, however, there are several changes. The broad peak at ~3700 — 3000 cm^{-1} at 300 and 425 K is due to the OH stretch of hydroxyl groups of the alumina surface. After heating to 525 K, the reduced intensity on the high frequency side and increased intensity on the low frequency side of this peak, along with the appearance of a peak at 1625 cm^{-1}, indicates that there has been some combination of the hydroxyl groups to form molecular water. The peaks at 3019 and 1307 cm^{-1}, as well as the rotational structure associated with the former peak, are assigned to gas phase CH_4. Since no $^{13}CH_4$ is formed when ^{13}CO adsorbed on Rh/alumina is heated, it is suggested that some of the acetone used in the sample preparation is retained by the sample and decomposes upon heating. No CH stretching bands were observed before the sample was heated to 525 K.

In contrast to the H_2O and CH_4 bands, the other peaks below 1700 cm^{-1} in Fig. 1 remain after the sample is evacuated and treated with O_2 or H_2 at 450 K. Their identification is facilitated by reference to the infrared spectra of alumina heated in the presence of CO or CO_2 at 425 and 525 K, which are shown in Fig. 2. Upon exposure of alumina to either CO or CO_2 at 300 K, only a small amount of gas is taken up ($\lesssim 2$ μmol/g) and there is little change in the infrared spectra. Heating alumina in CO and CO_2 does cause changes in the infrared spectra. The most prominent bands present after heating alumina at 525 K in CO are at 1594, 1395 and 1383 cm^{-1}, and are assigned to a surface formate species **(28,29)**. Peaks at 1470 and 1455 cm^{-1} are due to carbonate species, referred to variously as free, basic or ionic **(30)**. The peaks at 1649 and 1231 cm^{-1} are due to carbonate species involved in more covalent bonding, probably the bicarbonate ion in this case **(31)**. Heating alumina in CO_2 produces the same three species, but more of the carbonate and bicarbonate and less of the formate than are formed by heating in CO.

Referring back to the spectrum in Fig. 1 of Rh/alumina heated to 525 K in CO, we see that of these three species, only the ionic carbonate is present. The band at ~ 1415 cm^{-1} lies at the lower end of the range of asymmetric OCO_2 stretching frequencies of ionic carbonates, and may indicate that there is yet another type. The bands at ~ 1365 and 1280 cm^{-1}, unaccompanied by corresponding bands above 1450 cm^{-1} are probably not due to a carbonate species, but may be from the COH bending and/or CH_x deformation modes of an acetone residue.

B. Infrared Spectra of Rh/Alumina Heated in CO_2

There is no change in the infrared spectrum in Fig. 3 upon exposure of Rh/alumina-90 to 55 Torr of CO_2 at 300 K. There has been much controversy about the conditions under which CO_2 will dissociate on Rh **(32,33)**, and relevant variables include temperature, exposure, dispersion of the Rh, and support material. There is also little change in the spectrum after heating the sample in CO_2 at 425 K.

After heating for 12 hr at 525 K and cooling to 300 K, though, substantial intensity appears in the CO stretching region. The presence of only two peaks, with maxima at 2044 and 1855 cm^{-1}, indicates that CO is adsorbed in the linear and bridging modes but not in the dicarbonyl mode. After the sample is evacuated at 300 K, and then exposed to 50 Torr of CO, the peaks of linear and bridging CO are more intense and shifted to higher frequencies compared to those before exposure to CO. Again, no dicarbonyl species are present. The spectral lineshape is quite comparable to but ~ 1.5 times more intense than that obtained after heating Rh/alumina-90 in CO at 525 K. The sample that had been heated in CO_2 was further heated in CO at 525 K. This caused little change in the peak intensities or frequencies. As with heating Rh/alumina in CO, the low frequency part of the spectrum of Rh/alumina heated in CO_2 indicates the

presence of carbonate, water and methane, but no formate or bicarbonate species.

C. Infrared Spectra of CO Adsorbed on Rh/Alumina Previously Heated at 525 K.

The effect of heating Rh/alumina *in vacuo* on the sites for adsorption of CO was also studied using infrared spectroscopy. However, Rh/alumina-115 was used instead of Rh/alumina-90 as in the above studies. The dispersion of the Rh was greater for Rh/alumina-115 because of the greater surface area of the alumina. For reference, the infrared spectrum of CO adsorbed at 300 K on unheated Rh/alumina-115 is shown in Fig. 4. The dicarbonyl doublet is more intense, per unit weight and surface area of sample and more intense relative to the bands of linear and bridging CO, than for CO adsorbed on Rh/alumina-90 The band of the linear CO is present but is not resolved from the bands of the dicarbonyl. This was demonstrated with a different Rh/alumina-115 sample. It was prepared similarly and had a similar infrared spectrum after CO was adsorbed at 300 K. Upon exposure to 10 Torr of O_2 at 300 K, there was a loss of intensity at 2070-2060 cm^{-1} and at ~ 1850 cm^{-1} due to selective removal of the linear and bridging CO, as observed by other workers using similar treatments **(10,12,34)**.

A cell containing Rh/alumina-115 which had been reduced in H_2 and evacuated is closed, heated at 525 K for 12 hr, and cooled to 300 K. The sample is then exposed to CO at 300 K, and an infrared spectrum recorded. Some redistribution of the CO adsorption sites is evident from the specctrum in Fig. 4. The dicarbonyl doublet is somewhat less intense and the peaks of linear and bridging CO are more intense compared to those in the spectrum of CO adsorbed on unheated Rh/alumina-115. The change is not nearly so great as upon heating in

the presence of CO or CO_2, though. The spectrum also indicates, as after heating Rh/alumina in the presence of CO or CO_2, that ionic carbonate, water and methane (evacuated before adsorption of CO), but not formate or bicarbonate, are formed.

D. Gas Uptake and Evolution Measurements

In order to obtain quantitative information about the redistribution and deactivation of the sites for adsorption of CO on Rh/alumina that were indicated by the infrared spectra, quantitative measurements were made of the gases taken up by and evolved from the samples upon heating. The results are summarized in Table 2. Experiments were also carried out with ^{13}C-enriched CO and the gases analyzed mass spectrometrically. These were used to verify the accuracy of the manometric measurements and the lack of interference from any residue of acetone that may have been retained during the sample preparation.

Quantitative measurements for Rh/alumina heated in CO were made for both Rh/alumina-115 and Rh/alumina-90 samples. Upon exposure of Rh/alumina-115 and -90 to a few Torr of CO at 300 K, 286 and 194 x 10^{-6} mol of CO per gram of sample, respectively, are taken up, that is, removed from the gas phase. These are equivalent to ratios of CO molecules adsorbed per Rh atom in the sample of 1.47 and 1.00, respectively. After heating Rh/alumina-115 at 425 K in CO, during which the only major change in the infrared spectrum was a decrease in intensity of the dicarbonyl doublet, CO and CO_2 are evolved in a ratio of 3.4 to 1. Upon heating to 525 K, after which there are no infrared bands of the dicarbonyl, CO and CO_2 are again evolved, in a ratio of 3.1 to 1. The amount of CO adsorbed at this point can be estimated by the amount of CO that readsorbs after evacuation, H_2 treatment, and reevacuation at 450 K and cooling to 300 K, since the infrared spectra of the sample before and after this procedure are

very similar (see Fig. 1). The amount of CO adsorbed on Rh/alumina-90 is greater than that on the Rh/alumina-115, both in absolute value, 38 vs. 14 μmol/g, and relative to that adsorbed on an unheated sample, 5 vs. 20%. In both cases, this is a dramatic loss in the capacity for CO adsorption. The total amount of CO and CO_2 evolved upon heating plus the CO that remains adsorbed account for 275 of the 286 μmol/g or 96% of the CO taken up at 300 K by Rh/alumina-115. The amount of H_2 in the gas phase after heating Rh/alumina-115 in CO at either 425 or 525 K is less than 11 μmol/g. Also, there is less than 1 μmol/g of CO_2 and H_2 after heating alumina in CO without Rh at 425 and 525 K.

From the data in Table 2, we also observe a strong dependence of the decrease in capacity for CO adsorption on Rh/alumina upon the gas present during heating to 525 K. After heating Rh/alumina-115 in CO and CO_2, the respective losses are 95 and 83% of the amounts of CO adsorbed on unheated samples. The losses after heating Rh/alumina-115 in the presence of O_2, H_2 and after heating an evacuated sample are much less: 3, 19 and 32%, respectively. After heating in O_2, H_2 or *in vacuo*, there are one or more CO molecules adsorbed per Rh atom, indicating that dicarbonyl species are present. This had been determined independently for CO adsorbed on Rh/alumina-115 previously heated *in vacuo* from the infrared spectrum in Fig. 4. We also note that Rh/alumina-115 which had been heated in H_2 is deactivated by subsequently heating in CO at 525 K, during which $CO_{(g)}$ and CO_2 are evolved. There is little additional deactivation of Rh/alumina-115 which had been heated by CO_2 by subsequently heating in CO, in agreement with the infrared spectra in Fig. 3.

4. Discussion

A. Deactivation of Rh/Alumina Upon Heating in CO

We first consider the possibility that sites for adsorption of CO on Rh/alumina that had been previously heated in CO could be blocked by species strongly adsorbed on the Rh. Surface carbon could be deposited by disproportionation of CO:

$$2CO_{(ad)} \rightarrow CO_2 + C_{(ad)} \qquad (1)$$

which occurs on several Group VIII transition metals **(35-37)**. However, all but 11 μmol/g (4%) of the carbon atoms of the CO adsorbed on unheated Rh/alumina-115 is accounted for as $CO_{(g)}$, $CO_{(ad)}$ or CO_2 after heating to 525 K. Therefore, this is an upper limit for the concentration of surface carbon after heating. It is not reasonable that 11 μmol/g of $C_{(ad)}$ could block the adsorption of 272 μmol/g, or all but 4%, of the CO that adsorbs on unheated Rh/alumina-115. By the same argument, the concentration of other carbon-containing species formed from CO, such as adsorbed carbonates, bicarbonates or carboxylates, is also limited to 11 μmol/g. Therefore, their formation cannot explain the extent of deactivation observed.

We also consider that adsorbed oxygen, which could be formed by dissociation of CO, could block the sites for adsorption of CO. However, the number of oxygen atoms in the $CO_{(g)}$ and CO_2 evolved and $CO_{(ad)}$ after heating Rh/alumina-115 in CO is greater than the number of oxygen atoms in the CO adsorbed on the sample before heating. Thus, it is unlikely that oxygen is being deposited on the Rh. It indicates, rather, that there is a net transfer of oxygen from the surface to the CO in forming CO_2.

Another possible cause of the deactivation of sites for adsorption of CO is that the Rh agglomerates upon heating in CO, so that a large fraction of the Rh is no longer able to adsorb CO. The deactivation is facilitated by the CO since heating Rh/alumina *in vacuo* does not cause much deactivation. We also recall

that while heating Rh/alumina in CO, some of the CO reacts with oxygen from the surface to form CO_2. Little CO_2 was formed in the absence of Rh. The amount of CO_2 that is produced increases with increasing initial dispersion of the Rh (as determined by the initial uptake of CO) as shown in Table 3. Since there is greater deactivation of the more highly dispersed Rh/alumina, this further supports the involvement of CO_2 formation in the deactivation process. In addition, we recall that the dicarbonyl species, which contain Rh^I, are eliminated by heating Rh/alumina in CO. The Rh of the dicarbonyl species would have a greater tendency to agglomerate if it were reduced from Rh^I to Rh^0 because of a loss in ionic bonding to the alumina support. These observations suggest that CO is oxidized to CO_2 and that Rh^I is reduced to Rh^0 upon heating Rh/alumina in CO as in the reaction

$$CO + 2Rh^I + O^{2-} \rightarrow CO_2 + 2Rh^0 \qquad (2)$$

As a check of this mechanism, we predict the amount of CO_2 that would be formed by the reaction in Eq. (2) and compare it to the observed value. The amount of CO_2 observed is within 20% of that actually formed while heating, based on the amount of CO adsorbed before heating that is not accounted for as $CO_{(ad)}$, $CO_{(g)}$ or CO_2 after heating. We can predict the amount of CO_2 that would be formed according to Eq. (2) by estimating the amount of dicarbonyl-forming Rh^I that is present before heating. Using CO uptake and primarily ^{13}C NMR measurements, Duncan et al. **(9)** determined the distribution of CO among the dicarbonyl, linear and bridging sites. For samples essentially identical to the Rh/alumina-90 samples used in this study, they found that the ratio of linear to bridging CO was 2 to 1, that the ratio of CO adsorbed on the clustered Rh to the surface Rh atoms of the Rh clusters was 3 to 4, and that 12% of the Rh of a freshly prepared sample was not involved in bonding to CO in any of the three modes of CO adsorption.

We assume that these results are true for the samples in the present study. We can then use the ratio of total CO adsorbed to total Rh atoms in the sample to calculate the distribution of Rh in the dicarbonyl, clustered and inactive forms (as well as the distribution of CO in the dicarbonyl, linear and bridging modes). The sensitivity of the calculated distributions to the assumptions made is such that an error of 5% in the amount of inactive Rh or an error of 0.05 in the ratio of CO to surface Rh atoms for the Rh clusters or an error of 0.1 in the overall CO to Rh ratio would result in an error of 15-20% in the calculated values.

The Rh and CO distributions of three samples of different dispersions before heating in CO at 525 K were calculated. The amount of CO_2 produced upon heating these samples in CO, along with the calculated concentrations of dicarbonyl-forming Rh^I are shown in Table 3. The ratio of Rh^I to CO_2 formed for all three samples agrees with the stoichiometry of Eq. (2) well within the uncertainty of $\pm$ 0.4 determined by an uncertainty in the calculated Rh^I concentration of 20%. Thus, Eq. (2) can account for most, if not all, of the CO_2 produced upon heating.

B. Mechanism of Reduction of Rh^I by CO

It is possible that the Rh^I could facilitate the reaction of CO directly with oxygen of the surface. However, in studies of supported Rh formed from $Rh_6(CO)_{16}$ **(13,14)** or $Rh_4(CO)_{12}$ **(38)**, H_2O was found to promote the conversion of dicarbonyl species to Rh that adsorbs CO in the linear and bridging modes. The surfaces as prepared in the present study are highly hydroxylated (2900 μmol(OH)/g, or 15 per 100 Å^2, as determined by ^1H NMR). Also, the infrared spectra indicate that molecular water is formed upon heating the samples to 525 K, presumably by condensation of the surface hydroxyl groups:

$$2HO^- \rightarrow H_2O + O^{2-} \quad (3)$$

Therefore, we consider the implications of the results of the present study for the possible participation of H_2O in the deactivation process.

Water is known to react with CO groups bound in transition metal complexes to produce CO_2, during which either the H_2O or the metal may be reduced. The former would be part of the water gas shift reaction:

$$CO + H_2O \rightarrow CO_2 + H_2 \quad (4)$$

which is catalyzed by metal carbonyls **(39-41)**, Pt^{II} and Pt^0 complexes **(42,43)**, and Rh complexes such as $RhHL_3$ and $Rh(OH)(CO)L_2$, L = $P(i - C_3H_7)_3$ **(44)**. Water or HO^- reacts with metal-bound CO to form, presumably, a carboxylate or formate intermediate, which decomposes to CO_2 and a metal hydride complex. Eventually, the hydrogen bound to the metal forms H_2.

An example in which the metal of a complex is reduced during the reaction of H_2O with metal-bound CO is the reduction of the Rh^{III} complex, $RhCl_3$ to the Rh^I complex, $Rh_2(CO)_4Cl_2$ **(45)**. There is most likely some bonding between Rh^I atoms in crystalline $Rh_2(CO)_4Cl_2$ **(46)**. It is possible to further reduce the Rh^I to the Rh^0 of $Rh_6(CO)_{16}$ in the presence of H_2O according to the following stoichiometry **(47)**:

$$3Rh_2(CO)_4Cl_2 + 7CO + 3H_2O \rightarrow Rh_6(CO)_{16} + 3CO_2 + 7HCl \quad (5)$$

The reduction of the Rh in the di-Rh^I complex may be compared to the reduction of H_2O with the complex $Rh(OH)(CO)(P(i\text{-}C_3H_7))_3$ **(44)**, which contains only one Rh^I atom. Two electrons are transferred per molecule of CO that is oxidized to CO_2. Apparently, when the metal is able to accept these two electrons, the metal, rather than the H_2O, is reduced.

The present study is a case in which the metal rather than H_2O is reduced.

The ratio of Rh^I present before heating to the CO_2 that is produced while heating agrees well with the ratio predicted assuming the Rh^I is reduced to Rh^0 [Eq. (2)]. Also, agglomeration of the Rh^0 that results provides an explanation of the deactivation of the sites for adsorption of CO.

In contrast, both the reduction of H_2O as in the water gas shift reaction [Eq. (4)] and the reduction of H_2O and Rh^I simultaneously are not consistent with the results of the present study. Unless the water gas shift reaction was limited kinetically, which seems unlikely, the amount of CO_2 formed would not be related to the amount of dicarbonyl-forming Rh^I that is present, in contrast to the results in Table 3. If the Rh^I and H_2O were reduced simultaneously, as in:

$$CO + Rh^I + O^{2-} + H_2O \rightarrow CO_2 + Rh^0 + HO^- + H \qquad (6)$$

the ratio predicted for the Rh^I present before heating to CO_2 formed while heating would be 1.0, compared to the observed ratio of 1.9 ± 0.4 (Table 3). H_2 that is present in the gas phase or adsorbed on the Rh or alumina or that has reacted to form CH_4 after heating Rh/alumina-115 in CO is less than 5 μmol/g, as determined by mass spectrometric and gas uptake and evolution measurements. This is equivalent to a ratio of H_2 to CO_2 formed of less than 0.08, compared to ratios of 1 and 0.5 that would be predicted using Eqs. (4) and (6), respectively.

If H_2O does facilitate the reduction of Rh^I by CO in the present study, the Rh^I must be able to accept the two electrons transferred for each CO that is oxidized. Production of hydrogen that could reduce other Rh^I species cannot be involved since heating Rh/alumina in H_2 did not cause much deactivation (see below). We recall that H_2O was reduced by CO in the presence of $Rh(OH)(CO)(P(i\text{-}C_3H_7))_2$ **(44)**, which contains one Rh^I atom, but that the Rh^I was reduced by CO in the di-Rh^I complex, $Rh_2(CO)_4Cl_2$ **(47)**. We then speculate that

each Rh^I is near at least one other Rh^I before it is reduced to Rh^0.

Structures of supported Rh derived from $Rh_6(CO)_{16}$ and $Rh_4(CO)_{12}$ in which the Rh atoms are near each other, perhaps bonded to each other have been proposed **(13,14,38)**. Dicarbonyl species are formed by addition of oxygen to the supported complexes. The complexes can be reformed by addition of CO and H_2O, and the analogy to the synthesis of $Rh_4(CO)_{12}$ and $Rh_6(CO)_{16}$ from $Rh_2(CO)_4Cl_2$ **(47)** has been noted **(13,38)**. Since there are Rh-Rh bonds in the complexes from which the supported Rh was formed, it was not apparent that dicarbonyl-forming Rh^I species of supported Rh that was formed by reducing $RhCl_3$ in H_2 would also be near each other. The results of the present study suggest that this is the case.

Though the dicarbonyl-forming Rh^I species may be near each other at some time before they are reduced by CO, this does not imply that the dicarbonyl species are near each other. During thermal programmed desorption of CO-covered Rh/alumina, Fujimoto et al. observed that only CO desorbs at temperatures less than 373 K, during which the dicarbonyl doublet in the infrared spectrum is removed **(21)**. At higher temperatures, CO_2 desorbs. Apparently one CO is removed from the dicarbonyl species before the Rh^I is reduced. It is thus possible that the formation of the dicarbonyl, which is known to be an activated process **(12,20)**, could involve migration of Rh^I species away from each other in order to bind two CO molecules per Rh^I.

C. Rh/Alumina Heated in CO vs. H_2

The reduction of Rh^I to Rh^0 by heating Rh/alumina in CO at 525 K is nearly quantitative, as shown by the agreement of the Rh^I:CO_2 ratios with those predicted by Eq. (2) and by the lack of the dicarbonyl doublet in the infrared spectrum after heating in CO (Fig. 1). In contrast, only ~ 42 of the 125 μmol/g,

or 34% of the Rh^I is reduced by heating at 525 K in H_2, according to calculations of the distribution of CO among the various adsorption modes that was described above. We may speculate that the binding of two CO groups to a single Rh^I facilitates the reduction in CO, as it does the exchange with gas phase CO **(20)**. However, the thermal programmed desorption results discussed above suggest that one CO is removed from the dicarbonyl before the Rh^I is reduced. It is also unlikely that a metastable state is formed after the removal of CO from the dicarbonyl since its reformation is activated, as was its original formation **(48)**.

The difference in the ability of CO and H_2 to reduce the Rh^I may be due to the stronger bonding of CO to the Rh^I sites, increasing its availability for reaction with oxygen of the surface. More likely, the reaction of CO directly with oxygen of the surface or with H_2O is a lower energy path by which the Rh^I may be reduced, compared to the paths available for reduction by H_2. Thus, the specific reactions that a gas may undergo, rather than simply the reducing or oxidizing nature of the gas strongly influence the effect of the gas on the supported Rh.

D. Rh/Alumina Heated in CO_2

The infrared spectra and uptake measurements suggest that the effects of heating Rh/alumina in CO_2 at 525 K are similar to those of heating in CO. Rh/alumina heated in CO_2 (or CO) adsorbs CO in the linear and bridging but not in the dicarbonyl mode, as shown in the infrared spectra. The capacity for adsorption of CO after heating Rh/alumina-115 in CO_2 is 48 μmol/g, or only 17% of the amount of CO adsorbed on an unheated sample. This is similar to the amount of CO adsorbed in the linear and bridging modes on unheated Rh/alumina (34 μmol/g), according to the calculations described above.

We might suppose that adsorbed CO, formed by decompostion of CO_2 on the clustered Rh, could migrate to and reduce the Rh^I to Rh^0 as proposed for heating in the presence of CO. The newly formed Rh^0 would most likely migrate to a Rh cluster. The adsorbed O may be absorbed into the Rh cluster, a process that occurs for O adsorbed on Rh(111) at 400 K **(49)**. Considering 1/2 O for each of the 125 μmol/g of Rh^I of Rh/alumina-115 and one O for each of the 11 μmol/g of adsorbed CO formed from CO_2 dissociation, one calculates an O:Rh ratio of 0.38.

However, there is little, if any, color change upon heating Rh/alumina in CO_2, in contrast to the darkening upon heating CO. The lack of color change is not due to a difference in the color of a Rh^0 cluster and a partially oxidized Rh cluster since a sample which had turned dark upon heating in CO did not become lighter when heated at 525 K in O_2 for 12 hr. It thus appears that the mechanism proposed for deactivation by heating Rh/alumina in CO is not responsible for the deactivation by heating in CO_2.

Another possibility is that oxygen, which could be formed by the dissociation of CO_2, could bind to the dicarbonyl-forming sites and block subsequent binding of CO at these sites. This is unlikely, based on thermochemical estimates. We assume that a species with the stoichiometry Rh_2O is stable with respect to decomposition to O_2 and Rh metal and that the stability of a dicarbonyl-forming Rh^I with an additional oxygen bound to it is similar to that of Rh_2O_3. The reaction

$$2CO_{2(g)} + Rh_2O \rightarrow Rh_2O_3 + 2CO_{(g)} \qquad (7)$$

is endoergic by more than about 75 kcal/mol **(50)**. The reaction is more favorable if the CO that is produced is adsorbed on the Rh. However, only ~ 34 μmol/g of CO is adsorbed on linear and bridging sites of unheated Rh/alumina-

115, or ~ 29% of the amount of Rh^I that forms dicarbonyl species. Thus, there are not enough sites to adsorb the CO that would be formed by deactivation of all of the dicarbonyl species according to the stoichiometry of Eq. (7).

Another argument against deactivation of Rh/alumina by the reaction in Eq. (7) is that we might have expected that heating in O_2 would deactivate Rh/alumina by a similar process. In contrast to this, heating in O_2 caused almost no loss in the capacity of Rh/alumina to adsorb CO, as shown in Table 2. In other studies **(10,12,34)**, after treatment of Rh/alumina with O_2 at 300 or 473 K, the amount of dicarbonyl species formed upon exposure to CO had either increased or remained unchanged compared to that without the pretreatment in O_2. A new peak in the infrared spectrum appeared at 2128-2120 cm^{-1} after the pretreatment in O_2 and subsequent exposure to CO **(10,12)**. No peak is observed at these frequencies in the infrared spectra after heating Rh/alumina in CO_2 and after subsequent exposure to CO in the present study.

Yet another possibility is that the CO_2 could react with the dicarbonyl-forming Rh^I to form a species that would block the adsorption of CO on these sites. There are Rh complexes in which carbonate **(51,52)**, bicarbonate **(51,53)** and carboxylate **(51,53,54)** groups are bonded in unidentate and bidentate configurations. These Rh complexes are often synthesized by reaction of CO_2 with other Rh complexes **(51-54)**. However, upon heating Rh/alumina in CO_2, there is little change in the infrared spectrum at the frequencies expected for such species **(51-54)**. Uncertainty about the extinction coefficients of the infrared peaks that would be due to Rh carbonate and carboxylate species prevents us from concluding that these species are not present, though. Thus, additional experiments are necessary to determine the cause of deactivation of the dicarbonyl-forming sites of Rh/alumina which results from heating in CO_2. Perhaps ^{13}C NMR or X-ray photoelectron spectroscopy will be useful in resolving this problem.

(THIS PAGE IS BLANK, DUE TO ERROR IN PAGINATION)

E. Surface Species Bound to the Alumina

The final point we would like to discuss is the difference in surface species bound to the alumina after heating in the presence and absence of Rh. Heating alumina in either CO or CO_2 produces surface formate, carbonate and bicarbonate species, whereas in the presence of Rh, only carbonates are formed. We might expect formate and bicarbonate species to be formed by reaction with surface hydroxyl groups as follows:

$$CO + HO^{-}_{(ad)} \rightarrow HCOO^{-}_{(ad)} \quad (8)$$

and

$$CO_2 + HO^{-}_{(ad)} \rightarrow HOCOO^{-}_{(ad)} \quad (9)$$

These reactions may take place with hydroxyl groups, that are blocked by the Rh or are replaced by the chloride ions introduced as $RhCl_3$. Peri **(55)** observed that infrared bands in the region 1900 — 1350 cm^{-1} that appeared upon exposure of alumina to CO or CO_2 were not present if the alumina was previously exposed to chloride or fluoride ions. The concentration of chloride ion remaining after reduction of Rh/alumina in H_2 is 305 μmol/g **(9)** and the Rh concentration is 195 μmol/g. These are much less than the total hydroxyl group concentration of 2900 μmol/g. This may indicate that the formate and bicarbonate species are formed from particular hydroxyl groups that are also preferentially blocked by the Rh or are replaced by chloride ions.

5. Conclusions

The behavior of Rh/alumina upon heating in the presence of CO, CO_2, H_2 and O_2 was studied using infrared spectroscopy and quantitative measurements of gases taken up and evolved during various procedures. By combining the results with estimates of the distribution of CO and Rh among the dicarbonyl, linear

and bridging modes of CO adsorption we find that:

A. The loss in the capacity of Rh/alumina to adsorb CO upon heating at 525 K in the presence of various gases increases in the order: O_2, H_2, vacuum < CO_2 < CO.

B. The Rh^I that forms dicarbonyl species is reduced with CO by 525 K, yielding CO_2 and Rh^0. The Rh^0 agglomerates, accounting for the substantial loss in capacity for adsorption of CO. There is little or no disproportionation of CO.

C. Reduction of Rh^I by heating in CO is much more extensive than by heating in H_2 most likely because of a greater reactivity of CO toward oxygen of the surface or the stronger bonding of CO to the Rh^I, increasing its availability for reaction.

D. The dicarbonyl-forming Rh^I species are also deactivated by heating in CO_2. The resulting loss in capacity to adsorb CO is nearly as great as that from heating in CO.

Acknowledgments

This study was supported by the Office of Naval Research under contract NOOO14-79-F-0014. We thank Dr. G. R. Rossman for the use of his infrared spectrometer and M. Templeton for obtaining the mass spectra. Helpful comments were offered by Drs. W. H. Weinberg, T. M. Duncan and S. I. Chan.

References

1. Yang, A. C. and Garland, C. W., J. Phys. Chem. **61**, 1504 (1957).

2. Sheppard, N. and Nguyen, T. T., Advan. Infrared Raman Spectr. **5**, 67 (1978).

3. Kellner, C.S. and Bell, A. T., J. Catal. **71**, 296 (1981).

4. Smith, A. K., Besson, B., Basset, J.M., Psaro, R., Fusi, A. and Ugo, R., J. Organometal. Chem. **192**, C31 (1980).

5. Deeba, M. and Gates, B. C., J. Catal. **67**, 303 (1981).

6. Knozinger, H. and Zhao, Y., J. Catal. **71**, 337 (1981).

7. Yates, J. T., Jr, Duncan, T. M., Worley, S. D. and Vaughan, R. W., J. Chem. Phys. **70**, 1219 (1979).

8. Yao, H. C. and Rothschild, W. G., J. Chem. Phys. **68**, 4774 (1978).

9. Duncan, T. M., Yates, J. T., Jr. and Vaughan, R. W., J. Chem. Phys. **73**, 975 (1980).

10. Rice, C. A., Worley, S. D., Curtis, C. W., Guin, J. A. and Tarrer, A. R., J. Chem. Phys. **74**, 6487 (1981).

11. Yates, D. J. C., Murrell, L. L. and Prestridge, E. B., J. Catal. **57**, 41 (1979).

12. Primet, M., J. Chem. Soc. Faraday Trans. I **74**, 2570 (1978).

13. Smith, A. K., Hugues, F., Theolier, A., Basset, J. M., Ugo, R., Zanderighi, G. M., Bilhou, J. L., Bilhou-Bougnol, V. and Graydon, W. F., Inorg. Chem. **18**, 3104 (1979).

14. Watters, K. L., Howe, R. F., Chojnacki, T. P., Fu, C.-M., Schneider, R. L. and Wong, N. B., J. Catal. **66**, 424 (1980).

15. Andersson, S. L. T., Watters, K. L. and Howe, R. F., J. Catal. **69**, 212 (1981).

16. Gleeson, J. and Vaughan, R. W., unpublished observations.

17. Yao, H. C. and Shelef, M., Proc. 7th Intern. Congr. Catal., paper A21, Preprints, Tokyo (1980).

18. Knozinger, H., Zhao, Y., Tesche, B., Barth, R., Epstein, R., Gates, B. C. and Scott, J. P., Faraday Discus. Chem. Soc. **72**, in press.

19. Yao, H. C., Japar, S. and Shelef, M., J. Catal. **50**, 407 (1977).

20. Yates, J. T., Jr., Duncan, T. M. and Vaughan, R. W., J. Chem. Phys. **71**, 3908 (1979).

21. Fujimoto, K., Kameyama, M. and Kunugi, T., J. Catal. **61**, 7 (1980).

22. Arai, H. and Tominaga, H., J. Catal. **43**, 131 (1976).

23. Yates, D. J. C. and Sinfelt, J. H., J. Catal. **8**, 348 (1967).

24. Yao, H. C., Yao, Y.-F. Yu and Otto, K., J. Catal. **56**, 21 (1979).

25. Okanoto, et al., J. Catal. **58**, 82 (1979).

26. Iizuka, T. and Lunsford, J. H., J. Mol. Catal. **8**, 391 (1980).

27. Fuentes, S. and Fuentes, F., J. Catal. **61**, 443 (1980).

28. Greenler, R. G., J. Chem. Phys. **37**, 2094 (1962).

29. Solymosi, F., Erdohelyi, A. and Kocsis, M., J. Catal. **65**, 428 (1980).

30. Little, L. H., *Infrared Spectra of Adsorbed Species*, p. 74, Academic, New York (1966).

31. Parkyns, N. D., J. Phys. Chem. **75**, 526 (1971).

32. Solymosi, F. and Erdohelyi, A., J. Catal. **70**, 451 (1981).

33. Iizuka, T. and Tanaka, Y., J. Catal. **70**, 449 (1981), and references therein.

34. Cavanaugh, R. R. and Yates, J. T., Jr., J. Chem. Phys. **74**, 4150 (1981).

35. Ponec, V., Catal. Rev. Sci. Eng. **18**, 151 (1978).

36. Rabo, J. A., Risch, A. P. and Poutsma, M. L., J. Catal. **53**, 295 (1978).

37. Doering, D. L., Poppa, H. and Dickinson, J. T., J. Vac. Sci. Tech. **18**, 460 (1981).

38. Theolier, A., Smithg, A. K., Leconte, M., Basset, J. M., Zanderighi, G. M., Psaro, R. and Ugo, R., J. Organometal. Chem. **191**, 415 (1980).

39. King, A. D. et al., J. Amer. Chem. Soc. **103**, 299 (1981).

40. Ungermann, C., Landis, V., Moya, S. A., Cohen, H., Walker, M., Pearson, R. G., Rinker, R. G. and Ford, P. C., J. Amer. Chem. Soc. **101**, 5922 (1979).

41. Darensbourg, D. J. and Rokicki, A., in *Catalytic Activation of Carbon Monoxide* (P. C. Ford, Ed.), p. 107, American Chemical Society, Washington, D.C., 1981.

42. Chen, C.-H. and Eisenberg, R., J. Amer. Chem. Soc. **100**, 5968 (1978).

43. Yoshida, T., Ueda, Y. and Otsuka, S., J. Amer. Chem. Soc. **100**, 3941 (1978).

44. Yoshida, T., Okano, T. and Otsuka, S., in *Catalytic Activation of Carbon Monoxide* (P. C. Ford, Ed.), p. 79, American Chemical Society, Washington, D.C., 1981.

45. James, B. R., Rempel, G. L. and Ng, F. T. T., J. Chem. Soc. A, 2454 (1969).

46. Dahl, L. F., Martell, C. and Wampler, D. L., J. Amer. Chem. Soc. **83**, 1761 (1961).

47. Chini, P. and Martinengo, S., Inorg. Chim. Acta **3**, 315 (1969).

48. Duncan, T. M., PhD Thesis, California Institute of Technology (1980).

49. Thiel, P. A., Yates, J. T., Jr. and Weinberg, W. H., Surface Sci. **84**, 54 (1979).

50. JANAF Thermochemical Tables, 2nd ed. (D. R. Stull and H. Prophet, Project Directors), U.S. National Bureau of Standards, Washington, D.C., 1971.

51. Eisenberg, R. and Hendriksen, D. E., Advan. Catal. **28**, 79 (1979).

52. Krogsrud, S., Komiya, S., Ito, T., Ibers, J. A. and Yamamoto, A., Inorg. Chem. **15**, 2789 (1976).

53. Yoshida, T., Thorn, D. L., Okano, T., Ibers, J. A. and Otsuka, S., J. Amer. Chem. Soc. **101**, 4212 (1979).

54. Volpin, M. E. and Kolmnikov, I. S., Organometal. Reactions **5**, 313 (1975).

55. Peri, J. B., J. Phys. Chem. **70**, 1482 (1966); **72**, 2917 (1968).

Figure Captions

Figure 1: Infrared spectra of Rh/alumina heated in ^{12}CO. (a) Clean Rh/alumina exposed to 50 Torr of ^{12}CO at 300 K; (b) The sample in (a) heated at 425 K for 12 hr; (c) The sample in (b), heated at 525 K for 12 hr; (d) The sample in (c) evacuated, exposed to 200 Torr of H_2, and reevacuated, all at 450 K (after which there were no infrared peaks due to CO stretching), then exposed to 50 Torr of ^{12}CO at 300 K.

Figure 2: Infrared spectra of alumina heated in 50 Torr of: *A.* ^{12}CO and *B.* $^{12}CO_2$. (a) 50 Torr of CO or CO_2 at 300 K; (b) The sample in (a), heated at 425 K for 12 hr; (c) The sample in (b), heated at 525 K for 12 hr.

Figure 3: Infrared spectra of Rh/alumina-90 heated in $^{12}CO_2$. (a) Clean Rh/alumina exposed to 55 Torr of $^{12}CO_2$ at 300 K; (b) The sample in (a), heated at 425 K for 12 hr; (c) The sample in (b), heated at 525 K for 12 hr.; (d) The sample in (c), evacuated at 300 K and exposed to 50 Torr of ^{12}CO at 300 K.

Figure 4: Infrared spectra of CO adsorbed at 300 K on: (a) unheated Rh/alumina-115; (b) Rh/alumina-115 previously heated at 525 K for 12 hr, then cooled to 300 K before exposure to CO. Note that the absorbance scale has been compressed by a factor of two, relative to the previous figures.

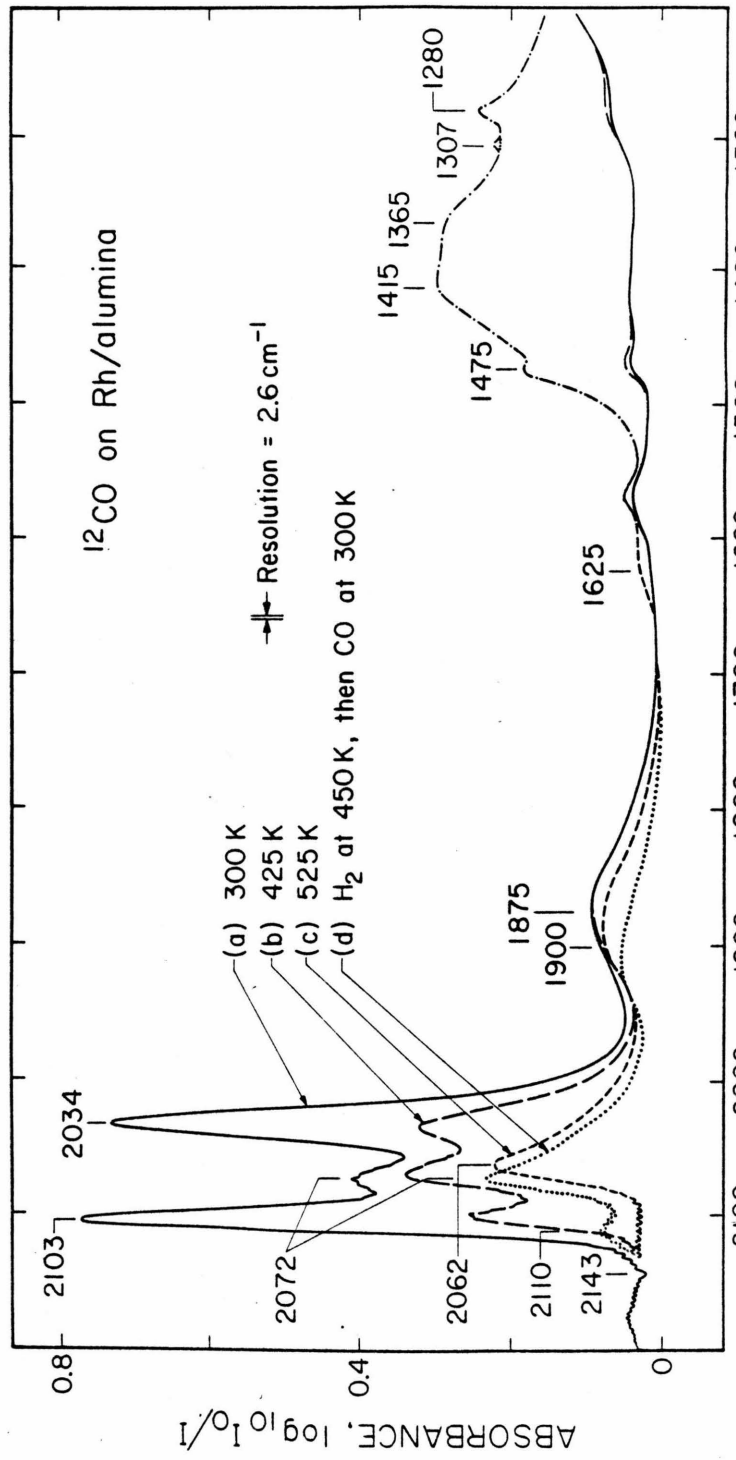
^{12}CO on Rh/alumina
Resolution = 2.6 cm^{-1}
(a) 300 K
(b) 425 K
(c) 525 K
(d) H_2 at 450 K, then CO at 300 K
2034
2103
2072
2062
2110
2143
1875
1900
1625
1415
1365
1307
1280
1475
ABSORBANCE, $\log_{10} I_0/I$
WAVENUMBER (cm^{-1})

Figure 1

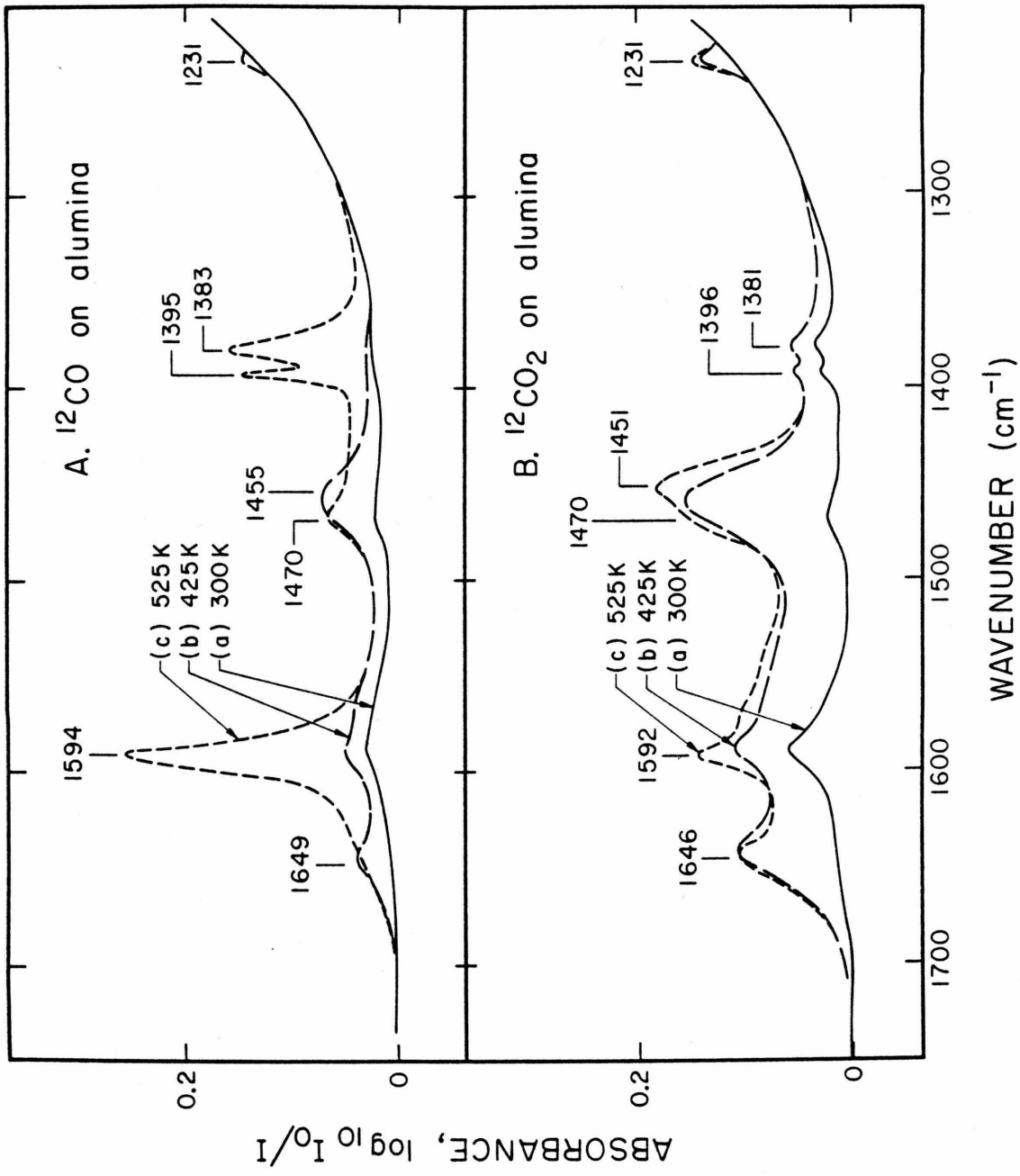
A. ^{12}CO on alumina
B. $^{12}CO_2$ on alumina
1231
1395
1383
1455
1470
1594
1649
(c) 525K
(b) 425K
(a) 300K
1451
1396
1381
1592
1646
0.2
0
1700
1600
1500
1400
1300
WAVENUMBER (cm^{-1})
ABSORBANCE, $\log_{10} I_0/I$

Figure 2

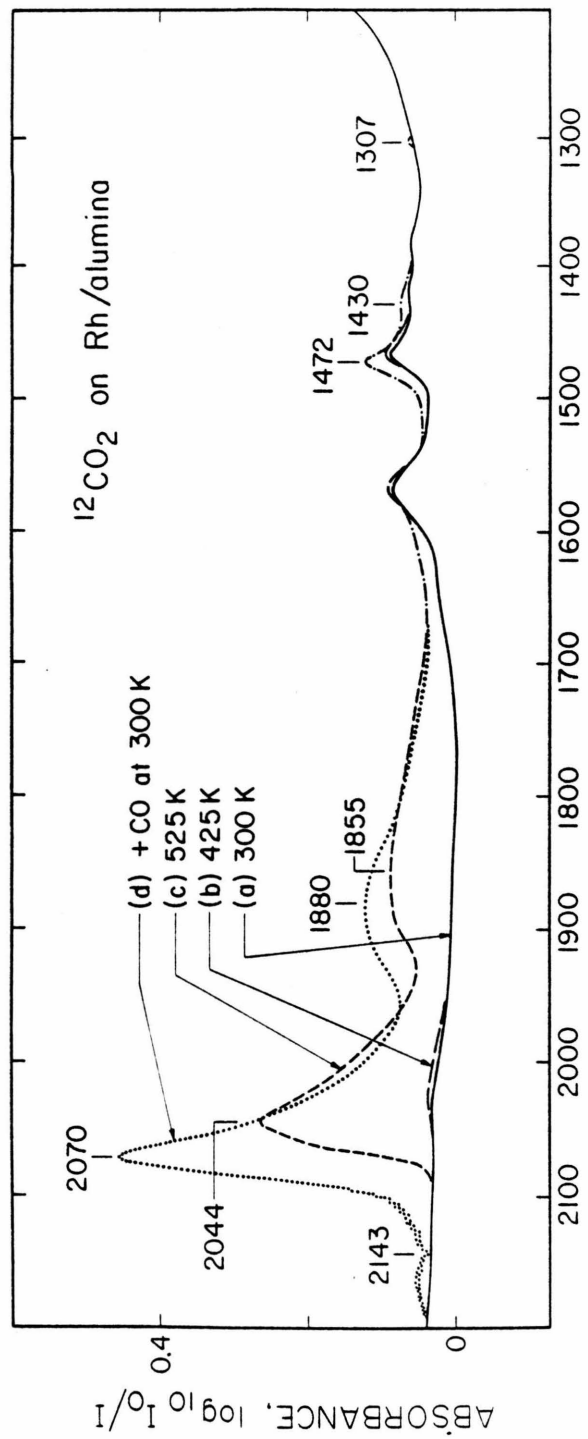
$^{12}CO_2$ on Rh/alumina
(d) + CO at 300 K
(c) 525 K
(b) 425 K
(a) 300 K
2070
2044
2143
1880
1855
1472
1430
1307
0.4
0
ABSORBANCE, $\log_{10} I_0/I$
2100
2000
1900
1800
1700
1600
1500
1400
1300
WAVENUMBER (cm^{-1})

Figure 3

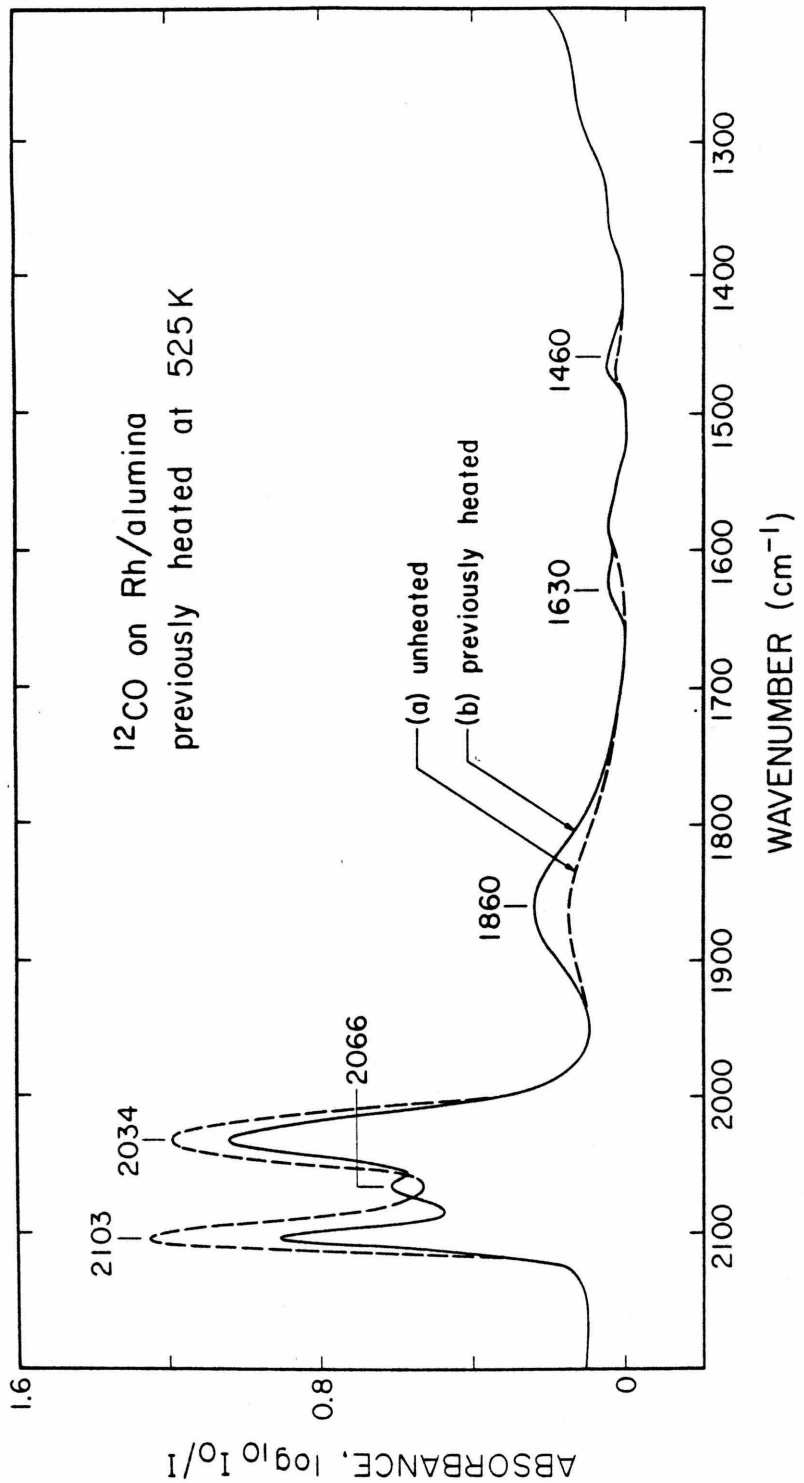
^{12}CO on Rh/alumina
previously heated at 525 K
(a) unheated
(b) previously heated
2103
2034
2066
1860
1630
1460
ABSORBANCE, $\log_{10} I_0/I$
1.6
0.8
0
2100
2000
1900
1800
1700
1600
1500
1400
1300
WAVENUMBER (cm^{-1})

Figure 4

Table 1

Frequencies and Assignments of Peaks in the Infrared Spectra between 2400 and 1200 cm^{-1}

Frequency (cm^{-1})	Species	Vibrational mode	Other Modes of the Species
∿2284	physically-adsorbed $^{13}CO_2$	asymmetric OCO stretch	
2143	gas phase ^{12}CO	CO stretch	
2103, 2034	dicarbonyl	symmetric CO stretch asymmetric CO stretch	
2072-2044	linear CO	CO stretch	
1900-1850	bridging CO	CO stretch	
1625	molecular water	HOH bend	∿3400 (OH stretch)
1649-1646, 1231	bicarbonate or bidentate carbonate	C=O stretch asymmetric OCO stretch	
1594-1592, 1396, 1381	formate	asymmetric OCO stretch CH in-plane bend symmetric OCO stretch	2915 (CH stretch)
1475-1430	ionic carbonate	asymmetric OCO_2 stretch	
1415,1365 1280	carbonate and/or alcohol impurity	asymmetric OCO_2 stretch, COH bend, and/or CH_x deformation	
1307	methane	CH_4 deformation	3019 (CH stretch)

Table 2

Amounts of CO and CO_2 Adsorbed on and Evolved from Rh/Alumina-115 upon Heating in Various Gases[a,b,c]

Gas	Heating T (K)	Additional Procedures	$CO_{(ad)}$	$CO_{(g)}$ Evolved	CO_2 Evolved[d]		Total
CO	300		286 (195)		1		286 (195)
	425			78	23	(28±10)	
	525			120	39		
		(evac, H_2, evac) at 450 K, + CO	14 (38)				
CO_2	525	evac at 300 K, + CO	37 (39)				
		(evac, H_2, evac) at 450 K, + CO	48				
H_2	525	evac 450 K, + CO	233				233
		heat in CO at 525 K		187	43		241
		(evac, H_2, evac) at 450 K, + CO	11				
O_2	525	(evac, H_2, evac) at 450 K,+ CO	277		1		
-	525	+ CO	194				

[a] Values are in μmol/g ± 5 μmol/g.

[b] Values in parentheses are for Rh/alumina-90.

[c] Rh concentration = 195 μmol/g.

[d] Amount of CO_2 in the gas phase or weakly adsorbed.

Table 3

The Amount of CO_2 Produced upon Heating Rh/Alumina Samples of Various Dispersions in CO at 525 K for 12 hr.[a]

Sample	$\frac{CO_{(ad)}}{Total\ Rh}$	CO_2 Formed (μmol/g)	Rh^I_{calc} (μmol/g)	$\frac{Rh^I_{calc}}{CO_2\ Formed}$[b]
Rh/alumina -115	1.47	63	125	2.0
Rh/alumina-115 previously heated in H_2 at 525 K	1.20	43	83	1.9
Rh/alumina-90	1.00	28 ± 10	53	1.9

[a] Total Rh concentration = 195 μmol/g.

[b] The theoretical $Rh^I_{calculated}/CO_2$ formed for Eq. (2) is 2.0

Chapter 5:

H_2S Adsorption and Interaction with CO on Rh/Alumina

Abstract

The adsorption of H_2S and its interaction with CO on Rh supported on alumina was studied using infrared spectroscopy and quantitative measurements of the gases taken up by and evolved from the samples. The dissociation of H_2S on the Rh at 300 K produces H_2 and is inhibited by preadsorbed CO. Rh also facilitates the reaction of H_2S with surface oxygen at $\leq$ 373 K, in which water is produced. After preexposure of the Rh to H_2S, CO adsorbs in the linear, but not in the dicarbonyl or bridging modes. Adsorption of H_2S onto a CO-precovered surface displaces much of the bridging CO, but only slowly removes the dicarbonyl and linear CO. Adsorption of H_2S strongly inhibits the removal of adsorbed CO by O_2, but exchange with $CO_{(g)}$ occurs readily.

1. Introduction

The modification of transition metal catalysts by adsorption and decomposition of sulfur-containing compounds is of great importance industrially **(1-3)**. The activity of the catalyst is generally lowered by adsorbed or absorbed sulfur. Occasionally, intentional exposure to sulfur-containing compounds is used to change the selectivity of a catalyst **(1,2)**.

The interaction of sulfur-containing compounds with Rh catalysts is especially interesting since among several of the Group VIII transition metals, Rh was shown to be particularly resistant to SO_2 poisoning of the catalytic reduction of NO **(4)**. The resistance of Rh and other metals to sulfur-poisoning was greatly enhanced by adding small amounts of O_2 to the reactants **(4,5)**. After NO was reduced in the presence of metal foils, oxygen was found in both the surface and subsurface region of the metal **(5)**. It is possible that this oxygen inhibited the adsorption of sulfur or bulk sulfide formation and/or reacted with the sulfur deposited. One may speculate that the resistance of supported Rh to sulfur-poisoning may be related to a strong interaction of Rh with the oxygen of the support.

The interaction of Rh with the support is reflected in its binding of CO. Using vibrational spectroscopies **(6-15)**, it has been shown that CO adsorbs on supported Rh in three distinct modes:

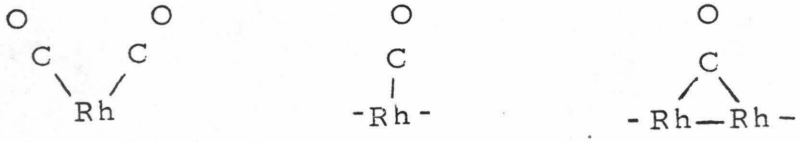

which we will refer to, respectively, as dicarbonyl, linear and bridged. The linear and bridged modes, which are typical of CO adsorbed on supported and unsupported Group VIII transition metals **(16)**, occur on two- or three-dimensional

clusters of Rh. Only on supported Rh, Ru **(17)** and Os **(18-20)** is there convincing evidence of dicarbonyl formation. The Rh of this species is most likely in an oxidation state of +1 and may be isolated from the clustered Rh, as discussed elsewhere **(8-10,12,14,21,22)**. Thus, it is particularly difficult to reduce all of the supported Rh to Rh^0, presumably due to a strong interaction of Rh with the support.

There have been two studies of the interaction of H_2S with CO on supported Rh. Guerra **(23)**, using infrared spectroscopy, found that exposing silica-supported Rh to H_2S inhibited subsequent adsorption of CO in the bridging, but not in the dicarbonyl or linear modes. Similarly, other workers observed that CO adsorbed in the linear but not in the bridging mode on supported Ni that had been exposed to H_2S or CS_2 **(24-28)**. Kroeker et al. **(29)**, using inelastic electron tunneling spectroscopy, found that adsorption of CO on alumina-supported Rh in all three modes was inhibited by preexposure to H_2S. Upon exposing a CO-precovered surface to H_2S, the CO that was adsorbed in the dicarbonyl and bridging, but not in the linear mode was displaced. They also obtained evidence that one CO molecule could be bound to a dicarbonyl-forming Rh that was perturbed by H_2S.

In the present study we investigate the adsorption of H_2S and its interaction with CO on alumina-supported Rh. We use infrared spectroscopy and also measure the amounts of H_2S and CO taken up by Rh/alumina and gases evolved during their adsorption to quantify the effects seen in the infrared spectra. By combining these results with estimates of the CO and Rh among the various adsorption modes, we determine the effect of H_2S on the modes of CO adsorption and the effect of CO on the modes which H_2S is found to adsorb in. We also examine the effect of H_2S on the exchange of adsorbed and gas phase CO and the removal of adsorbed CO by O_2.

2. Experimental Procedures

The 2.0% by weight Rh on alumina was prepared as described previously **(10)**. Briefly, $RhCl_3 \cdot 3H_2O$ was dissolved in a water:acetone (1:10) suspension of alumina and sprayed onto a CaF_2 disc preheated to 365 K. The disc, with a coverage of ~ 11 mg of sample per cm^2, was mounted in a stainless steel infrared cell with CaF_2 windows. The cell was then attached to a stainless steel vacuum system and heated under vacuum to 450 K. The Rh was reduced with three charges of H_2 (Matheson, 99.9995%) at 425 K and 200 Torr. The sample was then evacuated at 450 K for 12 hr and cooled to 300 K. We will refer to the sample at this point as clean Rh/alumina. The alumina samples were prepared exactly as were the Rh/alumina samples, except that no $RhCl_3 \cdot 3H_2O$ was added to the water:acetone suspension of alumina.

The amounts of H_2S and CO taken up by the samples and gases evolved during their adsorption were measured manometrically in the constant volume system at pressures of a few Torr with a Baratron capacitance manometer to ± 0.01 Torr. Due to the low mass of the infrared samples, precision uptake measurements were made on 0.2g samples packed loosely in the bottom of glass tubes and pretreated *in situ* as above. After the exposures to CO and H_2S, the only gas phase species present at concentrations greater than 5 μmol/g were CO, H_2S, H_2O and H_2 as shown by mass spectrometry. During the exposures, these components were conveniently monitored manometrically by condensing the H_2O in a glass tube at 195 K, condensing the H_2O and H_2S in a glass tube at 77 K, and condensing the CO on dehydrated alumina at 77 K.

Transmission infrared spectra were obtained with a Perkin-Elmer 180 grating spectrometer with the absorbance scale. The double beam mode was used without any compensating sample in the reference beam. The spectral resolu-

tion at 2000 cm^{-1} was set at 2.6 cm^{-1}. All spectra were recorded with the sample at approximately 310 K.

The ^{13}CO (Merck Isotopes, 90% enriched) and the unenriched CO (Matheson, Research) were obtained in glass breakseal bulbs and used without further purification. The O_2 (Matheson, Research) was also used without further purification. The H_2S (Matheson, C.P.) was purified by three freeze-pump-thaw cycles and sublimed at 195 K immediately before use. The alumina was "Alon-C" (Cabot), a fumed alumina with a particle size of ~ 15 nm and a BET surface area of 115 m^2/g.

3. Results

A. Infrared Spectra

(i). Adsorption of H_2S *on Rh/Alumina*

The infrared spectra of alumina and clean and CO-precovered Rh/alumina after exposure to H_2S are shown in Fig. 1. Before exposure to H_2S, there is a broad band in the spectrum at ~ 3700-3000 cm^{-1} due to the OH stretching mode of the hydroxyl groups of the alumina surface. Exposure at 300 K of clean Rh/alumina to 4.5 Torr of H_2S causes four changes in the infrared spectrum. A band appears at 1630 cm^{-1} and there is increased intensity on the lower frequency side of the band at 3700-3000 cm^{-1}. These are assigned to the HOH bending and OH stretching modes, respectively, of molecular water. The very weak band that appears at ~ 2480 cm^{-1} is assigned to an SH stretching mode of an HS or H_2S species involved in hydrogen bonding. For comparison, the asymmetric stretching mode for gaseous H_2S at 2627 cm^{-1} **(30)** is shifted down in frequency through hydrogen bonding to 2544 cm^{-1} in solid H_2S **(31)** and to 2482 cm^{-1} for H_2S dissolved in pyridine **(32)**. It will be argued later that the peak at 2067 cm^{-1} is due to adsorbed CO impurity that is

perturbed by adsorbed sulfur.

After alumina and CO-precovered Rh/alumina are exposed to 4.5 Torr of H_2S at 300 K, the bands due to molecular water are present, indicating that some H_2O is formed. However, these bands are less intense than for those after exposure of Rh/alumina to H_2S. The band at 2480 is present after exposure of CO-precovered Rh/alumina, but not alumina, to H_2S.

(ii). Sequential Adsorption of CO and H_2S

A Rh/alumina sample was exposed to CO and then to H_2S and another sample was exposed to H_2S and then to CO. Their infrared spectra are shown in Fig. 2. After CO is adsorbed on clean Rh/alumina, the intense doublet of the dicarbonyl species at 2103 and 2034 cm^{-1} and the broad band of the bridged-bonded CO near 1850 cm^{-1} are seen (Fig. 2A). A different sample, prepared similarly and having a similar infrared spectrum after adsorption of CO, was then exposed to 10 Torr of O_2 at 300 K. There was a loss of intensity at 2065-2070 cm^{-1} and at 1850 cm^{-1} due to selective removal of the linear and bridging CO, as observed by other workers using similar treatments **(9,14,33)**. Thus, there is intensity due to the linear CO, but it is not resolved from the intense doublet of the dicarbonyl.

For CO adsorbed on H_2S-precovered Rh/alumina, the maximum of the dominant peak is at 2079 cm^{-1} as shown in Fig. 2B, compared to 2060-2070 cm^{-1} for linearly-adsorbed CO on clean Rh/alumina. The broad band of the bridging species is missing completely. The lower frequency peak of the dicarbonyl doublet at ~ 2036 cm^{-1} is now only a shoulder on the peak of the linear CO, while the higher frequency peak is not resolved from that of the linear CO. The integrated intensity of the spectrum decreases by 10% upon evacuating the sample for 2 hr at 300 K.

Upon exposure of CO-precovered Rh/alumina to H_2S, the peak of the bridging CO decreases substantially in intensity and shifts down in frequency from 1850 to 1820 cm^{-1} (Fig. 2A). The spectrum between 2150 and 1950 cm^{-1} increases in intensity by ~ 25% and appears to be similar to a superposition of a dicarbonyl doublet and the spectrum of CO adsorbed on H_2S-precovered Rh/alumina. The latter was subtracted from the spectrum of a CO-precovered surface which had been exposed to H_2S to better resolve the peaks of the dicarbonyl from that of the linear CO. As shown in Fig. 2C, the intensity of the lower frequency peak of the dicarbonyl is reduced by ~ 15-20% upon exposure of a CO-precovered surface to H_2S. Also, the intensity of the peak of the linear CO increases to a value somewhat greater than that after adsorption of CO on an H_2S-precovered surface. Extended exposure of a CO-precovered surface to H_2S (120 hr) causes the intensity of the spectrum to decrease by ~ 25%, compared to that after exposure for 1.5 hr.

(iii). Exchange of Adsorbed CO with $^{13}CO(g)$

We wished to examine the effect of exposure to H_2S on the ability of the CO adsorbed on Rh/alumina to exchange with CO in the gas phase and also to verify that the infrared bands in the region 2200-1700 cm^{-1} are due to CO stretches. To do this, the samples were exposed to excess ^{13}C-enriched CO (enriched CO/adsorbed CO = 200) at 300 K and a pressure of 12 Torr. Nearly all CO adsorbed on H_2S-precovered Rh/alumina exchanges with $^{13}CO(g)$ in 20 hr, as shown in Fig. 3B. The shoulder at ~ 2070 cm^{-1} is assigned to adsorbed ^{12}CO that either does not exchange with $^{13}CO_{(g)}$ or that is from the 10% ^{12}CO in the ^{13}C-enriched $CO_{(g)}$ used for the exchange. The exchange that takes place is ~ 90% complete after 0.5 hr. This is somewhat slower than the exchange in the absence of H_2S, which is complete in ≤ 0.2 hr **(10)**.

Much of the CO adsorbed on Rh/alumina, which had then been subsequently exposed to H_2S also exchanges with $^{13}CO_{(g)}$ in 20 hr, as shown in Fig. 3A. However, a significant fraction of the adsorbed species with infrared intensity at 2070-2080 cm^{-1} does not exchange. This is indicated by the peak at ~ 2078 cm^{-1} and the loss of intensity between the peaks of the dicarbonyl, both of which are now resolved at 2051 and 1988 cm^{-1}. The high frequency peak of the mixed dicarbonyl, $Rh(^{12}CO)(^{13}CO)$ would be expected at ~ 2086 cm^{-1} **(10)**. It may contribute to the 2078 cm^{-1} peak and shift it somewhat higher in frequency. The bridged-bonded CO that remains after exposure to H_2S and has its CO stretch at 1820 cm^{-1} does not exchange with $^{13}CO(g)$. Again, the exchange that does occur is ~ 90% complete after 0.5 hr.

(iv). Reactivity of Adsorbed CO Toward O_2

The effect of exposure to H_2S on the reactivity of the CO adsorbed on Rh/alumina toward O_2 was also investigated. The samples were exposed to excess O_2 (O_2/adsorbed CO = 200) at 300 K and a pressure of 12 Torr. Even after 20 hr, the intensity of the peaks from CO adsorbed on an H_2S-precovered surface is reduced by only ~ 35%, as shown in Fig. 3B. In the absence of H_2S, the linear and bridging CO species are removed by O_2 within 0.2 hr as found for similar samples here and by other workers **(14,33)**. O_2 preferentially removes the, linearly-adsorbed CO, allowing the higher frequency peak of the $Rh(^{13}CO)_2$ doublet to become visible as a shoulder at ~ 2051 cm^{-1} and supporting the assignment of the 1988 cm^{-1} peak to the lower frequency peak of this doublet. At least some of the adsorbed species that did not exchange with $^{13}CO(g)$ are also not removed by O_2, since the shoulder at ~ 2070 cm^{-1} is still present.

CO adsorbed on Rh/alumina which is then exposed to H_2S is also only slowly removed by O_2. Much of the peak at ~ 2078 cm^{-1} due to adsorbed species that

did not exchange with $^{13}CO(g)$ remains after the sample is exposed to O_2. An additional check that the peak at 2078 cm^{-1} is not from adsorbed hydrogen rather than unreactive adsorbed CO was performed. After exposure to O_2 the sample was evacuated and exposed to 12 Torr of D_2 at 300 K. A very broad peak with a maximum at 2700 cm^{-1} due to OD stretching is observed, indicating that D_2 is able to dissociated on this surface. The infrared spectrum between 2200 and 1700 cm^{-1}, however, is unchanged. Adsorbed hydrogen would have been expected to exchange with dissociated D_2 and infrared peaks due to adsorbed hydrogen would have been shifted down in frequency by a factor of $\sqrt{2}$ for adsorbed deuterium.

B. Gas Uptake and Evolution Measurements

Shown in Table 1 are the results of manometric measurements of the H_2S and CO taken up, that is, removed from the gas phase, by various surfaces. On clean Rh/alumina, 220 x 10^{-6} mol of H_2S per gram of sample are taken up, or nearly 1.1 molecules of H_2S for each Rh atom in the sample. Of the hydrogen in the H_2S taken up, 28% appears in the gas phase as H_2, most of it within 0.25 hr. To test for reversible adsorption of the H_2S and for the presence of H_2O, which was suggested by the infrared spectra in Fig. 1, the sample was heated at 373 K for 2 hr while continuously trapping the desorbing H_2S and H_2O at 77 K. We see in Table 2 that of the H_2S taken up, 38 μmol/g (H_2S/Rh = 0.19), or 17%, desorbs as H_2S, in addition to 5 μmol/g of $H_{2(g)}$ (H_2/Rh = 0.03). Also, a considerable amount of H_2O desorbs, ~ 70 μmol/g (H_2O/Rh = 0.36) or 32% of the amount of H_2S taken up. Due to adsorption of H_2O on the alumina and on the walls of the vacuum system, the uncertainty in the measurement of H_2O is large, and is estimated to be ± 25 μmol/g. We cannot be sure what fraction of the H_2O which desorbs upon heating is formed upon adsorption of H_2S at 300 K and what fraction is formed

while heating. The amount of CO that adsorbs on this sample after this heating procedure is the same, within experimental error, as that which adsorbs on unheated, H_2S-precovered Rh/alumina.

The adsorption of H_2S on alumina and the desorption of species upon heating at 373 K were also carried out. Of the 36 μmol/g of H_2S taken up, 28 μmol/g, or 78% desorbs as H_2S, in addition to ~ 6 μmol/g of H_2O. Thus, 74% of the H_2S that desorbs from Rh/alumina may be attributed to desorption from the alumina support, while most of the water is formed only in the presence of Rh.

After exposure of CO-precovered Rh/alumina to 4.5 Torr of H_2S for 0.25 hr, 104 μmol/g of H_2S are taken up and 8 μmol/g of $H_{2_{(g)}}$ are evolved. The amount of H_2S taken up that does not produce $H_{2_{(g)}}$ is equal, within experimental error, to that taken up in the same time in the absence of preadsorbed CO. Also, after 0.25 hr, only 14 μmol/g of CO, or 5% of that adsorbed previously, was displaced into the gas phase. Between 0.25 and 10 hr of exposure to H_2S, the amount of H_2S taken up is similar to the amounts of $H_{2_{(g)}}$ evolved and CO displaced into the gas phase during this period.

The effect of exposing Rh/alumina to H_2S on the amount of CO that it takes up was also examined. On clean Rh/alumina 224 μmol/g of CO (CO/Rh = 1.15) is taken up within 0.25 hr, and 268 μmol/g (CO/Rh = 1.38) is taken up in 20 hr. On an H_2S-precovered Rh/alumina, the CO/Rh ratios are only 0.10 and 0.21 at 0.25 and 20 hr, respectively, or 8% and 15%, respectively, of those in the absence of preadsorbed H_2S. Less than 1 μmol/g of CO adsorbs on the alumina support.

Less than 1 μmol/g of H_2S could be displaced into the gas phase by exposure of H_2S-precovered Rh/alumina to CO. To determine if there was any hydrogen adsorbed on the Rh/alumina after it was exposed to H_2S, we attempted to displace adsorbed hydrogen by CO. To prevent adsorbed hydrogen from desorbing

upon evacuation, the H_2S which was not taken up by the Rh/alumina was removed by condensing at 77 K and 99% of the $H_{2(g)}$ above the sample was removed without evacuating the sample itself. After then exposing the sample to CO, there was less than 1 μmol/g of $H_{2(g)}$.

4. Discussion

A. Adsorption of H_2S on Rh/Alumina

When H_2S adsorbs on clean Rh/alumina, $H_2(g)$ is evolved. H_2S has been shown to adsorb dissociatively on Group VIII transition metal crystals **(34-36)** and films **(37-39)**, producing $H_{2(g)}$ and adsorbed sulfur:

$$H_2S \rightarrow S_{(ad)} + H_2 \qquad (1)$$

This reaction occurs at temperatures as low as 193 K **(37-39)**. The sulfur adsorbed on crystal surfaces of Rh **(36)** and other metals **(40)** was shown to occupy high coordination sites by using Low Energy Electron Diffraction. The surfaces of Rh **(40)** and Pt **(34,35)** crystals that had been heated in excess H_2S at 525-575 K had 0.25 and 0.5-0.75 adsorbed sulfur atoms per surface metal atom, respectively.

There is evidence that there is also adsorbed sulfur in high coordination sites on the clustered Rh of the present study. Preexposing Rh/alumina to H_2S prevents CO from absorbing in the bridging mode, as shown in the infrared spectra of Fig. 2B. In addition, bridging CO is displaced by subsequent exposure to H_2S. Preadsorbing CO does, however, slow the dissociation of H_2S, as reflected in the amount of $H_{2(g)}$ evolved (Table 1).

We also wish to compare the coverage of sulfur adsorbed on the metal crystals with that on the Rh/alumina. The amount of adsorbed sulfur atoms is equal to the amount of $H_{2(g)}$ evolved at or below 373 K, 66 μmol/g, if all of the

$H_{2(g)}$ is produced by reaction (1). We can calculate the amount of Rh that is involved in dicarbonyl formation, that is on the surface of the Rh clusters, and that is not involved in bonding to CO by using the results of Duncan et al. **(21)**, who studied Rh/alumina samples that were prepared similarly to those used here.

By using CO uptake and primarily ^{13}C NMR measurements, they found that the ratio of linear to bridging CO was 2.0, that the ratio of CO molecules adsorbed on the clustered Rh to the surface Rh atoms of the clusters was 0.75, and that 12% of the Rh of a freshly prepared sample was not involved in bonding to CO in any of the three adsorption modes. Assuming that these are true for the samples in the present study, we can use the ratio of the total CO molecules adsorbed to the total Rh atoms in the sample to calculate the distribution of Rh in the dicabonyl, clustered and inactive forms (as well as the distribution of CO in the dicarbonyl, linear and bridging modes). The results of this calculation are given in Table 3. The sensitivity of the calculated distributions to the assumptions made is such that an error of 5% in the amount of inactive Rh or an error of 0.05 in the ratio of CO to surface Rh atoms for the Rh clusters or an error of 0.1 in the overall CO to Rh ratio would result in an error of 15-20% in the calculated values.

The calculated ratio of adsorbed sulfur atoms to the surface Rh atoms of the Rh clusters is then 66/59 = 1.1. This is larger than any of the values found for Rh **(36)** or Pt **(34,35)** crystal surfaces (0.25-0.75). The larger values for Rh/alumina indicate either that there is more extensive sulfur deposition on the clustered Rh than on the crystal surfaces or that some $H_{2(g)}$ is produced by adsorption of H_2S on the dicarbonyl-forming Rh. We are unable to differentiate between these possibilities at this time.

In the present study, H_2O is also formed upon exposure of the samples to H_2S. The infrared spectra in Fig. 1 suggest that more H_2O is produced when H_2S is adsorbed at 300 K on clean Rh/alumina than on alumina. This is in accord with the amounts of H_2O that desorb upon heating these surfaces at 373 K. Only ~ 9% of H_2O formed by adsorption of H_2S on clean Rh/alumina can be accounted for by adsorption of H_2S on the alumina.

The H_2O may be formed by the reaction of H_2S with surface oxygen:

$$H_2S + O^{2-}_{(ad)} \rightarrow H_2O + S^{2-}_{(ad)} \qquad (2)$$

It is likely that this reaction is facilitated by the dicarbonyl-forming Rh^I, rather than the clustered Rh. The Rh^I facilitates the reaction of CO with surface oxygen at 425-525 K **(22)**. The amount of CO_2 produced upon heating Rh/alumina in CO, 63 μmol/g, is similar to the amount of H_2O produced from the adsorption of H_2S on Rh/alumina, 64 μmol/g, and is approximately half of the amount of Rh^I that is present before these reactions. Reactions similar to (2) may occur in the treatment of metal oxides with H_2S in preparing metal sulfide catalysts **(41)**.

Of the hydrogen in the H_2S that is taken up by clean Rh/alumina at 300 K, all but ~ 20% (46 μmol/g) is accounted for by the H_2 evolved at 300 and 373 K and by the H_2S and H_2O desorbed at 373 K. Only 2 μmol/g of H_2 are taken up by clean Rh/alumina at 373 K. Thus, the hydrogen that is not accounted for is not bound directly to the Rh. It is presumably either still bound to the sulfur or is bound to the surface oxygen but is not desorbed as H_2S or H_2O below 373 K. This hydrogen may contribute to the bands in the infrared spectra (Fig. 1) that were assigned to SH and OH groups.

Preadsorbed CO does not inhibit greatly the uptake of H_2S by Rh/alumina. The amount of H_2 that is evolved upon exposure of CO-precovered Rh/alumina to H_2S for 0.25 and for 10 hr and after heating to 373 K is 14, 41 and 83%,

respectively, of the H_2 that evolves under the same conditions from Rh/alumina that had been exposed only to H_2S. This suggests that the amount of H_2S taken up that eventually dissociates to yield H_2 is similar for clean and CO-precovered Rh/alumina, but that the dissociation itself is inhibited by the CO. In contrast, the H_2S taken up by clean Rh/alumina that produces H_2O appears to be inhibited by preadsorbed CO, as shown by the infrared spectra (Fig. 1) and by the amount of H_2O that desorbs upon heating (Table 2). The difference in the amount of H_2O that desorbs from clean and CO-precovered Rh/alumina is similar to the diference in the amount of H_2S taken up by the two surfaces. As with H_2S adsorbed on clean Rh/alumina, a substantial amount (62 μmol/g) of the hydrogen in the H_2S adsorbed at 300 K on CO-precovered Rh/alumina is not accounted for by the H_2, H_2S and H_2O desorbed at or below 373 K. Again, the hydrogen may be bound as SH and/or OH groups based on the observation of infrared bands that were assigned to these species.

B. Effect of H_2S on the Adsorption of CO

Preadsorption of H_2S on Rh/alumina greatly inhibits formation of the dicarbonyl species and adsorption of CO in the bridging but not in the linear mode, as indicated by the infrared spectra in Fig. 2B. The amount of CO taken up by H_2S-precovered Rh/alumina, 41 μmol/g, may be compared to the calculated amount of CO adsorbed in the dicarbonyl and linear modes on clean Rh/alumina, 224 and 30 μmol/g, respectively. Thus, a maximum of 37% of the dicarbonyl-forming Rh can adsorb one CO. We may expect some CO to adsorb in the linear mode on the clustered Rh, based on the results of others using supported Ni **(24-28)**. However, there is less CO adsorbed in the linear mode on a clean surface than CO on an H_2S-precovered surface. Therefore, it seems likely that, on an H_2S-precovered surface, CO is adsorbed linearly on both the clustered and

dicarbonyl-forming Rh.

The effect of H_2S on the adsorption of CO on Rh/alumina is less if the CO is adsorbed before than after exposure to H_2S. Only 25 of the 268 μmol/g, or 9% of the CO adsorbed on a clean surface is displaced into the gas phase by exposure to 4.5 Torr of H_2S for 1.5 hr. The intensity of the infrared peak of the bridging CO is reduced by a factor of ~ 4 by exposure to H_2S, probably due to displacement of the CO from the high coordination sites preferred by adsorbed sulfur, as discussed above.

The infrared peaks of the dicarbonyl also decrease somewhat in intensity upon exposure of CO-precovered Rh/alumina to H_2S for 1.5 hr. It is likely that a significant fraction of the 25 μmol/g of displaced CO was bound in the dicarbonyl and bridging modes. Therefore, at least some of the 30 μmol/g CO that is bound linearly to the clustered Rh appears to be present after exposure of Rh/alumina to H_2S for 1.5 hr. However, there must be a loss of 10-25 μmol/g, or 4-10% in the combined amount of CO adsorbed in the linear and dicarbonyl modes, depending on whether the bridging CO is displaced to other adsorption sites or into the gas phase. Surprisingly, there is an increase of $\sim 25\%$ in the infrared intensity between 2150 and 1950 cm^{-1} under these conditions.

It would seem possible that there could be infrared intensity in the region 2150-1950 cm^{-1} due to adsorbed hydrogen formed by dissociation of the H_2S. Metal-hydrogen stretching modes in metal hydride complexes occur at these frequencies **(38)**. Evidence that there is little adsorbed hydrogen present (< 5 μmol/g) after adsorption of H_2S on clean Rh/alumina was presented above. When clean Rh/alumina samples prepared similarly to those used here were exposed to 500 Torr of H_2, no changes in the infrared spectrum resulted **(43)**. Thus, even if adsorbed hydrogen was present, it is not likely that it would be

observed in the infrared spectra. In addition, Kroeker et al. **(29)** did not observe any vibrational modes in the tunneling spectrum due to deuterium after Rh/alumina was exposed to D_2S. Thus, the increase of infrared intensity in the region 2150-1950 cm^{-1} is not due to adsorbed hydrogen.

Instead, the increase is attributed to an average increase in the infrared extinction coefficient of CO adsorbed in the linear and/or dicarbonyl modes. We can estimate the extinction coefficient of CO adsorbed linearly on clean Rh/alumina by exposing CO-precovered Rh/alumina to excess O_2 at 300 K and at a pressure of 10 Torr and then measuring the loss in intensity in the region 2150-2000 cm^{-1}. This treatment does not change the intensity of peaks of the dicarbonyl but removes the peaks of the linear and bridging CO **(9,14,33)**. The amount of linearly-adsorbed CO is estimated as above. The extinction coefficient for CO adsorbed on H_2S-precovered Rh/alumina is obtained directly from the CO uptake and the intensity of the infrared spectrum [Fig. 2B(b)], since CO adsorbs almost exclusively in the linear mode. We find that CO adsorbed linearly on H_2S-precovered Rh/alumina has an integrated extinction coefficient which is ~ 5 times that for CO adsorbed on clean Rh/alumina.

We may suppose that much of the increase of the infrared intensity in the region 2150-1950 cm^{-1} upon exposure of CO-precovered Rh/alumina to H_2S could also be due to an increase in the extinction coefficient of the linearly-adsorbed CO by the H_2S. We can remove much of the contribution of the linear CO from the spectrum by subtracting from the spectrum, that of CO adsorbed onto H_2S-precovered Rh/alumina, which was done in Fig. 2C. It can then be seen that the peaks of the dicarbonyl have decreased in intensity compared to those before exposure to H_2S. A displacement into the gas phase of both CO groups of 11% of the dicarbonyls would account for all of the CO displaced into the gas phase by exposure to H_2S. The CO displaced can also be accounted for if all of

the bridging CO and one CO of 19% of the dicarbonyls are displaced.

In studies by other workers using supported Ni **(25,26,28)**, it was sometimes noticed that the intensity of the bands due to linearly-bound CO could be increased by either exposure of the surface to H_2S before adsorbing CO or by exposing a CO-precovered surface to H_2S. This was interpreted as indicating that the number of linear CO species was increased by exposure to H_2S **(28)**. The results of the present study would suggest that the increase in intensity of the band due to linear CO could alternatively be caused by an increase in its infrared extinction coefficient.

From the arguments presented above, the infrared peak at 2067 cm^{-1} which is present after clean Rh/alumina is exposed to H_2S is not due to adsorbed hydrogen. One might suppose that the CO_2 impurity (0.1%) in the H_2S could produce adsorbed CO by decomposition on the Rh. However, only 1 μmol/g of CO_2 is adsorbed on a clean surface at 300 K. Also there is no change in the infrared spectrum between 2200 and 1700 cm^{-1} after exposure to 50 Torr of CO_2 at 300 K. **(22)**. There is, however, a small amount of adsorbed CO present on the "clean" surface, as shown by the very weak band at ~ 2040 cm^{-1} in the background spectra of Fig. 2B. Subsequent adsorption of H_2S could increase the intensity of the band of linear CO by increasing its extinction coefficient, as described above, or by displacing bridging CO to linear adsorption sites. The peak could be shifted up in frequency from ~ 2040 cm^{-1} before exposure to H_2S by an electronic effect of adsorbed sulfur and/or by interactions with other adsorbed CO **(44)**.

The results in the present study are somewhat different from those of other investigators. After exposure of H_2S-precovered Rh/silica to CO, Guerra **(23)** observed the band of linear CO but not that of bridging CO in the infrared spec-

trum, as found here and by other workers using supported Ni **(24-28)**. However, Kroeker et al. **(29)** did not observe bands in the inelastic electron tunneling spec trum from either linear or bridging CO on H_2S-precovered Rh/alumina. Kroeker et al. also did not observe a band from the dicarbonyl, in agreement with the present results (the bands of the dicarbonyl were extremely weak), whereas Guerra observed bands which most likely should be assigned to dicarbonyl species. Exposure of a CO-precovered surface to H_2S decreased the intensity of the bands of the dicarbonyl and bridging CO more in the study of Kroeker et al. than in the present study. The difference in results most likely indicates the sensitivity of the nature of the supported Rh to the support used and the method of preparation.

C. Effect of H_2S Adsorption on the Reactivity of Adsorbed CO

The dicarbonyl species and most of the CO adsorbed linearly on Rh/alumina that had been exposed to H_2S before or after exposure to CO were found to exchange with $^{13}CO(g)$ within 0.5 hr. Since the desorption of the CO is much slower than this, as shown by its stability toward evacuation, the exchange must take place by an associative mechanism, as found for Rh/alumina without H_2S **(10)**. The bridging species that remain after H_2S adsorption on a CO-precovered surface does not exchange with $^{13}CO(g)$ or with adsorbed CO that exchanges with $^{13}CO(g)$, even after 20 hr. Since the exchange of linear and bridging CO would be expected to take place much faster than this **(45)**, these bridging CO groups must be isolated from other adsorbed CO, presumably by adsorbed S, HS or H_2S species.

In contrast to the exchange of adsorbed CO with $^{13}CO(g)$, the removal of adsorbed CO with O_2 is inhibited greatly by previous exposure of Rh/alumina to H_2S. The presence of adsorbed dioxygen has been proposed to explain isotopic

exchange experiments of O_2 over Rh/alumina that had been derived from $Rh_6(CO)_{16}$ dispersed on alumina **(13)**. We might have expected for the samples used here that dioxygen could displace adsorbed CO as in the exchange reaction with $^{13}CO(g)$. Arguing against this, however, is that H_2S inhibits the removal of adsorbed CO by $^{13}CO(g)$ much less than by O_2. The rate of oxidation of adsorbed CO by O_2 over a Pt(100) surface that had been partially covered with adsorbed sulfur by decomposition of H_2S was shown to be limited by the rate of dissociative adsorption of O_2 **(34)**. Inhibition of O_2 dissociation by H_2S could also prevent CO removal by O_2 in the present study.

5. Conclusions

We have studied the adsorption of H_2S and its interaction with CO on Rh/alumina by using infrared spectroscopy and gas uptake and evolution measurements. We find that:

1. On clean Rh/alumina, H_2S adsorbs dissociatively at 300 K, producing H_2, and also reacts with surface oxygen at $\leq$ 373 K, producing water.

2. Little or no CO adsorbs in the dicarbonyl and bridging modes on an H_2S-precovered surface, while the amount of adsorption in the linear mode is not changed greatly. H_2S adsorbing onto a CO-precovered surface displaces much of the bridging CO, but only slowly removes the dicarbonyl and linear CO.

3. Exposure of Rh/alumina to H_2S strongly inhibits the removal of adsorbed CO by O_2, but exchange of adsorbed CO with CO(g) takes place readily.

From the present results, we can conclude that the particular resistance of Rh catalysts to poisoning by SO_2 **(4)** cannot be due to the presence of dicarbonyl-forming Rh^I species that do not bind sulfur. It is possible that the Rh^I and

clustered Rh may react differently toward H_2S and SO_2 or that the ease of removal of sulfur from these sites may be different.

Acknowledgments

This study was supported by the Office of Naval Research under contract NOOO14-79-F-0014. We thank Dr. G. R. Rossman for the use of his infrared spectrometer and M. Templeton for obtaining the mass spectra. Helpful comments were offered by Drs. W. H. Weinberg and T. M. Duncan.

References

1. Oudar, J., Catal. Rev. Sci. Eng. **22**, 171 (1980).

2. Madon, R. J. and Shaw, H., Catal. Rev. Sci. Eng. **15**, 69 (1977).

3. Shelef, M., Otto, K. and Otto, N. C., Advan. Catal. **27**, 311 (1978).

4. Summers, J. C. and Baron, K., J. Catal. **57**, 380 (1979).

5. Tsai, J., Agrawal, P. K., Sullivan, D. R., Katzer, J. R. and Manogue, W. H., J. Catal. **61**, 204 (1980).

6. Yang, A. C. and Garland, C. W., J. Phys. Chem. **61**, 1504 (1957).

7. Arai, H. and Tominaga, H., J. Catal. **43**, 131 (1976).

8. Yao, H. C. and Rothschild, W. G., J. Chem. Phys. **68**, 4774 (1978).

9. Primet, M., J. Chem. Soc. Farad. Trans. I **74**, 2570 (1978).

10. Yates, J. T., Jr., Duncan, T. M., Worley, S. D. and Vaughan, R. W., J. Chem. Phys. **70**, 1219 (1979).

11. Yates, D. J. C., Marrell, L. L. and Prestridge, E. B., J. Catal. **57**, 41 (1979).

12. Smith, A. K., Hugues, F., Theolier, A., Basset, J. M., Ugo, R., Zanderighi, G. M., Bilhou, J. L., Bilhou-Bougnol, V. and Graydon, W. F., Inorg. Chem. **18**, 3104 (1979).

13. Watters, K. L., Howe, R. F., Chojnacki, T. P., Fu, C-M., Schneider, R. L. and Wong, N.-B., J. Catal. **66**, 424 (1980).

14. Rice, C. A., Worley, S. D., Curtis, C. W., Guin, J. A. and Tarrer, A. R., J. Chem. Phys. **74**, 6487 (1981).

15. Kroeker, R. M., Kaska, W. C. and Hansma, P. K., J. Catal. **57**, 72 (1979).

16. Sheppard, N. and Nguyen, T. T., Advan. Infrared Raman Spectr. **5**, 67 (1978).

17. Kellner, C. S. and Bell, A. T., J. Catal. **71**, 296 (1981).

18. Smith, A. K., Besson, B., Basset, J. M., Psaro, R., Fusi, A. and Ugo, R., J. Organometal. Chem. **192**, C31 (1980).

19. Deeba, M. and Gates, B. C., J. Catal. **67**, 303 (1981).

20. Knozinger, H. and Zhao, Y., J. Catal. **71**, 337 (1981).

21. Duncan, T. M., Yates, J. T., Jr. and Vaughan, R. W., J. Chem. Phys. **73**, 975 (1980).

22. Gleeson, J. W. and Vaughan, R. W., submitted.

23. Guerra, C. R., J. Col. Interface Sci. **29**, 229 (1969).

24. Garland, C. W., J. Phys. Chem. **63**, 1423 (1959).

25. Crell, W., Hobert, H. and Knappe, B., Z. Chem. **8**, 396 (1968).

26. Marx, von G., Hobert, H., Hopfe, V., Knappe, B., Vogelsberger, W., Mackrodt, P. and Meyer, K., Z. Chem. **12**, 444 (1972).

27. Rochester, C. H. and Terrell, R. J., J. Chem. Soc. Farad. Trans. I, 609 (1977).

28. Rewick, R. T. and Wise, H., J. Phys. Chem. **82**, 751 (1978).

29. Kroeker, R. M., Kaska, W. C. and Hansma, P. K., J. Catal. **63**, 487 (1980).

30. Allen, H. C. and Plyler, E. K., J. Chem. Phys. **25**, 1132 (1956).

31. Reding, F. P. and Hornig, D. F., J. Chem. Phys. **27**, 1024 (1957).

32. Josien, M. L. and Saumagne, P., Bull. Soc. Chim. France, 937 (1956).

33. Cavanagh, R. R. and Yates, J. T., Jr., J. Chem. Phys. **74**, 4150 (1981).

34. Bonzel, H. P. and Ku, R., J. Chem. Phys. **58**, 4617 (1973); **59**, 1641 (1973).

35. Fischer, T. E. and Kelemen, S. R., J. Catal. **53**, 24 (1978). (1980).

36. Hengrasmee, S., Watson, P. R., Frost, D. C. and Mitchell, K. A. R., Surface Sci. **87**, L249 (1979); **92**, 71 (1980).

37. Saleh, J. M., Kemball, C. and Roberts, M. W., Trans. Faraday Soc. **57**, 1771 (1961).

38. Roberts, M. W. and Ross, J. R. H., Trans. Faraday Soc. **62**, 2301 (1966).

39. Saleh, J. M., Trans. Faraday Soc. **67**, 1830 (1971); **66**, 1830 (1970).

40. Somorjai, G. A. and Van Hove, M. A., Structure and Bonding **38**, 123 (1979).

41. Weisser, O. and Landa, S., *Sulfide Catalysts, Their Properties and Applications*, p. 23, Pergamon Press, New York, 1973.

42. Kaesz, H. D. and Saillant, R. B., Chem. Rev. **72**, 231 (1972).

43. Yates, J. T., Jr., Worley, S. D., Duncan, T. M. and Vaughan, R. W., J. Chem. Phys. **70**, 1225 (1979).

44. Crossley, A. and King, D. A., Surface, Sci. **68**, 528 (1977).

45. Engel, T. and Ertl, G., Advan. Catal. **28**, 1 (1979).

46. Yates, J. T., Jr., Duncan, T. M. and Vaughan, R. W., J. Chem. Phys. **71**, 3908 (1979).

Figure Captions

Figure 1. Infrared spectra of H_2S adsorbed at 300 K on *(a)* Rh/alumina for 3.5 hr, *(b)* CO-precovered Rh/alumina for 1.5 hr, and *(c)* alumina for 1.5 and 3.5 hr. The background is the spectrum of Rh/alumina before exposure to H_2S. The samples were evacuated for 0.2 hr following exposure to H_2S before the spectra were recorded. The peaks in the region 2200-1700 cm^{-1} are due to adsorbed CO.

Figure 2. Infrared spectra for H_2S and CO adsorbed sequentially on Rh/alumina at 300 K. **A.** *(a)* A clean surface exposed to 2.5 Torr of ^{12}CO for 20 hr; *(b)* the sample in *(a)*, evacuated for 0.2 hr, then exposed to 5 Torr of H_2S for 1.5 hr; *(c)* for 120 hr. **B.** *(a)* A clean surface exposed to 5 Torr of H_2S for 3.5 hr and evacuated for 0.2 hr; *(b)* the sample in *(a)*, exposed to 2 Torr of ^{12}CO for 20 hr. The background is the spectrum before exposure to H_2S. **C.** The difference spectrum between a CO-precovered surface exposed to H_2S (**A** *(b)*) and CO adsorbed on an H_2S-precovered surface (**B** *(b)*). The spectrum of CO adsorbed on a clean surface (**A** *(a)*) is shown for comparison.

Figure 3. Infrared spectra of the exchange of $^{13}CO_{(g)}$ and the reaction of O_2 with Rh/alumina that had been exposed sequentially to H_2S and ^{12}CO. **A.** A CO-precovered surface exposed to H_2S for 120 hr [same as Fig. 2A(c)] *(a)* evacuated for 1 hr, then exposed to 10 Torr of ^{13}CO for 20 hr; *(b)* the sample in (a), evacuated for 0.2 hr, then exposed to 10 Torr of O_2 for 20 hr. **B.** *(a)* An H_2S-precovered surface exposed to 2 Torr of ^{12}CO for 20 hr [same as Fig. 2B*(b)*]; *(b)* the sample in *(a)* evacuated for 2 hr, then exposed to 10 Torr of ^{13}CO for 20 hr; *(c)* the

sample in *(b)* evacuated for 0.2 hr, then exposed to 10 Torr of O_2 for 20 hr.

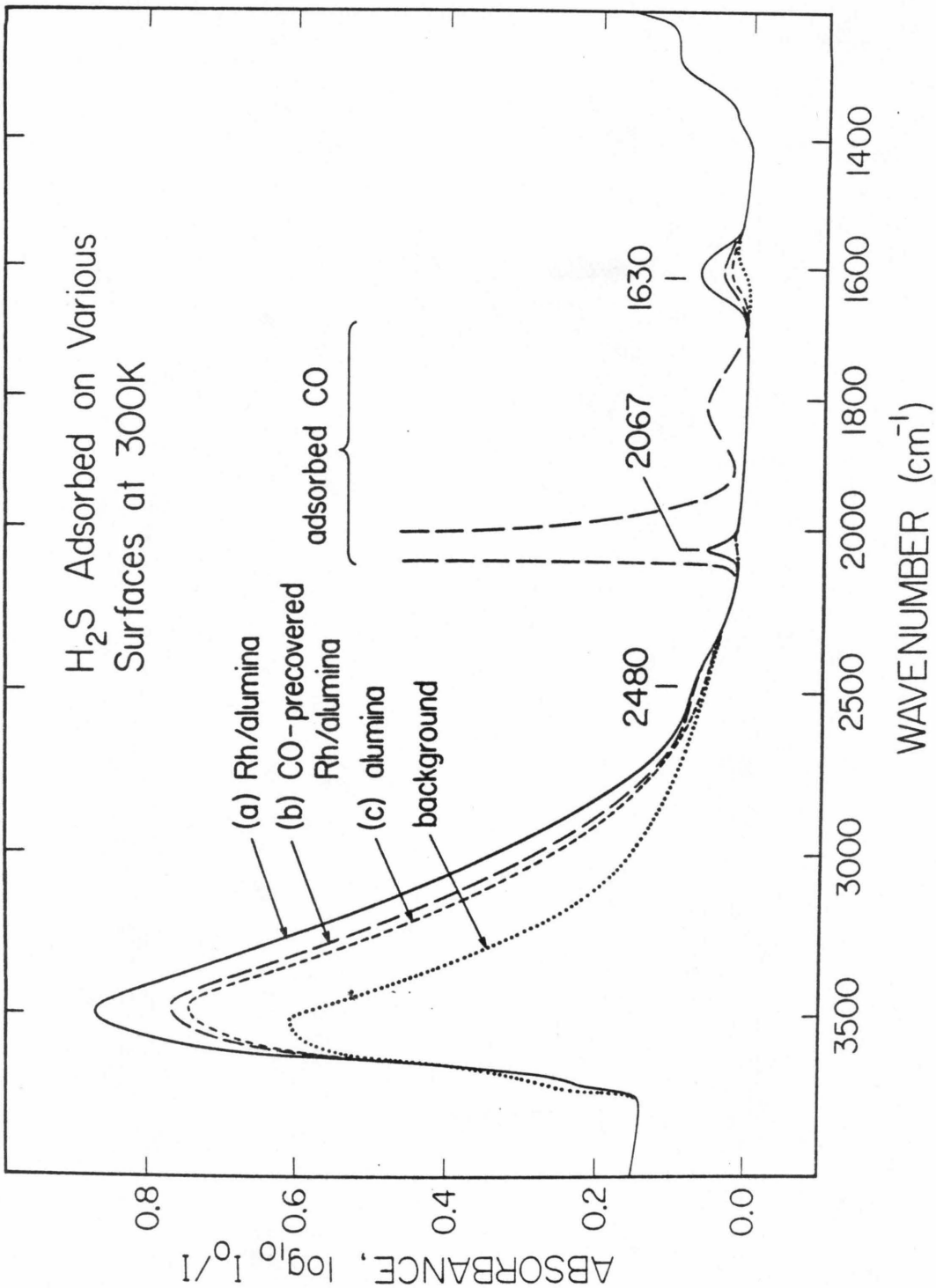
H_2S Adsorbed on Various Surfaces at 300K
(a) Rh/alumina
(b) CO-precovered Rh/alumina
(c) alumina
background
adsorbed CO
2480
2067
1630
ABSORBANCE, $\log_{10} I_0/I$
0.0
0.2
0.4
0.6
0.8
3500
3000
2500
2000
1800
1600
1400
WAVENUMBER (cm^{-1})

Figure 1

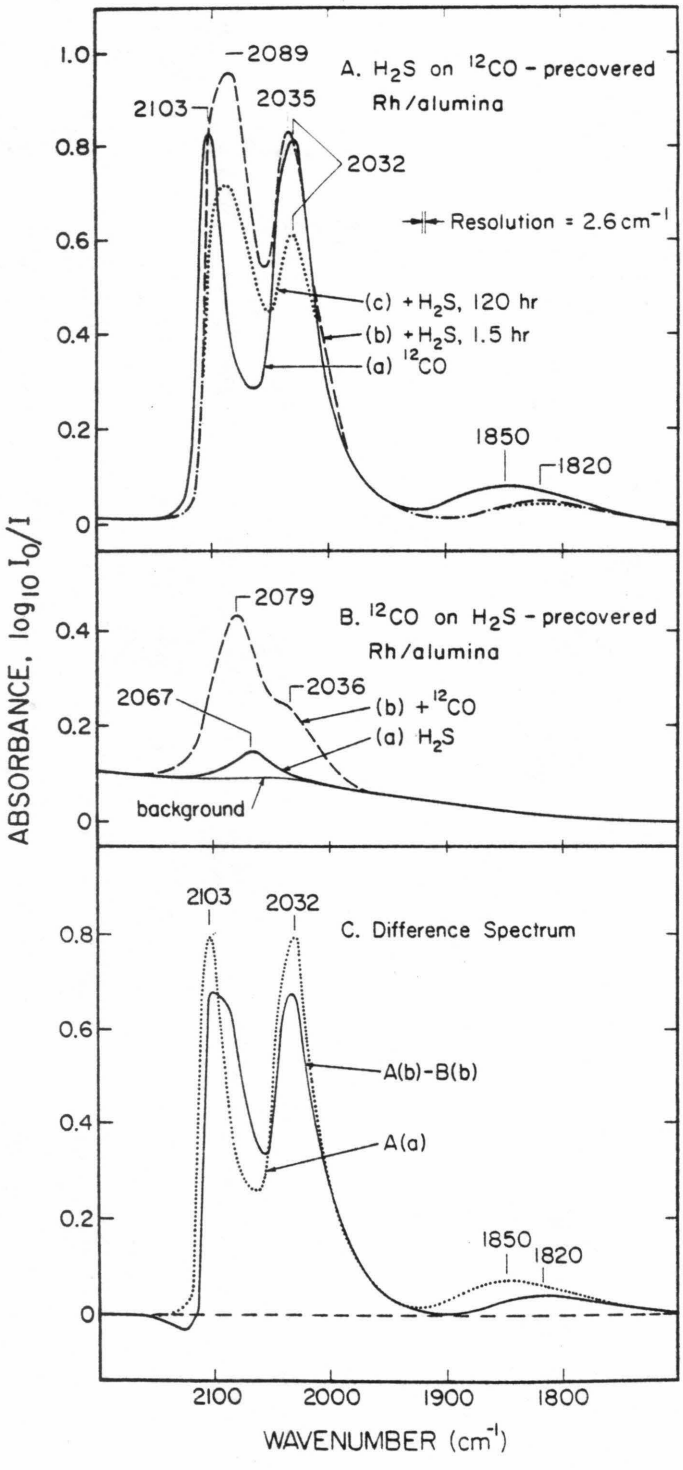
A. H_2S on ^{12}CO - precovered Rh/alumina
2089
2103
2035
2032
Resolution = 2.6 cm^{-1}
(c) + H_2S, 120 hr
(b) + H_2S, 1.5 hr
(a) ^{12}CO
1850
1820
B. ^{12}CO on H_2S - precovered Rh/alumina
2079
2067
2036
(b) + ^{12}CO
(a) H_2S
background
C. Difference Spectrum
2103
2032
A(b)-B(b)
A(a)
1850
1820
ABSORBANCE, $\log_{10} I_0/I$
WAVENUMBER (cm^{-1})

Figure 2

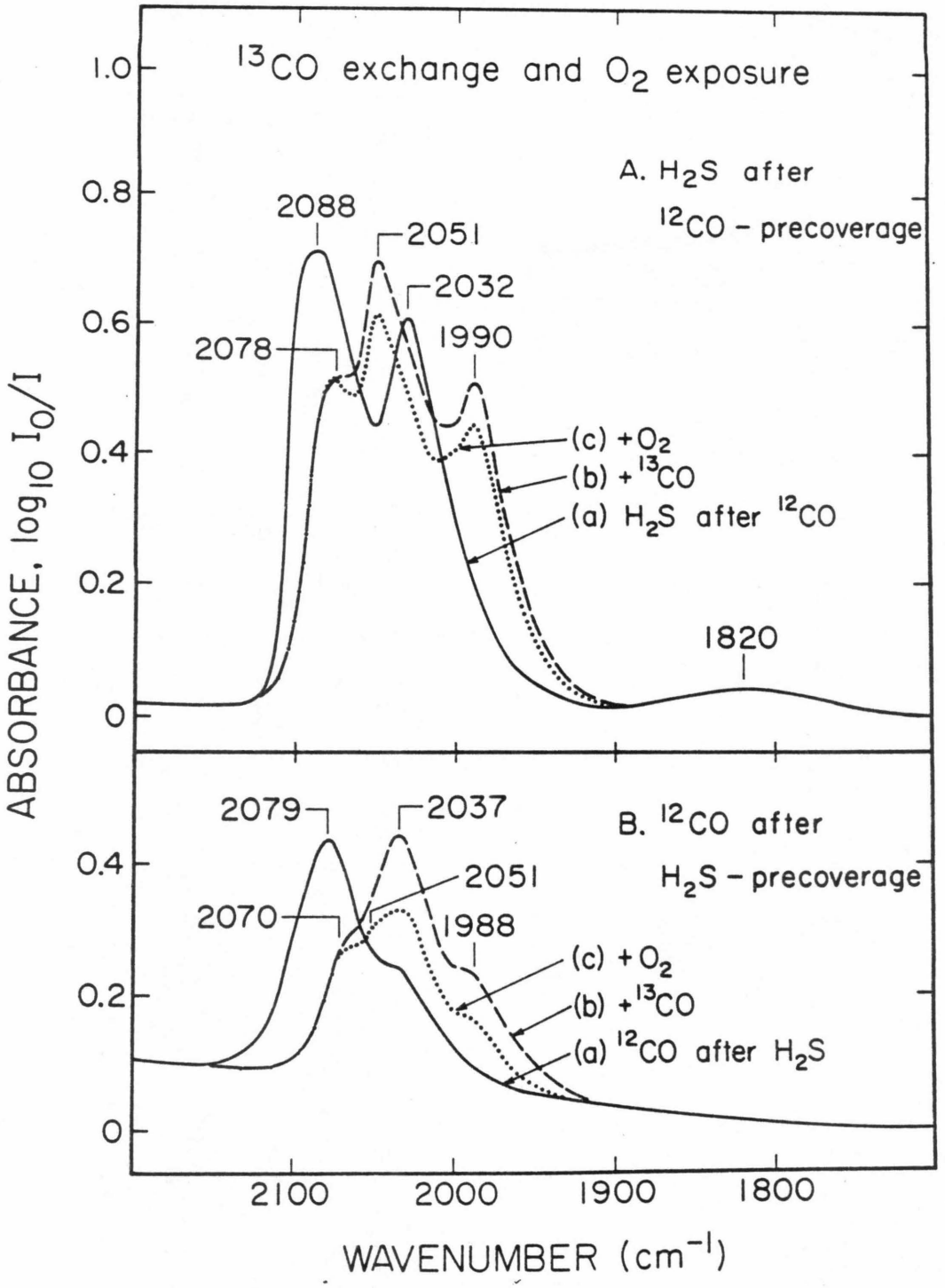
^{13}CO exchange and O_2 exposure
A. H_2S after ^{12}CO – precoverage
2088
2051
2032
1990
2078
(c) + O_2
(b) + ^{13}CO
(a) H_2S after ^{12}CO
1820
B. ^{12}CO after H_2S – precoverage
2079
2037
2051
2070
1988
(c) + O_2
(b) + ^{13}CO
(a) ^{12}CO after H_2S
ABSORBANCE, $\log_{10} I_0/I$
1.0
0.8
0.6
0.4
0.2
0
2100
2000
1900
1800
WAVENUMBER (cm^{-1})

Figure 3

Table 1

The Amounts of H_2S and CO Taken up by Various Surfaces and of Gases Evolved during their Adsorption at 300 K. [a-c]

Adsorbate	Surface	Time of Exposure (hr)	Uptake	Preadsorbate Displaced into Gas Phase	H_2(g) Evolved
H_2S	Rh/alumina	0.25	160	-	51
		10	220	-	61
	CO-precovered	0.25	104	14	8
		1.5	130	25	14
	Rh/alumina	10	165	55	25
	Alumina	0.25	27	-	<1
		10	36	-	<1
CO	Rh/alumina	0.25	224	-	-
		20	268	-	-
	H_2S-precovered	0.25	19	<1	
	Rh/alumina	20	41	<1	<1
	Alumina	0.25	<1	-	-
		20	<1	-	-

[a] Values are in μmol/g ± 5 μmol/g.

[b] Rh concentration = 195 μmol/g.

[c] P_{H_2S} = 4.5 Torr; P_{CO} = 2.5 Torr.

Table 2

Hydrogen Balance for Adsorption of H_2S at 300 K and Desorption of Species at 373 K from Various Surfaces[a,b]

Surface	H_2O Uptake	H_2 Evolved at 300 K	Desorbed Species			Total H_2X[e] Produced	
			H_2S	H_2O[d]	H_2	μmol/g	fraction of H_2S Uptake
Rh/alumina	220	61	38	70	5	174	.79
CO-precovered Rh/alumina[c]	165	25	32	15	30	102	.62
alumina	36	<1	28	6	<1	34	.94

[a] Values are in μmol/g ± 5 μmol/g.

[b] Rh concentration = 195 μmol/g.

[c] CO uptake 268 μmol/g; 55 μmol/g of CO displaced at 300 K; 138 and 11 μmol/g of CO and CO_2, respectively desorbed at 373 K.

[d] ±25 μmol/g.

[e] X = S, O, - .

Table 3

Calculated Distribution of Rh and CO for CO-covered Rh/alumina[a]

Rh Distribution	μmol/g	CO distribution	μmol/g
dicarbonyl	112	dicarbonyl	224
clustered	59	linear	30
inactive	23	bridging	15
total	194	total	269

[a] Total CO/Total Rh = 1.38.

APPENDIX:

C_2H_2 Adsorption and Interaction with CO on Rh/Alumina

1. Introduction

Heterogeneous and homogeneous catalysts containing Rh are among the most active for hydrogenation and dimerization of unsaturated hydrocarbons **(1-3)**. It has also been found that the activity for hydrocarbon reactions may depend on the oxidation state of the Rh. For zeolite-supported Rh, Rh^0 was much more active than Rh^I for hydrogenation of C_2H_2, while Rh^I was more active than Rh^0 for the dimerization of C_2H_4 **(4)**. On alumina, Rh also exists as Rh^0 and Rh^I **(5)**. Rh^0 adsorbs CO in the linear and bridging modes whereas Rh^I forms a dicarbonyl species **(5)**. They can be distinguished by their vibrational spectra **(6-8)**. We report here a preliminary study of the adsorption of C_2H_2 and its interaction with CO on alumina-supported Rh using infrared spectroscopy and measurements of the amounts of C_2H_2 and CO taken up.

2. Experimental Procedures

The preparation of the 2.0% Rh/alumina and the procedures for recording the infrared spectra were described in Chapters 4 and 5 of this thesis. The alumina used in this study had a BET surface area of 115 m^2/g. The C_2H_2 (Matheson, C.P.) was purified by three freeze-pump-thaw cycles and sublimed at 178 K. All adsorption measurements and treatments of the samples after the initial preparation of the Rh/alumina were made at 300 K.

3. Results

A. Uptake of C_2H_2

After exposure of Rh/alumina to 2 Torr of C_2H_2 at 300 K for 38 hr, the sample and the gases above it were exposed to a trap at 77 K for 5 min. The condensed material was analyzed by gas chromatography and 1.5 and 0.1 μmol/g of C_2H_4 and C_2H_6, respectively, were found. We assume that components other than

C_2H_2 are not present in the gas phase and calculate the amount of C_2H_2 taken up by the sample, i.e. removed from the gas phase, from the decrease in pressure during exposure to C_2H_2. Data for the uptake measurements are listed in Table 1.

The uptake of C_2H_2 is approximately linear in time$^{1/2}$ from ~ 15 hr to at least 38 hr, as shown in Fig. 1. After 38 hr, the uptake is 211 μmol/g, which is equivalent to a ratio of molecules of C_2H_2 taken up to Rh atoms in the sample of 1.09. A ratio of 1.37 was reached for another sample that exhibited the same type of behavior. The sample was then evacuated for 3 hr at 300 K and reexposed to 2 Torr of C_2H_2. After ~ 20 hr, the uptake again became linear in time $^{1/2}$.

Less detailed studies of C_2H_2 adsorption on alumina and CO-precovered Rh/alumina were carried out and the results are illustrated in Fig. 1. After exposure of alumina to 1.0 Torr of C_2H_2 for 30 hr, only 15 μ mol/g of C_2H_2 are taken up. After exposure of CO-precovered Rh/alumina to 1.5 Torr of C_2H_2 for ~ 15 hr, 134 μmol/g of C_2H_2 are taken up, which is 72% of that taken up in 15 hr by clean Rh/alumina.

B. Infrared Spectra and Uptake Measurements of C_2H_2 and CO Adsorbed Sequentially

A Rh/alumina sample was exposed to 5 Torr of ^{12}CO for 15 hr, at which point the amount of CO taken up was 284 μmol/g, or 1.46 molecules per Rh atom in the sample. The changes that occur in the infrared spectrum in the region recorded, 4000-1200 cm^{-1}, compared to before exposure to CO, are due to the CO stretching modes of CO adsorbed on the Rh, as shown in Fig. 2A(a). The infrared spectrum of CO adsorbed on Rh/alumina has been explained in previous studies **(6-8)**. The intense peaks at 2103 and 2034 cm^{-1} are assigned to the

dicarbonyl species and the broad peak at ~1855 cm^{-1} is assigned to CO *adsorbed* in a bridging configuration on clustered Rh. The presence of a peak from CO adsorbed linearly on the clustered Rh may be inferred from the loss of intensity at 2070-2060 cm^{-1} upon exposure of CO-precovered Rh/alumina to 10 Torr of O_2 at 300 K. This treatment removes the linear and bridging CO but not the dicarbonyl species **(8-10)**.

The sample which gave the infrared spectrum in Fig. 2A(a) after exposure to CO, was evacuated for 0.2 hr and then exposed to 1.5 Torr of C_2H_2 at 300 K. The uptake of C_2H_2 on this sample after 15 hr was 134 μmol/g, or 0.69 molecules per Rh. During this time, the amount of CO displaced into the gas phase was 32 μmol/g, or 11% of the CO previously adsorbed on the Rh/alumina and equivalent to a displaced CO to Rh ratio of 0.16. The infrared spectrum after exposure to C_2H_2 for 15 hr is shown in Fig. 2A(b). The peaks of the dicarbonyl have changed little by exposure to C_2H_2. The band of the bridging CO has decreased in intensity and shifted lower in frequency while that of the linear CO has decreased in intensity and/or shifted lower in frequency.

A Rh/alumina sample was exposed to 2 Torr of C_2H_2 for 10 hr, at which point the ratio of C_2H_2 molecules taken up to the number of Rh atoms in the sample was 1.37. Without evacuating the sample, the infrared spectrum from 4000 to 1200 cm^{-1} was recorded. No changes were observed compared to before C_2H_2 was adsorbed on the sample [(a) in Fig. 2B].

The sample was then evacuated for 3 hr, exposed to 2.5 Torr of ^{12}CO. After 15 hr, 82 μmol/g of CO had been taken up, or 29% of that by a clean surface in the same time. At this point the infrared spectrum was recorded. All the changes occurred between 2200 and 1700 cm^{-1} and are shown in Fig. 2B(b). The peaks of the dicarbonyl species at 2099 and 2030 cm^{-1}, and the band of bridging CO at

~ 1830 cm^{-1} are evident. They are, however, substantially reduced in intensity, those of the dicarbonyl by ~ 70%, compared to the intensities of the peaks from the dicarbonyl and bridging CO adsorbed on clean Rh/alumina shown in Fig. 2A(a). Changes in the infrared intensity from the linearly-adsorbed CO are difficult to follow in the spectra presented due to the much greater intensity of the dicarbonyl doublet.

4. Discussion

Preadsorbing C_2H_2 on Rh/alumina was found to inhibit the adsorption of CO on the dicarbonyl-forming Rh^I and on the clustered Rh. Thus, to inhibit adsorption of CO on both types of Rh, C_2H_2 must also interact with both types of Rh.

Only 1% of the C_2H_2 that is taken up is hydrogenated to C_2H_4 or C_2H_6. The lack of hydrogenation is in contrast to the results for Rh/silica exposed to C_2H_2 **(11)**. The C_2H_2 is presumably hydrogenated by adsorbed hydrogen from acetylene that had dissociated. In the present study, then, either little of the C_2H_2 dissociated, or the C_2H_4 or C_2H_6 that would be expected to form reacted further.

We obtained values of molecules of C_2H_2 taken up per Rh atom in the sample as large as 1.37, with no indication that the uptake had reached a maximum. The amount of CO taken up by the sample was 1.46 molecules per Rh atom. The ratio of CO molecules adsorbed on the Rh clusters to clustered Rh atoms is only 0.75 **(5)**. The greater overall ratio observed is due to formation of dicarbonyl species in addition to the adsorption of CO on clustered Rh. Formation of a species with more that one acetylene bound to a single Rh atom could explain the large values of C_2H_2 taken up by a clean Rh/alumina surface. Examples of organometallic complexes with more than one C_2H_4 bound to a single Rh atom are $(\eta^5 - C_5H_5)Rh(C_2H_4)_2$ and $[Rh(C_2H_4)_2Cl]_2$.

Considering the adsorption of C_2H_2 on CO-precovered Rh/alumina, however, this explanation would appear unlikely. A sample which had adsorbed 1.46 molecules of CO per Rh was subsequently exposed to C_2H_2 for 15 hr. The ratio of CO displaced into the gas phase per Rh was 0.16. However, there were 0.69 molecules of C_2H_2 taken up per Rh, or 72% of the C_2H_2 taken up in the same time by clean Rh/alumina. The infrared spectra in Fig. 2A supports the idea that the adsorbed CO has not been perturbed greatly by exposure to C_2H_2. Thus an average of 1.99 molecules of CO + C_2H_2 would be bound per Rh, causing very strong steric interactions.

An explanation for the large values of C_2H_2 taken up per Rh which seems more likely is that the C_2H_2 is oligomerizing or polymerizing. During hydrogenation of C_2H_2 over Rh/alumina, C_4 hydrocarbons were observed **(12)**. Also, after exposure of Rh/silica to C_2H_2, C_4 hydrocarbons and benzene could be desorbed by evacuating at 291 K **(11)**. Preadsorbing CO on the Rh/silica did not greatly affect the amount of benzene formed **(12)**. Also, preadsorbed CO on Rh/alumina did not strongly affect the subsequent uptake of C_2H_2 in this study.

Oligomerization or polymerization of C_2H_2 would not greatly relieve the steric crowding on the Rh if all of the product was bound to the Rh. For example, the saturation coverage of benzene chemisorbed on the Ni(100) and (111) surfaces at 300 K is one molecule per 8 and 12 Ni surface atoms, respectively **(13)**. However, the benzene may migrate onto the alumina support or desorb into the gas phase in the present study. The linearity of the amount of C_2H_2 taken up versus (time of exposure)$^{1/2}$ would be consistent with the uptake being limited by diffusion of benzene from a constant number of Rh sites onto the support. This is not the only explanation of the shape of the uptake versus time, and the dependence of the shape on temperature and C_2H_2 pressure would certainly be required to fully characterize the kinetics of the uptake process.

It is interesting that Reid et al. **(16)** also proposed that surface species migrated from the Rh onto the silica or alumina support. They proposed, however, that the species that migrated was C_2H_2, rather than a product of oligomerization. It is not clear why the migration of C_2H_2 would be facilitated by the Rh, as they observed. None of their data contradicts the migration of a product of oligomerization, rather than C_2H_2.

From the infrared spectra in Fig. 2A, we saw that CO adsorbed on the clustered Rh was perturbed by subsequent exposure to C_2H_2 while the dicarbonyl species was apparently nearly unaffected. Preadsorbing CO on Rh/alumina only reduced the uptake of C_2H_2 by ~ 28%. Also, preadsorbing CO on Rh/silica did not affect the formation of benzene greatly **(11)**. Thus, we suspect that there is much oligomerization and/or polymerization of C_2H_2 on clustered Rh. This is somewhat surprising since the clustered Rh is most likely in the zerovalent state **(5)**, and Rh^I, but not Rh^0 was found to be active for C_2H_4 dimerization **(4)**.

The final point we comment on is the lack of change in the infrared spectrum after as much as 1.37 molecules of C_2H_2 were taken up by Rh/alumina. We do not wish to discuss the reason we did not observe changes, since the factors that determine the extinction coefficients of bands in infrared spectra in general **(15)** and in infrared spectra of surface species in particular **(16,17)** are not well understood. We wish only to point out that considerable caution must be used in interpreting the intensities and absence of bands in the infrared spectra of adsorbed hydrocarbons.

Conclusions

We have studied C_2H_2 adsorption and interaction with CO on alumina-supported Rh with infrared spectroscopy and measurements of the amounts of

C_2H_2 and CO taken up. We find that:

1. C_2H_2 adsorbs on both the dicarbonyl-forming and clustered Rh.
2. There is oligomerization and/or polymerization of the C_2H_2 upon adsorption on the Rh, at least some of which takes place on the clustered Rh.

Acknowledgments

This work was supported by the Office of Naval Research under contract NOOO14-79-F-0014.

References

1. R. S. Mann and T. R. Lien, J. Catal. **15**, 1 (1969).

2. R. E. Harmon, S. K. Gupta and D. J. Brown, Chem. Rev. **73**, 21 (1973).

3. R. Cramer, J. Amer. Chem. Soc. **87**, 4717 (1965).

4. Y. Okamoto, N. Ishida, T. Imanaka and S. Teranishi, J. Catal. **58**, 82 (1979).

5. Chapter 4 of this thesis, and references therein.

6. A. C. Yang and C. W. Garland, J. Phys. Chem. **61**, 1504 (1957).

7. J. T. Yates, Jr., T. M. Duncan, S. D. Worley and R. W. Vaughan, J. Chem. Phys. **70**, 1219 (1979).

8. M. Primet, J. Chem. Soc. Faraday Trans. I **74**, 2570 (1978).

9. R. R. Cavanagh and J. T. Yates, Jr., J. Chem. Phys. **74**, 4153 (1981).

10. C. A. Rice, S. D. Worley, C. W. Curtis, J. A. Guin and A. R. Tarrer, J. Chem. Phys. **74**, 6487 (1981).

11. J. U. Reid, S. J. Thomson and G. Webb, J. Catal. **30**,, 378 (1973).

12. G. C. Bond and P. B. Wells, J. Catal. **5**, 419 (1966).

13. J. C. Bertolini, G. Dalmai-Imelik and J. Rousseau, Surface Sci. **67**, 478 (1977).

14. J. U. Reid. S. J. Thompson and G. Webb, J. Catal. **30**, 372 (1973).

15. D. Steele, Advan. Infrared Raman Spect. **1**, 232 (1975).

16. L. H. Little, *Infrared Spectra of Adsorbed Species*, p. 382, Academic Press, New York, 1966.

17. H. A. Pearce and N. Sheppard, Surface Sci. **59**, 205 (1976).

Table 1

The Amounts of C_2H_2 and CO Taken up by Various Surfaces at 300 K.[a,b]

Adsorbate	Surface	Time of Exposure (hr)	Pressure (Torr)	Uptake (μmol/g)	Preadsorbed CO Displaced into Gas Phase (μmol/g)
C_2H_2	Rh/alumina	15	2.0	186	-
		38	2.0	211	
	CO-precovered Rh/alumina	15	1.5	134	32
	alumina	15	1.0	15	-
CO	Rh/alumina	15	5	284	-
	C_2H_2-precoverd Rh/alumina	15	2.5	82	-

[a] Rh concentration = 195 μmol/g.

[b] The measurements were made manometrically assuming that only C_2H_2, C_2H_4, C_2H_6 and CO were present in the gas phase.

Figure Captions

Figure 1. C_2H_2 taken up by various surfaces at 300 K. The uptake was measured manometrically, assuming that only C_2H_2, C_2H_4, CO and C_2H_6 were present in the gas phase. The gas pressures during uptake on the Rh/alumina, CO-precovered Rh/alumina and alumina were 2.2-1.8, 1.5-1.4 and 1.0-0.9 Torr, respectively. The Rh concentration was 195 μmol/g.

Figure 2. Infrared spectra for C_2H_2 and CO adsorbed sequentially on Rh/alumina at 300 K. A. (a) Clean Rh/alumina exposed to 5 Torr of ^{12}CO for 15 hr; (b) the sample in (a) evacuated for 0.2 hr, then exposed to 2 Torr of C_2H_2 for 15 hr. B. (a) Clean Rh/alumina exposed to 2 Torr of C_2H_2 for 10 hr; (b) the sample in (a) evacuated for 0.2 hr, then exposed to 2.5 Torr of CO for 15 hr. During all of these treatments, there were no changes in the infrared spectra between 4000 and 1200 cm^{-1} at frequencies outside the region shown.

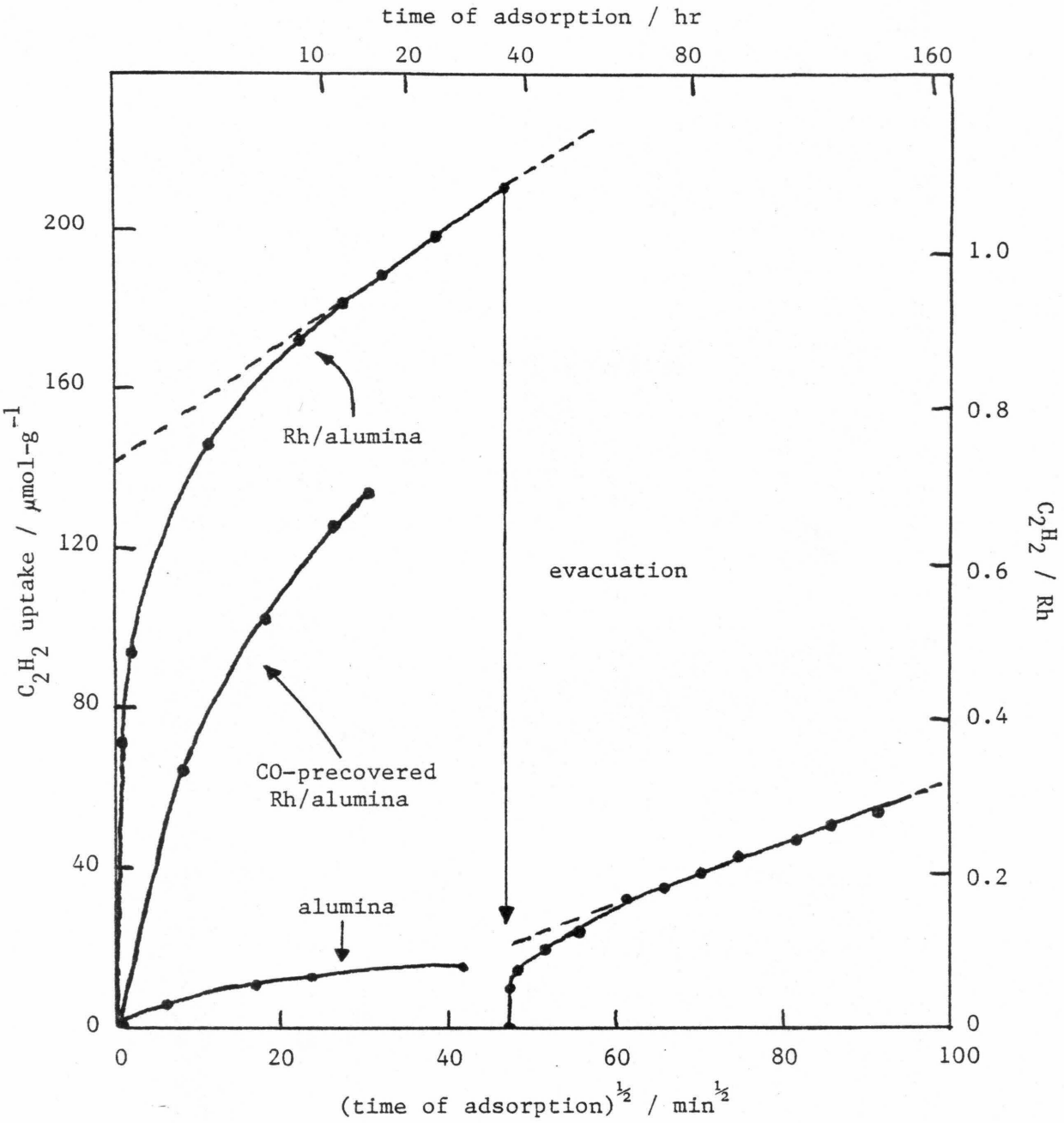
time of adsorption / hr
10
20
40
80
160
200
160
120
80
40
0
C_2H_2 uptake / μmol-g^{-1}
1.0
0.8
0.6
0.4
0.2
0
C_2H_2 / Rh
Rh/alumina
evacuation
CO-precovered
Rh/alumina
alumina
0
20
40
60
80
100
(time of adsorption)^{½} / min^{½}

Figure 1

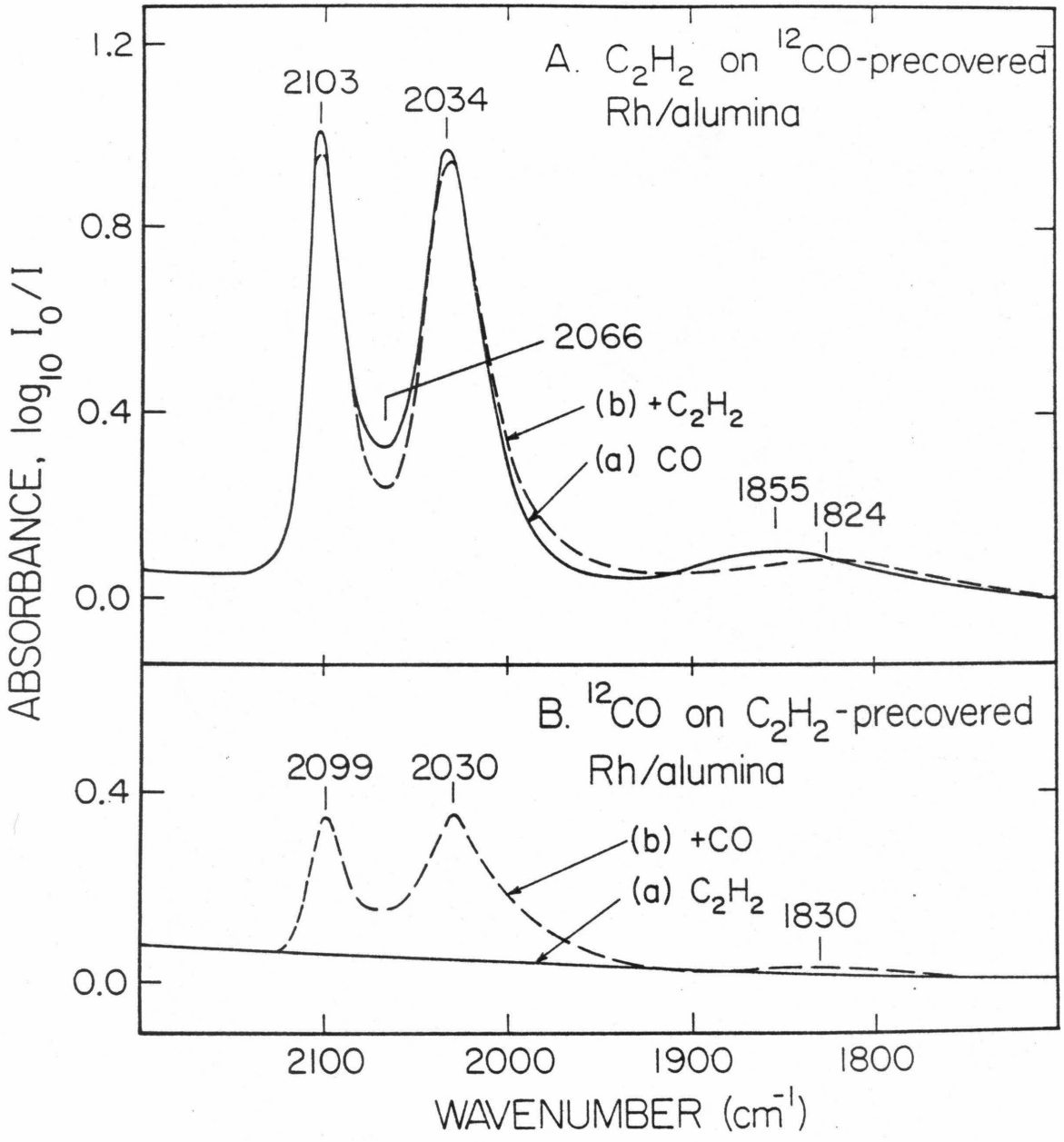
A. C_2H_2 on ^{12}CO-precovered Rh/alumina
2103
2034
2066
(b) + C_2H_2
(a) CO
1855
1824
B. ^{12}CO on C_2H_2-precovered Rh/alumina
2099
2030
(b) +CO
(a) C_2H_2
1830
ABSORBANCE, $\log_{10} I_0/I$
1.2
0.8
0.4
0.0
0.4
0.0
2100
2000
1900
1800
WAVENUMBER (cm^{-1})

Figure 2

CONCLUSIONS

In this thesis, the binding of small molecules to transition metals was studied with the goal of better understanding the fundamental interactions between reactants and catalysts. In Part I, the bonding of the CO in metal carbonyls was examined by determining the ^{13}C nuclear magnetic resonance chemical shift tensors of several metal carbonyls. It was found that for CO bound terminally, the electron orbitals are symmetric about the C-O internuclear axis. In contrast, for CO bound in a bridging configuration between two or three metal atoms, there is significant asymmetry in the electron orbitals.Both types of bonding are unlike that in organic carbonyls.

In Part II of this thesis, the surface chemistry of rhodium supported on alumina was studied using infrared spectroscopy and quantitative measurements of gases taken up and evolved during various procedures. In the first study, the deactivation of the CO adsorption sites upon heating the alumina-supported Rh was found to depend strongly on the gas phase present while heating. The deactivation was much greater if the sample was heated in CO or CO_2 than in O_2, H_2 or *in vacuo*. The specific reactions that the gases undergo, rather than simply the reducing or oxidizing nature of the gas determines the extent of deactivation.

In the second study, another deactivation mechanism was examined, the poisoning of CO adsorption sites of alumina-supported Rh by exposure to H_2S. Though the adsorption of CO was not completely inhibited by H_2S, nor was the ability of adsorbed CO to exchange with gas phase CO, the reactivity of adsorbed CO toward oxygen was greatly reduced. The particular resistance of Rh catalysts to SO_2 poisoning cannot be due to an inability of the dicarbonyl-forming Rh to bind sulfur, as might have been speculated.

Some of the present results may be relevant to the use of Rh-

containing catalysts. For example, in reactions in which the presence of dicarbonyl-forming Rh is advantageous, it would be important to limit the temperature during the reaction or the concentrations of CO, CO_2 and perhaps H_2O and to limit the concentration of sulfur-containing compounds.

It is hoped that the value of identifying various surface species, as well as estimating their concentrations, has been demonstrated. The observation of a surface species does not, however, imply that it is an active intermediate in the catalyzed reaction. It is quite possible that it is involved in an unproductive side reaction. Changes in its concentration during a reaction must be consistent with the kinetics of the overall reaction if it is an active intermediate. Also, isotopic labeling of the reactants and analysis of the distribution of the label in the products can assist in demonstrating the involvement of a surface species in a reaction. In the future, we should expect a trend toward studies in which surface species are observed while kinetic and/or isotopic measurements are made in order to determine mechanisms of catalytic reactions.